POLITECNICO DI MILANO

School of Industrial an Information Engineering

Master of Science in Mechanical Engineering

MODELLING THE RESPONSE OF THE HUMAN FEET TO VERTICAL WHOLE-BODY VIBRATION

Supervisor: Ing. Marco TARABINI

Co-supervisors: Stefano MARELLI, Pietro MARZAROLI, Alex MOORHEAD

Author:

Sabrina MAUGERI

882621

Academic Year 2018-2019

A Marco,
colui che realizza tutti i miei Sogni

Contents

If you want to find the secrets of the universe,
think in terms of energy, frequency and vibration.

Nikola Tesla

Ringraziamenti

A conclusione di questo lavoro di tesi, è doveroso porre i miei più sentiti ringraziamenti alle persone che ho avuto modo di conoscere in questo importante e lungo periodo della mia vita e che mi hanno aiutato a crescere sia dal punto di vista professionale che umano. È difficile in poche righe ricordare tutte le persone che, a vario titolo, hanno contribuito a rendere migliore questo percorso.

Un ringraziamento sentito per la guida competente e solerte va al Professor Marco Tarabini: la mia stima per lui è dovuta, oltre che alla sua profonda esperienza e conoscenza nel campo delle misure meccaniche, alla grande umanità e simpatia con la quale ha saputo incoraggiarmi in tutti i momenti di difficoltà.

Un ringraziamento particolare va a Pietro Marzaroli, Stefano Marelli e Alex Moorhead che con pazienza e spirito critico mi hanno insegnato, sostenuto, consigliato e aiutato durante tutto lo svolgimento della tesi.

Non possono mancare tutte quelle persone con cui ho iniziato e trascorso i miei studi, con le quali ho condiviso momenti indimenticabili, instaurando una sincera amicizia e una profonda collaborazione.

Un Grazie speciale va a Khadija, che con pazienza e Amore mi ha saputo sempre aiutare quando ne ho avuto bisogno. Tu e Sara siete state le prime persone che ho conosciuto e resterete sempre nel mio cuore per i bei momenti passati insieme.

Quanti i pomeriggi di studio "sprecati" per bere un caffè, che poi durava ore con i miei Amici Andrea, Cristina e Edoardo. Voi avete reso sereni anche i giorni più bui in cui tutto sembrava… non funzionare! Io per questo vi ringrazio e vi auguro con tutto il cuore di affrontare tutte le avversità della vita come voi le avete fatte affrontare a me: con lo sguardo avanti e il sorriso sulle labbra.

Come non parlare ora delle Amiche che ho avuto la fortuna di incontrare ancora prima dell'inizio di questo percorso e che hanno saputo esserci sempre: nei giorni difficili ma soprattutto nei giorni sereni di questi ultimi undici anni. Elena, Sara, insieme possiamo dire di essere davvero cresciute: siamo tutte cambiate, ma siamo sempre noi.

Un pensiero anche alle Amiche ritrovate, la leggerezza dello spirito che ho avuto rivedendovi nella mia vita non ha prezzo. Grazie.

Un enorme Grazie anche ai miei compagni di progetto, in particolare a Giovanni che ha affrontato e superato con successo assieme a me i momenti più ardui di ammissione alla Laurea Magistrale. Sei stato per me vitale in quel periodo e te ne sarò sempre grata.
Non cito uno ad uno il resto degli amici, perché vi assicuro che sono talmente tanti che ci vorrebbe un'altra tesi, ma sappiate che siete tutti qui. Se ho raggiunto questo traguardo lo devo anche alla vostra continua presenza, per avermi fatto capire che potevo farcela, incoraggiandomi a "non mollare mai".

Un sincero e profondo grazie anche a tutta la mia grande Famiglia, in particolare al mio Papà, a mia Mamma, mio Fratello Antony, a Roberta, ai miei Nonni, e mia cugina Laura che per me è come una sorella. Voi mi avete vista crescere e con voi desidero condividere la gioia di questo giorno.
Non so se trovo le parole giuste per ringraziarvi, però vorrei che questo mio traguardo raggiunto, per quanto possibile, fosse un premio anche per voi e per i sacrifici che avete fatto. Un infinito grazie per esserci sempre, per sostenermi, ma soprattutto sopportarmi. Senza di voi certamente non sarei la persona che sono. Grazie per i vostri consigli, per le vostre critiche che mi hanno fatta crescere.
Vorrei anche ringraziare Gianni, Morena, Sara e tutta la famiglia, che in questi anni mi hanno accolta e sostenuta in ogni mio progetto. Giorno dopo giorno mi avete donato ed insegnato il meglio di voi.

Infine, un immenso Grazie a Marco, che mi ha insegnato cosa sono l'Amore vero e la vera gioia di vivere tutti i giorni. A Te dedico questa grande vittoria, che è solo un esempio di tutto quello che insieme Noi riusciamo a fare. Ora che questo duro e lunghissimo percorso è finito, non vedo l'ora di scoprire insieme cosa il Destino abbia in serbo per Noi.

Grazie per il vostro Amore

Abstract

Transfer of the external loading such as shock or vibration to whole body could cause harmful effects, depending on exposure time, frequency and magnitude. Researchers showed that the foot and ankle system (FAS) plays an important role in vibration transmission since the transmissibility of the FAS was dominant in lower leg. The vibration absorbing capability of the human FAS was investigated using experimental methods and model development. The vibration transmissibility of the FAS has been studied under vertical sinusoidal vibration. The transmissibility of the foot was qualitatively divided into 5 different areas, given the relevant differences in the response at the heel, midfoot, forefoot, ankle and toes.

A lumped parameter model was developed to reproduce the experimental transfer function of the FAS exposed to vertical excitation. The linearized model has been developed by deriving the equations of motion of the model and fitting the response with the experimental data in a least square sense. Different experimental conditions were considered, with or without the shoes and with the standing subject assuming different postures (leaning forward, backward or neutral). The model has also been improved to fit the apparent mass in addition to the vibration transmissibility.

Keywords: foot; transmissibility; apparent mass; vibration; model.

Astratto

Le vibrazioni possono causare effetti dannosi al corpo umano, con effetti via via più severi all'aumentare del tempo di esposizione e dell'ampiezza dell'oscillazione. Molte ricerche mostrano che il sistema formato dal piede e dalla caviglia (FAS) ha un ruolo molto importante nella trasmissione delle vibrazioni, essendo il punto di ingresso dello stimolo meccanico nel corpo. La trasmissibilità delle vibrazioni nel FAS è stata studiata attraverso lo sviluppo di un modello a parametri concentrati che riproduce quanto identificato sperimentalmente applicando una vibrazione verticale sinusoidale. I dati sperimentali di partenza hanno mostrato che la risposta differisce nelle cinque aree del piede (tallone, pianta del piede, avampiede, caviglia e dita).

Nel presente lavoro di tesi è stato sviluppato un modello a parametri concentrati per definire la funzione di trasferimento del piede soggetto a una vibrazione verticale. I parametri modali sono stati calcolati attraverso un'ottimizzazione ai minimi quadrati, e tutte le non linearità sono state semplificate nell'ipotesi di piccole oscillazioni rispetto alla posizione di equilibrio. Il modello è stato utilizzato per riprodurre la risposta in posture differenti e per riprodurre l'effetto delle calzature. Sono state altresì effettuate ottimizzazioni multi-obiettivo per riprodurre, oltre alla trasmissibilità, la massa apparente del corpo. I risultati hanno mostrato la validità del modello sperimentale e la possibilità quindi di utilizzare il modello per identificare le caratteristiche ottimali di una calzatura per ridurre le vibrazioni trasmesse ad alcuni segmenti del piede.

Parole chiave: piede; trasmissibilità; massa apparente; modello;

List of figures

List of tables

1 Introduction

1.1 Vibration

Vibration is defined as a continuing motion, repetitive and often periodic, of a solid or liquid body within certain spatial limits. Vibration is a mechanical phenomenon whereby oscillations occur around an equilibrium point. The oscillations may be periodic such as the motion of a pendulum or random such as the movement of a tire on a gravel road. Vibration can be generated by different causes and can assume different forms: sinusoidal, random, stationary and transient. For example, a sinusoidal vibration is a periodic motion that repeats itself over a certain time interval. Vibration occurs frequently in a variety of phenomena such as the motion of the oceans, in rotating and stationary machinery, in structures as buildings and ships, in vehicles, and in combinations of these various elements in larger systems. The sources of vibration and the types of vibratory motion and their propagation are complicated and depend on the characteristics of the systems being examined. Moreover, there is a strong coupling between the notions of mechanical vibration, the propagation of vibration and acoustic signals through both the ground and the air. This kind of vibration transmission can create discomfort, annoyance, and even physical damage to the people and structures adjacent to the source of vibration.

The human body is often subjected to vibrations from machines, on roads, or within vehicles. In general, human beings are exposed to external environmental forces intentionally or involuntarily such as various vibrations or shocks during routine life. In fact, we often use more and more powerful tools in work environments, and this involves a higher transfer of vibration to the subjects in working conditions. As a result, even if a part of the vibration is initially dissipated to the environment, a part of it is unavoidably transmitted to the body of the worker. Therefore, as vibration plays an important role in human health, it is very necessary to analyse and explore the human response to this kind of stress.

The biodynamic study on human beings started in 1918 when Alice Hamilton analysed the effects of vibrations on the workers in a quarry. Through experimental tests, she showed that the human body was subjected to, and in a certain sense, was damaged by the vibrations. Therefore, the health of the subject was affected by

the working environment. Considering this discovery, the effect of external forces and vibrations on the human body started to be the main topic of various scientific studies. The primary aim was to find the dynamic responses of the body to vibration and to explain the correlation between vibration and harmful effects.
There are two kinds of vibration: one is linear vibration, that can occur along three principal axes: vertical vibrations are measured along the z-axis, fore-aft vibrations are measured along the x-axis, and side-side vibrations are measured along the y-axis and the other is rotational vibration, that can be measured about the same axis. These kinds of vibrations result in a 6 degree of freedom signal: vertical, fore and aft, lateral, roll, pitch and yaw.

Riding transportation system, driving a car, using a heavy machinery (i.e. jackhammer) or more in general when a subject is placed in contact with a vibrating source, people experience “whole body vibration” (WBV). As the term suggests, WBV is a phenomenon which involves the whole human body without any particular local points affected.

1.2 Effects of vibration on the human body

Vibration can be transmitted to the whole body through a supporting surface or a vibrating platform, for example, through the buttocks of a seated person, the back of a recumbent person, or the feet of a standing person (ISO 2631-1, 1997). Recently, studies have reported that approximately 4-7% of workers in Canada, the United States and the European countries are exposed to vibration that can potentially cause negative health effects [1] [2]. Research [3] [4] [5] has started to evaluate vibration exposure in terms of comfort and health effects. When an individual is exposed to vibration, the energy is transmitted into the body through compression and rarefaction of tissues and fluids in the body [6]. Biodynamic research, focused on the relationship between human physiology and environmental stimuli, has shown that the human body response to vibration is dependent upon various factors [6].

The response of the human body to vibration depends on:

- the part of the body that is exposed
- the dominant frequency of the vibration exposure
- the amplitude of the vibration exposure.

The risks involved with vibration exposure are greater when the vibration magnitudes are high, the exposure durations long, frequent and regular over time, and if the vibration includes severe shocks or jolts. In this condition human body may be subjected to health risks. [6] [7].

Each segment or component of the human body has its own critical frequency at which it oscillates with maximum amplitude, producing maximum shear forces in the body tissue [8] [9]. This leads to maximum displacement between organs and skeletal structure which is translated into an unhealthy condition [8] [9]. Some data about the different resonant frequencies of each body area are reported in Table 1 (Pulkit Singh, 2013).

Body Parts	Resonant Frequency (as reported)	Reference
Eye balls	20-25 Hz	Mandal et al. (2006)
Knee	4-8 Hz	
Abdomen	4-8 Hz	
Chest	4-8 Hz	
Skull (sitting/reclining)	50-70 Hz	
Hand-arm	20-50 Hz	Dong et al. (2004)
Fingers	>80 Hz	Dong et al. (2010) Lundstrom (1984)
Spine	5 Hz	Mandal et al. (2006)
Feet	Currently not known	

Table 1 - Resonant frequencies of different body areas

However, if the vibration type is controlled by means of frequency, amplitude, and direction, it may offer some beneficial effects. Whole body or dynamic vibration therapy is a useful tool in the fitness and health industry for beauty, physical therapy, and rehabilitation. The current whole-body vibration equipment consists of a vibrating platform as the vibration source which can be set up in order to obtain different vibration parameters depending on the application: generating contraction in muscle fibres for training program, working at various speeds for physiotherapy, working at low speed/amplitude for preventing osteoporosis, improving blood circulation etc. There are studies that explore the favourable effect of human body vibration by WBV therapy or dynamic vibration therapy. It has been demonstrated that WBV can be utilized to enhance bone mineral density and muscle strength. Another example of vibration benefit was defined by Ferrario C. [10]. The objective was to determine the outcomes of whole-body vibration training (WBVT) on obese individuals. Typical interventions consist of three sessions per week of exercises performed on platforms vibrating at 25–40 Hz with a vibration amplitude: 1–2 mm. Interventions lasting 6 weeks improved cardiac autonomic function and reduced central/peripheral arterial stiffness in obese women; 10 weeks of WBVT produced significant weight/fat mass reduction, leg strength improvements as resistance training, and enhanced glucose regulation when added to hypocaloric diet. Although there are some benefits in this vibration therapy, it is

still considered controversial because of the unknown possible negative effects of vibration on human body.

The Directive 2002/44/EC of the European Parliament [11] aims at ensuring health and safety of each worker and at creating a minimum basis of protection for all Community workers by timely detection of adverse health effects arising or likely to arise from exposure to mechanical vibration, especially muscular-skeletal disorders. The Directive distinguishes between vibration affecting the hand-arm-system and WBV. Many studies completed in the last decades were about medical assessments related to physical damage due to exposure. Also, modelling attempts suitable for indirect evaluation of the stress transmitted from the working environment to the individual have been developed both from the mechanical and the mathematical point of view. These studies have shown that workers could be exposed to three main types of mechanical vibrations:

- Whole-body vibration (WBV)
- Hand-Arm vibration (HAV)
- Foot transmitted vibration (FTV)

1.2.1 Whole-body vibration (WBV)

Whole-body vibration (WBV) is a vibration that involves the whole human body. WBV can be experienced when sitting or standing on a vehicle or machine, travelling over rough ground or along a track, or the vibration when working near powerful machinery such as a rock crusher.

Health effects associated with WBV have been well documented and include low-back pain, spinal degeneration, neck problems, headaches, nausea, gastrointestinal tract problems, disturbed sleep, and autonomic nervous system dysfunction [6] [12] [13].

Major musculoskeletal health effects reported from WBV exposure include lumbago, early degenerative changes of the vertebrae and intervertebral disc herniations [14] [15] [13]. In 1986, Seidel and Heide reported that WBV may also contribute to the development of noise induced hearing loss [16]. Gastrointestinal disorders, and motion sickness [17] [18] are other examples of vibration effects on human health.

Recently, several researchers have estimated occupational exposure to WBV including Bovenzi [19] who suggested 4–7% of the workforce in North America and Europe were exposed annually to harmful levels of WBV, and Wasserman [20] who reported 7 million workers in the United States had annual exposure to WBV. More recently Palmer and his colleagues [21], estimated that 7.2 million men and 1.8 million women in Great Britain are exposed to occupational WBV.
Personal protective equipment (PPE) has also been developed specifically for WBV, e.g. in order to attenuate and limit the vibration or impact transmission, the mobile equipment seats are now designed with suspension and dampers [22] [23] [24].

1.2.2 Hand-arm vibration (HAV)

The term hand-arm vibration (HAV) is commonly used to refer to vibration transmitted into the hand and arms through the palm and fingers: this situation occurs when the worker handles a machine or a surface of a work piece or power tool that vibrates rapidly. This motion and the vibrations are transmitted into the hand and arm holding the equipment.
Multiple studies have shown that regular and frequent exposure to HAV can lead to permanent adverse health effects which are most likely to occur when contact with a vibrating tool or work process is a regular and significant part of a person's job. Hand-arm vibration can cause a range of conditions collectively known as hand-arm vibration syndrome (HAVS), as well as specific diseases such as white finger or Raynaud's syndrome, carpel tunnel syndrome and tendinitis. Vibration syndrome has adverse circulatory and neural effects in the fingers [25] [26] [27].
Prolonged HAV exposure can also lead to another symptom: vibration white-finger (VWF), that is a neurovascular change in fingers and hand which include blanching of the fingers due to a decrease of blood flow [28]tingling, numbness and reduced thermal and tactile sensations of the fingers and hands; and a reduction in muscular strength and dexterity [18] [29].
Epidemiological data are available for HAV exposure, suggesting that 1.7–5.8% of workers in the United States, Canada and European countries are exposed to occupational HAV [30]. Furthermore, the prevalence of vibration white finger is estimated at 0–5% amongst workers using vibrating tools in warm climates and

jumps up to 80–100% amongst workers exposed in countries at higher latitudes with colder climates [18] [6].

Various prevention/isolation strategies have been developed based on the transmissibility responses and resonant frequencies identified for WBV and HAV. For example, to protect workers from vibration exposure international standards have been introduced (ISO 2631-1, 1997 [31]; ISO 5349-1, 2001 [32]). As for WBV personal protective equipment (PPE) has also been developed specifically for HAV e.g. anti-vibration (AV) gloves (Figure 1) have been designed and developed to protect the worker's finger at resonance. Additionally, engineering controls have been implemented to prevent occupational exposure.

Figure 1 - Anti-vibration (AV) gloves. Designed and developed to protect the worker's finger at resonance

Another example of system used in order to minimize HAV exposure can be found considering mining activities: in the past miners used hand-held jack-leg drilling, they are replaced by jumbo drills, see Figure 2 [33].

(a) (b)

Figure 2 - HAV vibration reduction solution: (a) old methodology: Jack-leg drilling (b) New Technology: Jumbo Drill machine

Thanks to the adoption of this new technology, the HAV exposure has been reduced because the workers no longer holds in his hand the vibrating tool.

1.2.3 Foot-transmitted vibration (FTV)

Foot-transmitted vibration (FTV), is a vibration that is transmitted to lower limbs, feet and legs, from vibrating tools or vibrating machineries. For example, miners can be exposed to FTV when operating locomotives, bolters, jumbo drills, and drills attached to platforms where workers stand on. More specifically, miners who work with bolters, face unique circumstances whereby they are exposed at two contact points because they are standing on a vibrating platform (FTV) while handling a vibrating tool (HTV). Case reports suggest miners are experiencing pain, discomfort, and blanching in the toes more often than co-workers not exposed to vibration throug the feet. “Vibration-induced white foot” (VIWFt) is a quite recent medical term used to describe the foot vascular symptoms experienced with prolonged FTV exposure. VIWFt is an emergent condition whose incidence is expected to increase over the coming years [33] [34].

In the standing condition, the external vibration is transmitted to the whole body through the FAS since it behaves as the connection point between the shaking source and the human body.

Since the consequences of WBV on health can be considered acute, sometimes having immediate effects on the lower back, neck, or head, the majority of studies on standing vibration have focused on vibration transmissibility from the platform to these regions [6] [35].

To date, published epidemiological data has not classified FTV independent from general WBV. Therefore, isn't already not known how many people from the estimated WBV groups are primarily exposed to FTV.

Exposure to FTV may cause an analogous syndrome in the lower extremities; however, little is known about the characteristics of occupational FTV or clinical implications with prolonged exposure. Vibration exposure when standing, and the resulting health effects to feet, have received little attention and the impact of vibration frequency on feet is not fully understood yet.

In order to prevent FTV local injury or disease, the vibration transmissibility of different anatomical areas of the foot needs to be systematically identified, as it has been done with WBV and HAV [36]. However, research associated with FTV is limited, despite evidence of negative health effects of vibration at the foot, either with direct segmental exposure [37] or indirectly with ankle-foot vibration exposure [34] [38].

This limited knowledge on the bio-dynamic response of feet to FTV needs to be improved for better understanding of FTV and to identify interventions capable of attenuating harmful vibrations at the foot.

Understanding how vibration is transmitted in lower limbs is fundamental to find new solutions for preventing health issues and improving anti-vibration equipment.

The foot and ankle system is the starting location of WBV, indeed the FAS is a passive structure able to store and release the strain energy during dynamic loading. An important role of the foot and ankle is their capability to absorb shock and vibration. Joint degeneration is related to changes in this ability to attenuate shock waves. [17] [39] [35] [40]

In the standing condition, the external vibration is transmitted to the whole body through the FAS since it behaves as the connection point between the shaking source and the human body.

The Directive 2002/44/EC of the European Parliament [11], defines exposure limit values for HAV and WBV, respectively on basis of a standardized eight-hour reference period, simulating a work day.

The knowledge of the FAS response can't be considered complete, but the 'wrist and hand' in the upper extremity and 'ankle and foot' in the lower extremity of the human body appears to be constructed on structurally similar principles.

The local health effects associated with FTV have a similar symptomology to HAVS, including pain and numbness in the toes and feet, increased sensitivity to cold, blanching in the toes, and joint pain [33]. Researchers studying the effects of HAV syndrome have found a correlation between the neurological and vascular symptoms observed in the upper extremities and symptoms observed in the feet of workers affected by HAV syndrome [38] [41] [42].

The clinical term "Vibration-induced white foot" (VIWFt), was created by Thompson and colleagues and it is used to describe the foot vascular symptoms experienced with prolonged vibration exposure. Other pathological findings related to neurovascular structures, musculoskeletal structures, sympathetic nervous system etc., have also been reported following vibration exposure to the feet [34] [42] [43] [44] [45] [41].

Harazin and Grzesik [46] investigated the transmission of vertical WBV with a frequency range up to 250Hz (at a magnitude of 4m/s^2), to six body segments (metatarsus, ankle, knee, hip, shoulder and head) for 10 standing postures. Transmitted vibration amplitude was amplified in the range of frequencies:

- 4-10Hz and 31.5-125Hz at the metatarsus
- 4-10Hz and 25-63Hz at the ankle; implying the formation of a local resonance

Similarly, a laboratory study of FTV conducted on 30 male participants, identified the resonant frequency of the hallux to be 50Hz or higher, and the ankle to be lower than 25Hz [37]. The major limitations of this study were that only exposure frequencies from 25 to 50Hz were evaluated (at 5Hz intervals) and that the vibration magnitude was not held constant across the different exposure frequencies. However, these studies have found different transmissibility responses for the forefoot and rearfoot. This observation is consistent with previous HAV work which has reported differences in the vibration response at the fingers and palm of the hand [47] [48] [36]. These regional differences suggest that a systematic identification of resonance frequencies and vibration transmissibility for the foot must include a more precise study of this phenomenon. Therefore, during the experimental tests, numerous positions of the foot and ankle system

were considered to better understand and capture the dynamic response of the foot. However, there is limited knowledge on the bio-dynamic response of the feet to FTV and less is known about appropriate interventions to attenuate FTV.

1.3 General Features of the foot and ankle

As mentioned, the FAS is the starting location of WBV and it is also subject to FTV. It is a passive structure able to store and release the strain energy during dynamic loading. An important role of the foot and ankle is their capability to absorb shock and vibration [49] [50] [51] [52].

Indeed, the foot performs 2 major functions:

- support the body weight during standing position
- propel the body forward during walking, running, and leaping

This system is very complex, made of 24 bones, 33 joints, and a high number of muscles, tendons, and ligaments. The skeleton of the foot is arched, both longitudinally and transversely. In this paragraph a brief description of the anatomy of the arches of the foot, their bony and ligamentous structure, and the supporting tendons is provided.

The foot has three arches: the medial, longitudinal arch, lateral longitudinal arch, and transverse arch (Figure 3).

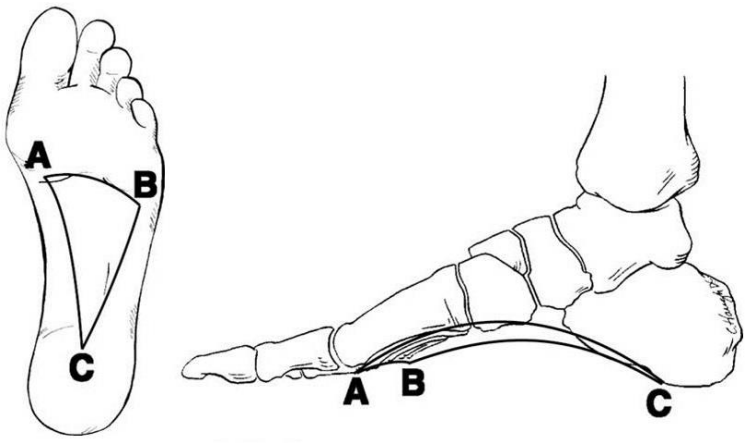

Figure 3 - Arches of the foot: A-B: Anterior Transverse Arch B-C: Lateral Longitudinal Arch; C-A: Medial Longitudinal Arch

These arches are segmented so they can endure the strain of weight and pushes at the optimum level. Their shape allows them to behave as a spring, bearing the weight of the body and absorbing the shock produced during work. The flexibility provided to the foot by these arches facilitates functions such as walking and running. The longitudinal arches of the foot are formed by the tarsal and metatarsal bones, strengthened by ligaments and tendons. The transverse arch is located in

the coronal plane of the foot. According to the height of the medial longitudinal arch, the foot can be rigid or flexible.

Figure 4 – Different anatomic condition of the arches of the foot - (A) Normal Arch; (B) High Arch; (C) Flat Arch

Considering the different anatomic conditions reported in Figure 4 the human foot is classified as:

- a normal arch foot;
- a high-arched foot (pes cavus)
- a flat-arched foot (pes planus)

High-arched feet have poor shock absorbing capability because they are generally more rigid structures while low-arched feet have flexible structural characteristics which can produce an excessive pronation.

The FAS can be divided into three parts (Figure 6):

- the forefoot
- the midfoot
- and the hindfoot/rearfoot

The forefoot is composed of five phalanges and five metatarsal bones. The midfoot is consists of the cuboid, navicular, and three cuneiforms. Only two bones, the calcaneus and talus form the rearfoot.

The primary tissues which connect the different bones are the plantar fascia and the Achilles tendon. The plantar fascia is a thick aponeurosis which supports the arch of the foot. It runs from the tuberosity of the calcaneus forward to the heads of the metatarsal bones (Figure 5).

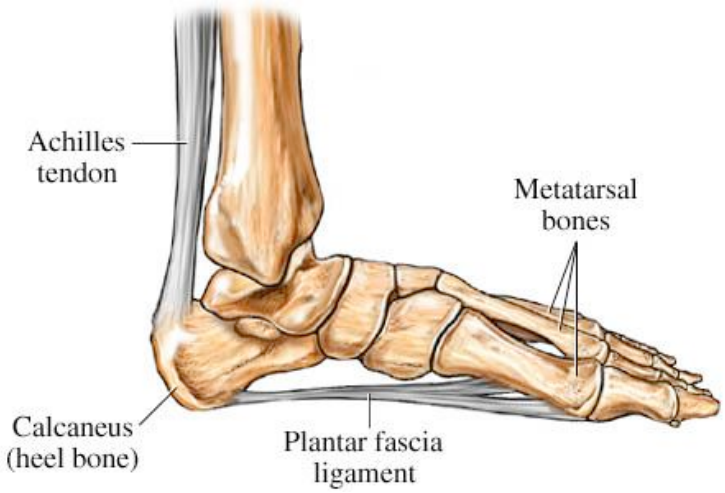

Figure 5 - Schematic representation of the plantar fascia ligament.

There are five main articular joints of the foot (Figure 6):

- Talocrural or ankle joint:

Located between the talus and tibia and between the fibula and tibia, and its axis is responsible for the rotation of the foot such as plantar flexion, dorsiflexion, abduction, and adduction.

- Lisfranc or tarsal-metatarsal joint:

Involves the cuneiform bones, the cuboid bone and the metatarsal bones.

- Metatarsal-phalangeal or MTP joint:

The joints between the metatarsal bones and the proximal phalanges of the toes.

- Subtalar (talocalcaneal):

Occurs at the meeting point of the talus and the calcaneus and allows supination and pronation, inversion and eversion of the foot, but plays no role in dorsiflexion or plantarflexion of the foot.

- Midtarsal (transverse tarsal):

Formed by the articulation of the calcaneus with the cuboid, and the articulation of the talus with the navicular.

As mentioned, a legislation defining limits and methods of vibration measurement exists, but the physical phenomenon of the transmission of vibrations is not yet fully explicit.

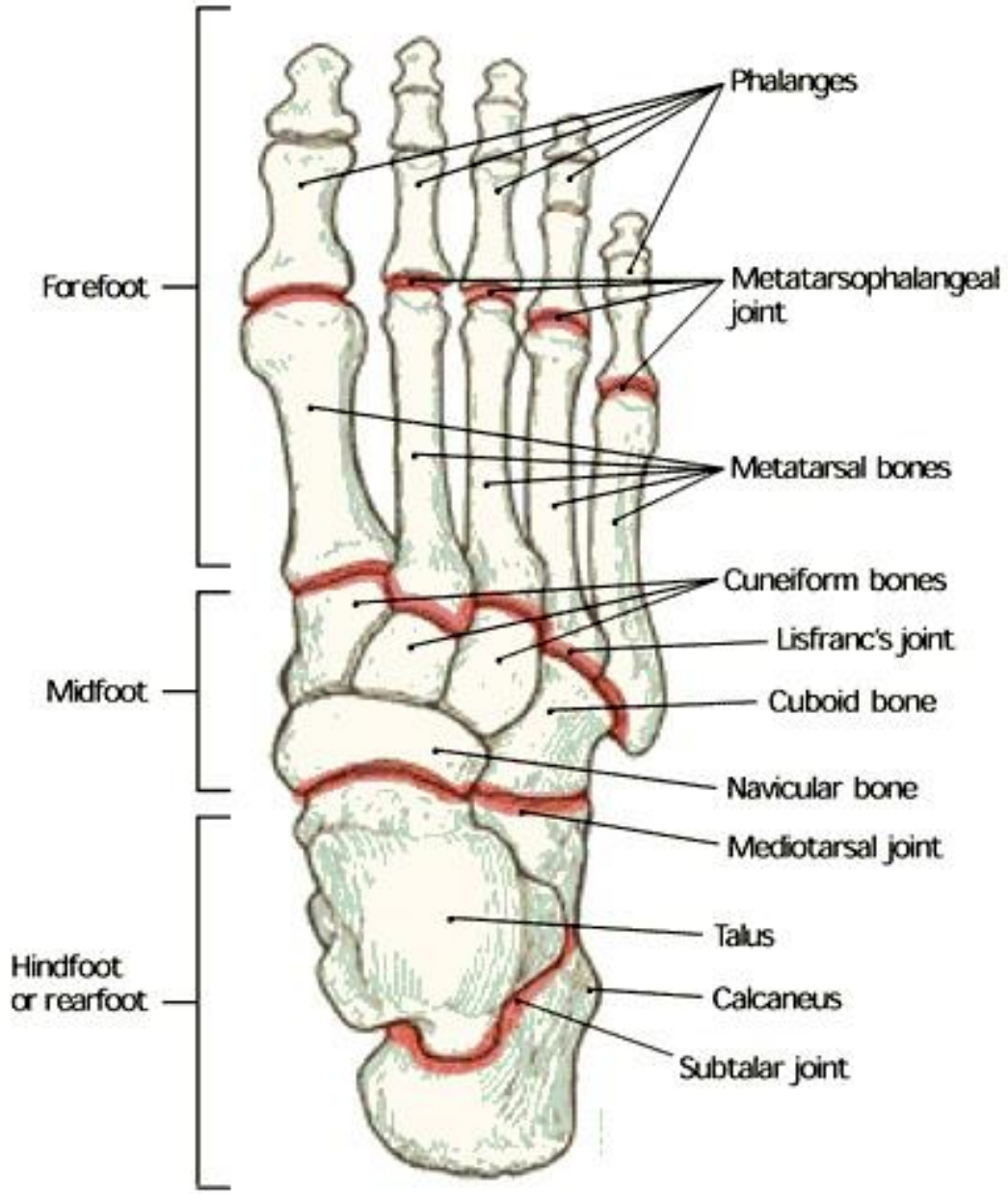

Figure 6 - Foot joints

1.4 The importance of modelling

In order to understand the behaviour of the FAS when subjected to vibration it is necessary to analyse both favourable and adverse effects. Automobiles, equipment, and industrial activities expose people to periodic, random and transient mechanical vibration which can interfere with comfort, activities and health. Vibration can cause a perception of discomfort to a person depending on the magnitude and frequency of vibration as well as the anthropometric properties of the subject. Alternatively, when a subject is exposed to vibration from a critical working environment, e.g. driving an industrial vehicle or agricultural machinery, or working with heavy machinery, there is a serious risk to the worker's health, in particular to the joints.

Understanding of the transmissibility response of different body segments, particularly the biodynamic response of the foot to vibration exposure becomes fundamental for injury prevention and mitigation.

By means of experimental tests a two-dimensional lumped parameter model, able to describe how the human body responds to external vibration has been designed and optimized [53]. Using this model, experimental tests were performed comparing three different body postures:

- Neutral standing
- Leaning forward
- Leaning backward

In order to evaluate and validate the lumped parameters of masses, springs and dampers a least square fitting between the model and measured data was done.

1.5 Dynamic vibration response of human body

Dynamics is the study of the relation between the applied forces or torques and the resulting motion. The foot is considered to be a dynamical system subjected to vibrations. As a dynamic system inertial component of forces are present:

$$F_i = m\ddot{x}$$

Therefore, if there is acceleration, inertial components influence the resultant of the forces.

For example (Figure 7) if a person is on a scale inside an elevator, the force applied on the scale is

$$F_{tot} = mg \mp m\ddot{x}$$

The inertial and the weight are summed up, and an apparent weight is read on the scale.

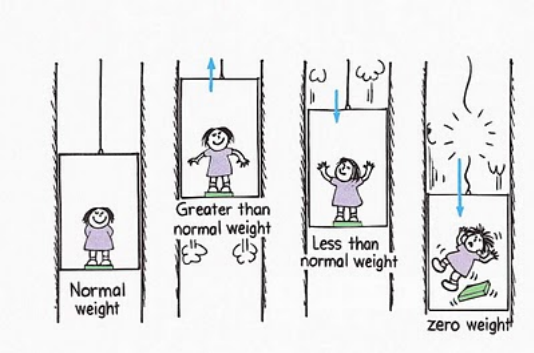

Figure 7 - Apparent mass in everyday life

The inertial force and the acceleration act on the same plane in the opposite direction. This is the reason why if the elevator is going upward the weight measured seems higher. Meanwhile if the elevator is going down the perceived weight is lower. In the case of a free-falling elevator, acceleration is equal to gravity, and the resulting force is zero.

Vertical vibration can be considered like a continual alternation between the two movements of the elevator. This effect, can be summarized in the so called apparent mass curve, that represents the apparent mass in frequency domain. Apparent mass, has great importance in human modelling for the vibration response because it evaluates the total forces between the vibrating surface and the

body. The current models measure either the transmissibility or the apparent mass. However, the two methods have yet to be combined.
This study attempts to develop a model that represents FAS in its kinematic, it reproduces the velocity components of points of interests, and they have not any effect on forces. In the following chapters will be clear that the model has to be improved, and the research of the linear lumped parameters have to be done by optimizing both transmissibility and apparent mass curve. In this way both velocity and forces are considered.
Once a dynamic load or other sources induce a vibration, the passive human body can present an effective mass of about 50-100% greater than its static mass [54]. The effect of the passive human body on the foot structure may therefore be underestimated by representing the human body as a rigid mass. This could result in unexpectedly high stresses in the elements of the structure affecting its integrity, or excessive vibration that might degrade its serviceability [55]. Knowing the apparent mass of the human body can be used to predict vibration transmission. Apparent mass should always be considered when the human body response to vibration is investigated.

Tarabini et al. [56] studied the influence of the body posture and of the foot support on the apparent mass distribution at the feet of standing subjects exposed to WBV. The apparent mass was measured using a capacitive pressure sensor matrix which allowed the separation of the contributions of the different foot regions. Static components of the pressure measurements were used to identify which fraction of the weight is supported by the rearfoot, midfoot and forefoot in the various test configurations. Factorial design of experiments on different response variables showed that the apparent mass is affected by the posture but not by the type of foot contact surface. Conversely, the presence of insoles varies with the apparent mass distribution on the different parts of the foot.

1.6 Insoles

Research of shock absorbing insoles can not only create products for better foot comfort, but also prevent foot injuries and disease due to different situations ranging from sports activities to vibration insolation. In order to control and isolate vibrations not only transmitted to the to human body but also to structures and machines, vibration isolators of different sizes and configurations are used with two objectives:

- decrease transmission of vibration to the surrounding structures due to rotational motion of components in a machine or equipment
- protect a machine, a human being or an equipment from vibration effects transmitted from supporting foundation structure

Vibration isolators are expected to fulfil one or more of the following purposes:

- Supporting the dead-weight of the structure that is isolated without failing and creeping
- Providing sufficient stiffness to protect from vibration transmission between the foundation structure and the machine or from the machine to the foundation structure [57]

Campbell et al. [58] examined the compressive behaviour of foam insoles under simulated use. These were all considered to be “cushioning” or “pressure-distributing” [59] [60] and they are generally felt by the subject to decrease shock transmission. So, they behave as an additional soft-tissue. The matching of the mechanical characteristics of the soft tissues of the foot to those of a material inserted into footwear is fundamental [61]. Various studies deal with the effects due to heat, perspiration and any mechanical degradation upon the insole material. However, the focus is to find a method for assessing the shock absorbing effects of insole materials and how these insoles interact with the human foot. For simplicity the mechanical characteristics of the elastomeric insoles’ materials are considered constant. This means that no variations of working conditions are considered.
Elastomer materials have mechanical properties similar to natural rubber.
They can be manufactured to achieve any for, stiffness, damping, mass, volume or binding characteristic required for any specific use. Elastomer vibration isolators

can sustain large deformations and can recover to their original state without any permanent deformation.

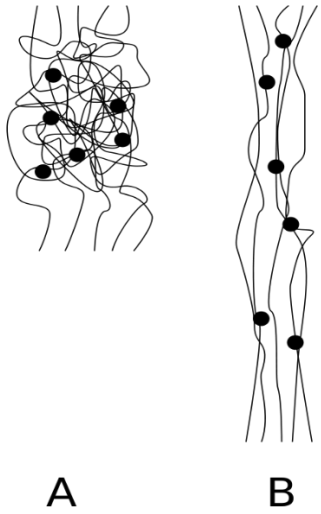

Figure 8 – Polymer chains in rest (A) and under traction stress (B)

In Figure 8 is possible to see the strain process of an elastomeric material. The polymer chains behave like wires connected in points called cross-link points. These points are strong chemical bonds. In the rest state (A) the polymer seems to be a tangle of polymer chains. During the traction (B) the chains becomes ordered in parallel lines.

Elastomer isolators may be used with different types of loading. These are compression, shear, tension, or buckling, or any combination of those. In most aerospace applications, conical elastomer vibration isolators are used because their stiffness characteristics can be arranged to be very close in all directions (iso-elastic behaviour [62]). They also occupy very little space in the axial direction, this is important for applications in which there is minimal space to place vibration isolators. These characteristics are particularly crucial when working with insoles because they should be thin and light.

Most important parameters of dynamic elastomer materials used in vibration isolators is that they are viscoelastic. The lumped parameters of viscoelastic materials depend on temperature, frequency, applied static preload and dynamic amplitude. Hence, stiffness and damping of a vibration isolator rely on the type of viscoelastic material, operating temperature, frequency, static load, dynamic amplitude, and finally geometry of vibration isolator.

In order to evaluate the material properties and characteristics according to ISO 6721-1, some important parameters have been computed:

- the storage modulus E' that represents the stiffness of a viscous-elastic material and is proportional to the energy stored during a loading cycle;
- the loss modulus E" that is proportional to the energy dissipated during one loading cycle. It represents, for example, energy lost as heat, and is a measure of vibrational energy that has been converted during vibration and that cannot be recovered. According to ISO 6721-1, modulus values are expressed in [MPa], but $[{}^{N}/_{mm^2}]$ are sometimes used.
- The loss factor $\eta = \tan\delta$ is the ratio of loss modulus to storage modulus. It is a measure of the energy lost, expressed in terms of the recoverable energy, and represents mechanical damping or internal friction in a viscoelastic system. The loss factor is expressed as a dimensionless number. A high η value is indicative of a material that has a high, non-elastic strain component, while a low value indicates one that is more elastic.

Therefore, from these parameters it is possible to calculate the equivalent stiffness and damping values to be used for the mechanical model of the insole. The stiffness, k, of a material is a measure of the resistance offered by an elastic body to deformation. And in this case, it can be computed using this formula:

$$k_{eq}\left[{}^{N}/_{m}\right] = E'Ah$$

A vibrating system is a system that can store energy in at least two forms. In the case of mechanical oscillators, they are kinetic and potential energy. Vibration involves a periodic transformation of energy between them. Since the efficiency of any energy transformation is always less than 100%, each time that energy is transformed, some of it is dissipated and free vibrations decay in time. This kind of damping is defined as viscoelastic damping. It can be described by using the stress-strain relationship referred to as Hooke's law. This stress-strain relationship, defining viscous-elastic material, is attributed to the Kelvin-Voigt model which is equivalent to a spring in parallel with a damper.

If material behaving in this way is subjected to harmonic loading, an elliptical hysteresis loop is followed in the strain-deformation (sigma-epsilon) plane. The hysteretic damping is a viscous damping with an equivalent damping coefficient:

$$c_{eq}\left[{}^{Ns}/_{m}\right] = \frac{k_{eq}\eta}{\omega}$$

The area of the enclosed hysteresis loop represents the total energy dissipated by the material (Figure 9). This dissipation is due to its viscoelastic behaviour.

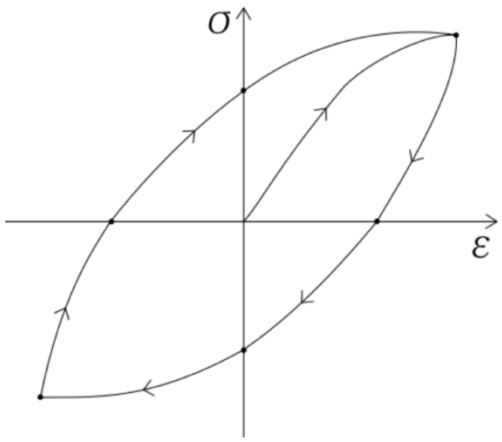

Figure 9 - Typical hysteresis cycle of a viscoelastic material, plotted in the stress- deformation plane. The enclosed area represents the amount of energy dissipated by the material

A model of the FAS that includes the insoles has been created. In this way is possible to evaluate how the lumped parameters of the foot and of the insoles change with the coupling between them and when vibration is applied. Moreover, thanks to this model is possible to predict how the application of a certain insole would change the foot response to vibration and its shock absorption capability.

2 Materials and methods

An important parameter when dealing with vibration is the frequency, that is expressed as the number of oscillatory motions completed in one second, and utilize as the standard international (S.I.) unit of measurement the Hertz [$Hz = {}^{1}/_{s}$] [63].
Vibration is often complex: contains many frequencies, occurs in several directions and changes over time (ISO 2631-1, 1997, [64]).
Another important characteristic of vibration signal is its magnitude or amplitude of signal oscillation, that can be expressed in terms of displacement [m], velocity [${}^{m}/_{s}$] or acceleration [${}^{m}/_{s^2}$].
Following, in this chapter are presented the most important response curve with respect to the analysis of how the vibration is transmitted inside a body:

- Transmissibility for the kinematic behaviour
- Apparent mass for the dynamic behaviour

For both the curves, are presented the experimental activities done, and how data were acquired.

2.1 Transmissibility

A fundamental parameter for understanding the response and the amount of vibrations absorbed by a subject is the transmissibility.

It is a measure of the ability of the body to either amplify or suppress input vibration.

The biodynamic responses, particularly those between the point at which the vibration enters the body and the point at which it is measured, are reflected in the transmissibility of the human body. The process of averaging the individual data to obtain a mean or median transmissibility curve loses the individual response and the large range of inter-subject variability [29]. Some of the variables which affect transmissibility are the type and magnitude of vibration, body posture and muscle tension.

When the majority of the vibration is transmitted through an object or body the transmissibility value obtained is considerable high (around 1.0). Conversely, if most of the vibration is attenuated, or not transmitted through the object or body, the transmissibility value will be low (around 0.0). A transmissibility value greater than 1.0 indicates that the vibration is amplified while passing through the body.

Transmissibility is defined as the ratio of the vibration measured between two points [7] therefore its value can be obtained using the following formula:

$$\text{Transmissibility of vibration} = \frac{\text{Vibration output}}{\text{Vibration input}}$$

The purpose of the present study was to investigate a structural dynamic response of the FAS exposed to the vertical vibration. For this reason, for the objectives of the present work, transmissibility is calculated between the vibrating ground and different points of the foot.

2.2 Modelling approach

As already mentioned, a legislation defining limits and methods of vibration measurement exists yet, but the physical phenomenon of the transmission of vibrations is not yet fully explicit.

ISO 2631, the reference standard for human exposure to vibration, provides a general method for measuring the effects of vibrations between 1 and 80 Hz on the human body. The effects of vibration on the musculoskeletal system were studied with varying frequency and shape of the vibration. This legislation, ISO 2631, does not consider how the vibrations are transmitted through the different parts of the human body, but it considers relevant only the quantity of vibrations entering the body itself.

On the contrary, a knowledge of how vibration is transmitted through the body can contribute in understanding the human body's biomechanical response to whole body vibration.

In general, it is possible to deal with the study of biodynamic responses of human beings through two methods:

- the statistical-experimental
- the analytical

The experimental procedure usually implies to evaluate the vibration-induced biodynamic responses (BR) of the human body by testing a large number of subjects. The obtained results are usually arithmetically averaged and used to represent their mean response. Then, the curves obtained are arithmetically averaged to form the reference mean response for standardization and other applications. This approach is obviously complex, so it is money and time consuming. Conversely, the reduction of the phenomenon to a more or less detailed mathematical model often allows an exhaustive approach for estimating transmitted stresses. The evaluation of the stresses transmitted to the individual is one of the most challenging issue to be faced because of the difficulty of the evaluation of the impedance of the human body along the three main directions.

The possibility to accurately calculate through a model the transmitted stresses allows to:

- better understand how vibrations are transmitted within the human body
- study different strategies for vibration reduction
- prevent vibration effects on human health

In order to simplify and reduce the number of experimental tests required, the purpose of this thesis is to develop a biomechanical model of the foot and ankle system for evaluating

the vibration transmissibility and so dynamic response to vertical vibrations in standing posture.

A two-dimensional lumped parameter model of the foot and ankle system has been designed. Experimental test on a population of 21 participants has been done. The arithmetically averaged measured transmissibility was directly compared with the response obtained from the aforementioned model. The experimental tests have the fundamental role of providing information on the behaviour of FAS since in order to be effective, the identification must be able to synthesize the information contained in the experimental tests. The final objective is in fact to implement a mathematical model that in the numerical simulations reflects in the most complete way the real dynamics of the FAS.

The modelling approach used, consider the FAS as a grey box, with one input (the vibration of the pedar) and a series of outputs: the movement of the points of interest on the foot. This is a theoretical-physical approach, it tried to determine the model structure and properties of its elements which can be described by a set of parameters. This approach uses some theoretical assumptions on model structure combined with experimental data. They are used to complete the model and estimate the unknown parameters in the derived equation.

The process is performed in an iterative way and trial and error method. Starting from a proper experimental test is possible to collect useful data. Once the model is chosen and derived with trial and error, it is possible to identify the selected model or estimate optimized first guess parameters of the derived model.

The general procedure of system identification is shown in Figure 10.

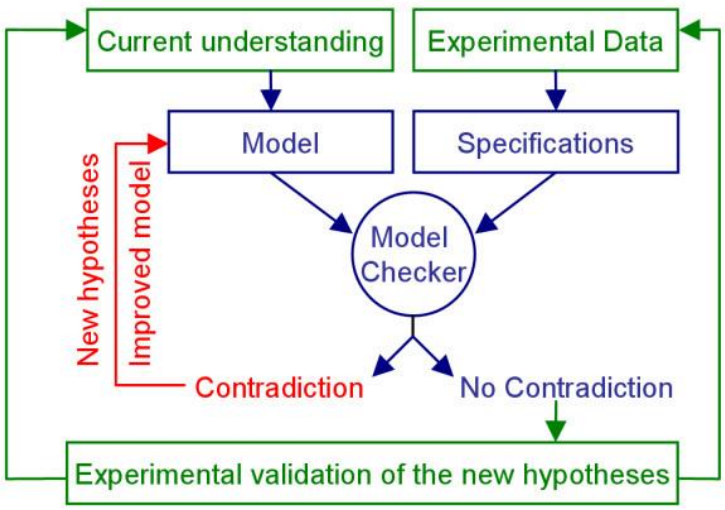

Figure 10 - General iteration procedure of System Identification.

2.3 FAS models in the state of the art

Modelling the complicated structure of the foot and ankle system remains a challenging problem since physical knowledge is not sufficient to describe the foot and ankle system.
Some studies modelled the foot and ankle structure exposed to the impact loading as a simple truss structure with only spring or spring and damping combination [65] [66] [67]. Gefen [65] and Simkin and Leichter [66] utilized a simple truss structure (two inclined rigid bodies hinged at the apex of the truss) for the foot and longitudinal arch and a spring (the connection between the ends of each bar) for the plantar fascia. Also, Kim and Voloshin [67] used a simple truss structure, but viscoelastic properties were utilized instead of a simple spring for the plantar fascia. In Figure 11 is possible to see how simple was this model: the beams represent the bones of the foot, while the ligaments are characterized by spring and dampers.

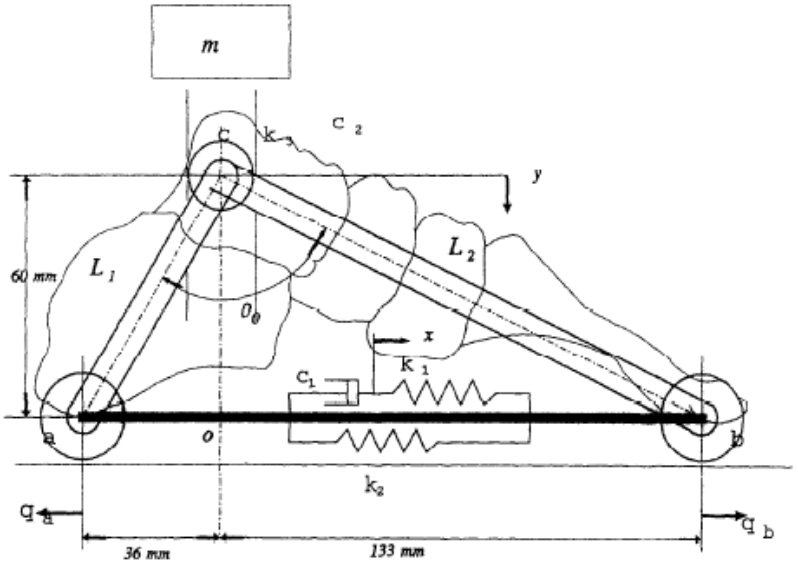

Figure 11 - Kim & Voloshin's model that describes the biomechanical behaviour of the human foot

Kim and Voloshin's model consider the foot composed by only two beams with masses connected by means of a pin. This pin also connects the foot with the mass of the body through a spring and damper. Another spring and damper system is placed between the other extremities of the beams, considering the viscoelastic properties of the ligaments and soft tissue.

2.4 Experimental activities

The model presented was made by a group of researchers of Politecnico di Milano [53] on a group of 21 subjects, computing the average transmissibility to vibration of the FAS of all the subjects. It was considered a frequency range 10-100Hz while standing in a neutral position. The transmissibility functions obtained for each part of the foot are called T1, T2, T3, T4 and T5 were computed between vibrating ground and the average response of the foot, measured by laser reference method. The experimental tests described in this chapter gave results that have been used to be directly compared with the response obtained from the model mentioned in the previous chapter.

In this way it is possible to use the information obtained for both:

- to modify the analytical model
- to be able to optimize the FAS parameters of mass, stiffness and damping

As it was done in the past for the whole-body vibration studies, the transmissibility between the vibrating source and different point of human body was measured. In this particular case the transmissibility of different point of foot and ankle were measured using a vertical sinusoidal vibration input acting on the foot sole. The resonance frequencies were identified for each foot anatomical location. Three different load distributions on the FAS have been tested (Figure 12):

- neutral standing position;
- backward position, with most of the weight loaded on the rearfoot;
- forward position, with the forefoot most loaded.

This has been done in order to implement different model configurations able to correctly describe different subject standing postures on the dynamic characteristics of the FAS.

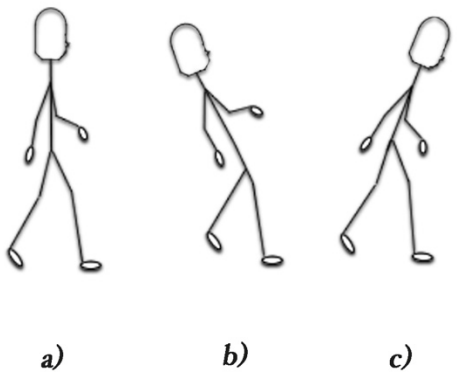

Figure 12 - Postures that have been tested: a) neutral standing b) leaning forward c) leaning backward

2.4.1 Experimental set up and acquisition method

Due to the limited research and the few studies done on the FTV, unfortunately only three studies can be taken into consideration. They are anyway different both for the measurement instrumentation and for the considered locations therefore they are useful in order to evaluate the reliability only of some of the obtained trends.
These three studies are described following:

- Goggins et al. (2016) [37] had the objective to measure vibration transmissibility from the floor-to-ankle and the floor-to-metatarsal, during exposure to FTV while standing. Another objective was to determine if FTV exposure frequency, or participant mass influences the transmission of FTV through the foot. These results can be compared with the ones obtained during our study on toe in position P3 and on foot in position M4
- Wee & Voloshin (2013) [68] instead, studied the FAS response of twenty subjects when exposed to sinusoidal vertical excitation (10-50 Hz with 5 Hz increments and peak to peak acceleration of 17.9 m/s^2) while sitting. The results showed that the FAS plays important role in vibration transmission of lower leg. They measured the lateral malleolus that can be compared with L4. These results, because are made on sitting subject, exclude the effect of the FAS on the body, or vice versa, the effects of the body in the FAS response.
- Finally, Harazin & Grzesik (1998) [46] evaluated the effects of body postures in standing position on the transmission of whole-body vibration to body segments.
  In particular they measured the magnitude acceleration in the *Z*-axis direction of six body segments (metatarsus, ankle, knee, hip, shoulder and head) during exposure to random vibration. Ten male subjects exposed to floor vibration stood in ten different postures. The transmissibility of random vibration from the floor to the body points was calculated at frequencies ranging from 4–250 Hz. Then, their results have been compared with the ones of the toe in position P3 and with the ones on the foot in position M4.

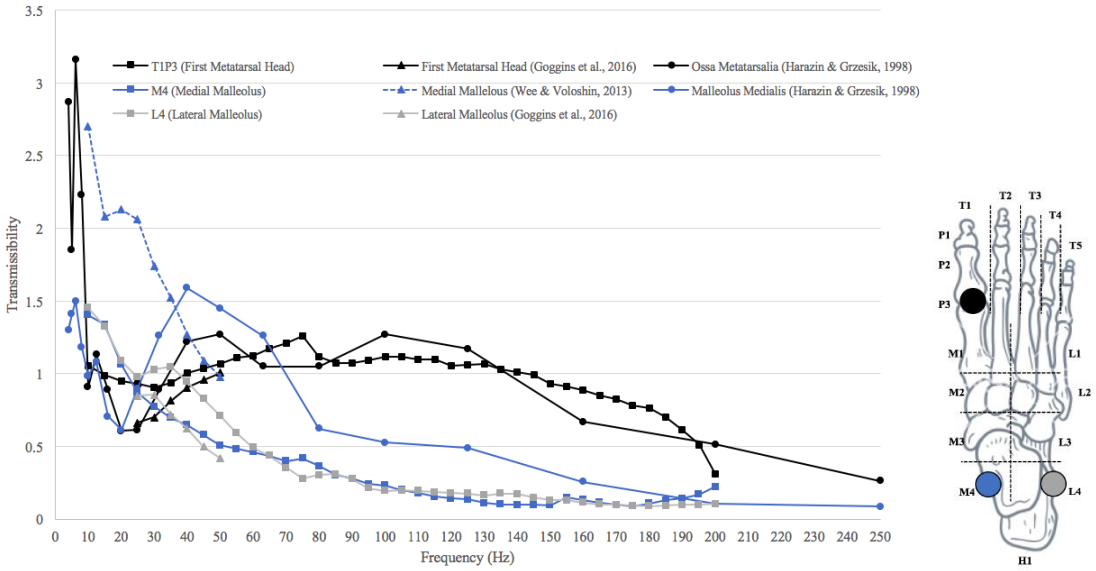

Figure 13 - Comparison of transmissibility results to the corresponding anatomical locations from three previously completed studies (Goggins et al., 2016; Wee & Voloshin, 2013; Harazin & Grzesik, 1998).

As can be seen in Figure 16 there are some differences between the results of the various studies. Equipment differences, accelerometers versus LDV, are probably responsible for the magnitude differences: indeed, the LDV used during this experimental test eliminates a number of problems due to misalignment of single-axis accelerometers, the effects of accelerometer mass on the skin, and the ability to maintain direct attachment to the skin during vibration exposure [36] [69]. On the other hand, among the studies a variation in the resonant frequency ranges could result from differences in vibration input. Another relevant issue is introduced by different subjects' position: for example, in Wee & Voloshin's research [68] the participants were sitting. Therefore, there was less weight baring capacity at the feet and this leads to a decrease in load and plantar pressure (concentrated mass to the feet) increasing amplitude in vibration transmissibility. Nevertheless, despite differences in magnitude, the overall trend of vibration transmissibility for these locations on the foot in a natural standing position are the same: an initial peak at low frequency, then a secondary peak, followed by a rapid decline. The linear phase response from the toes and the upper portion of the midfoot (Figure 13) was to be expected because these portions of the feet have individual mechanical elements, such as very small bony structures, with very little damping (excess tissue). The average phase angle measured at the medial malleolus (Ankle) is identical to the phase angle measured from 10-50Hz for a seated participant [68].

The following experimental tests and studies were performed in accordance with the ethical guidelines of Politecnico di Milano. This experimental activity represents the state of the art for the measuring procedure for the identification of FTV effects. The detailed description has already been published in the article "Biomechanical response of the human foot when

standing in a neutral position while exposed to vertical vibration" (K. Goggins, M. Tarabini, W. Lievers, T. Eger) [70].

The research was made on twenty-one participants, 6 females and 15 males, with an average (± standard deviation):

- age of 24 years (±7.8)
- height of 175.6 cm (± 9.1)
- mass of 70.1 kg (± 14.0)
- total foot length of 25.8 cm (± 2.0)

All the selected participants were in good health and with no particular symptoms or clinical situation. This experimental procedure implies to evaluate the vibration-induced biodynamic responses (BR) of different segments of the FAS. The obtained results have been arithmetically averaged and used to represent their mean response. The mean BR data reported were used to obtain a mean optimized value of the analytical model parameters.

Each subject got on a footboard, that is able to supply vertical vibration input through an electromagnetic shaker (LDS V830). The vibration platform acceleration was measured using Bruel & Kjaer 4508B accelerometer. The stimulus included a peak vertical vibration of 30 mm/s, with a sine sweep from 10-160Hz, lasting 51 seconds.

The general set-up of equipment is illustrated in Figure 14: the shaker provides a vertical sinusoidal input, the Laser Doppler Vibrometer (LDV) is used to measure the vertical output velocity, the accelerometer on the shaker plate is fundamental to measure the input velocity and finally there is the system for data transmission, conditioning and acquisition.

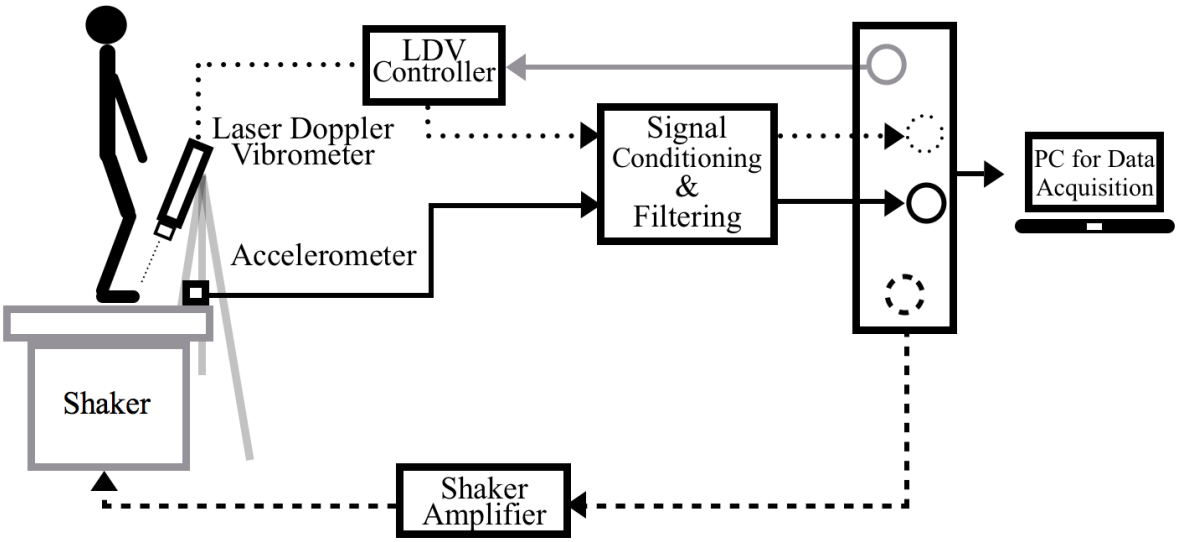

Figure 14 - Illustration of experimental setup and equipment connections: shaker providing sinusoidal input, LDV used to measure the output velocity; accelerometer to measure the input velocity; system for data transmission, conditioning and acquisition

On the foot twenty-four anatomical location have been identified: this positioning configuration have been chosen in order to have a complete view of transmissibility response of the different anatomical areas of the human foot. Each position has been chosen to better represent the muscle-skeletal configuration of the foot and ankle system. In Figure 15 it is possible to see the positions of markers in particular they are placed:

- three on each toe (letter T identifies the specific toe, from T1 to T5, while letter P identified the position: P1 = tip; P2 = mid; P3 = hub)
- six on the mid-foot (M1, M2, M3, L1, L2, L3)
- two on the ankle (M4 and L4)
- one on the heel (H1)

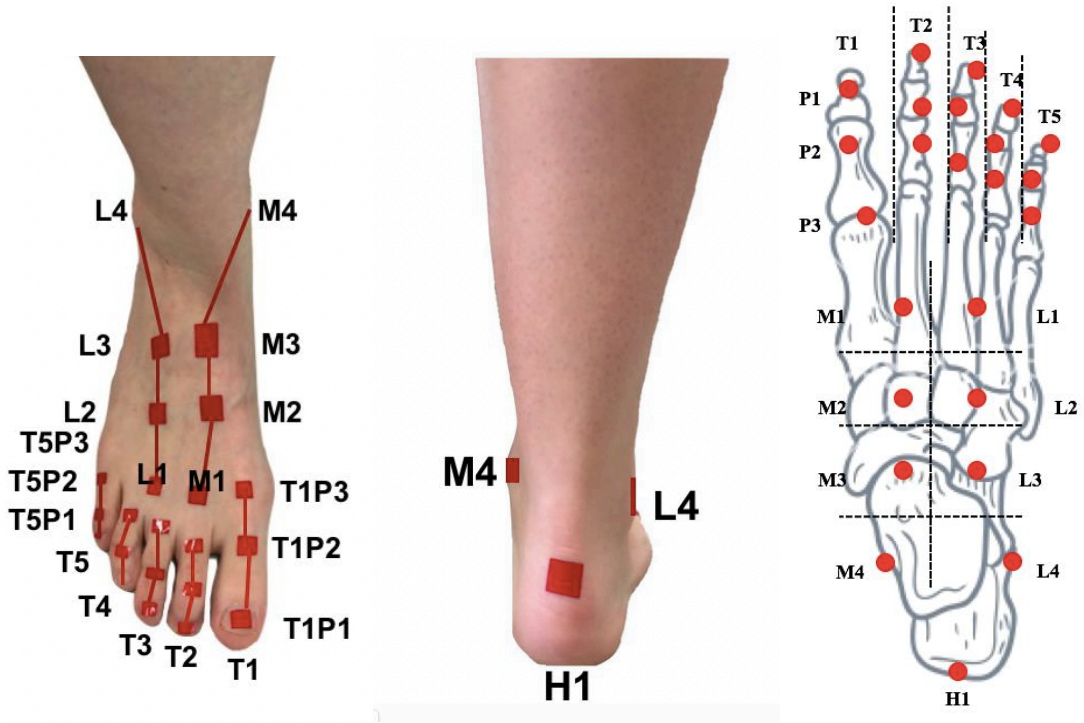

(a) (b) (c)

Figure 15 - Reflective marker set-up (a) anterior view, (b) posterior view, (c) topical anatomic representation.

The Laser Doppler Vibrometer (LDV) was used to measure the velocity at 24 anatomical locations on the foot while the participant was standing in their natural upright standing position, backward and forward position. These points of interest have been highlighted using 3M reflective tape in order to obtain small reflective markers. The LDV used during this experimental test eliminates a number of problems due to misalignment of single-axis accelerometers, the effects of accelerometer mass on the skin, and the ability to maintain direct attachment to the skin during vibration exposure [36] [69].

2.4.2 Overview on acquired data processing

All vibration data were processed using a combination of MeasLAB (Version 5.4) and LabVIEW (National Instruments, 2015). Some quantities of interest were calculated using a discrete Fourier transform (DFT):

- the cross-spectral densities (CSD)
- power-spectral densities (PSD)
- the auto-spectral densities (ASD)

The frequency response function, that in this case is transmissibility: T(f), was calculated across the frequency range (10-160Hz) for each of the 24 markers using the $H1$ frequency response function (FRF) [71]. The $H1$ FRF estimator is a modification of the cross spectral density (CSD) transfer function to deal with the noise from the output measurements recorded on the human skin [7]. In presence of noise affecting the output (response) measurement estimator becomes:

$$\widetilde{H_1}(f) = \frac{S_{x\tilde{y}}(f)}{S_{xx}(f)} = \frac{H(f) \cdot S_{xx}(f) + S_{nx}(f)}{S_{xx}(f)} = T(f)$$

Where:

- $S_{x\tilde{y}}(f)$ is the averaged CSD between the input signal and noisy response
- $H(f)$ being the Fourier transform in the impulse response
- $S_{xx}(f)$ is the auto spectral density (ASD) function of the input signal
- $S_{nx}(f)$ is the ASD function of the noise input

The coherence, that represents the degree of correlation between the input and output, was calculated using this formula:

$$Coherence(f)^2 = \gamma(f)^2 = \frac{\left|S_{xy}(f)\right|^2}{S_{xx}(f) \cdot S_{yy}(f)}$$

Where:

- $|S_{xy}(f)|^2$ is the modulus of the CSD
- $S_{xx}(f)$ and $S_{yy}(f)$ are the power spectral density (PSD) of the input and output respectively [56]

Coherence is a value between 0 and 1: the more correlation is near to one, the more the two signals being measured are correlated [7]. The coherence function can drop below unity for many reasons including contaminating noise on the input or output signals, leakage measurement errors not reduced by windowing, the system is nonlinear or not time

invariant, or because there are non-measured inputs affecting the output [56] Each test where coherence dropped below 0.5 has been repeated.

2.4.3 Experimental results

The transmissibility functions obtained from the experimental tests have been averaged between the 21 participants in order to get the mean transmissibility for each one of the 24 locations, and to eliminate the specific characteristics of each single subject.
Vibration transmissibility varied across the 24 measurement points in Figure 15.
The most evident differences are between three larger areas:

- the toes (15 locations)
- midfoot (M1, M2, L1, and L2)
- ankle (M3, M4, L3, L4, and H1)

The average coherence was maintained at unity for most points, except for M4, L4, and H1, where the average coherence gradually decreases to 0.6 at frequencies above 130Hz. The decrease in coherence was expected for these anatomical locations, due to some measurement system inaccuracies: taking a vertical measurement of a point within a horizontal plane can cause a reflection, or artefact, from which the LDV does not receive the whole return signal. The phase angle had two very distinct categories depending on the anatomical location: the average phase angles for the toes and upper portion of the midfoot were typically linear from 10-80Hz, and then between 80-160Hz the phase angle gradually dropped between approximately 20 and 60 degrees; while for the five points around the ankle (M3, M4, L3, L4, and H1), the phase shift drastically decreased, reaching -497^{o} for M4. The drastic phase changes observed at the ankle location likely resulted from the greater number of anatomic elements between the vibration input and measurement location compared to other regions of the foot. Vibration must pass through the heel fat pad, four-foot bones (cuboid, navicular, talus, and calcaneus) and one of two leg bones (tibia or fibula), as well as various tendons, ligaments, and muscles. Each of these components can be considered a combination of springs and dampers in the ankle mechanical systems. This more complicated transmission path amounts to a series of many mechanical elements in series which will result in the greater variability observed because the phase angle sums for each element. For the toes, the phase varied from 93-147 Hz (1.35-2.45); for the midfoot from 58-80Hz (1.36-1.53); for the ankle from 16-33Hz (1.29-1.91).
The maximum average peak transmissibility frequency (147Hz) occurred at T3P2, and the lowest (16Hz) occurred at H1.

Another important parameter when dealing with transmitted vibrations is the resonance peak. Human bodies exposed to vibration within their resonant frequencies have been shown to be associated with an increased risk of injury [6] [7]. The average peak FTV frequency and amplitude at 24 locations on the foot are reported in Figure 16, where is possible to note that there are notable differences in peak FTV resonance frequency and associated transmissibility magnitude between the different measurement location. The frequency range in which the magnitude of transmissibility has a peak is very different, depending on the considered foot segment:

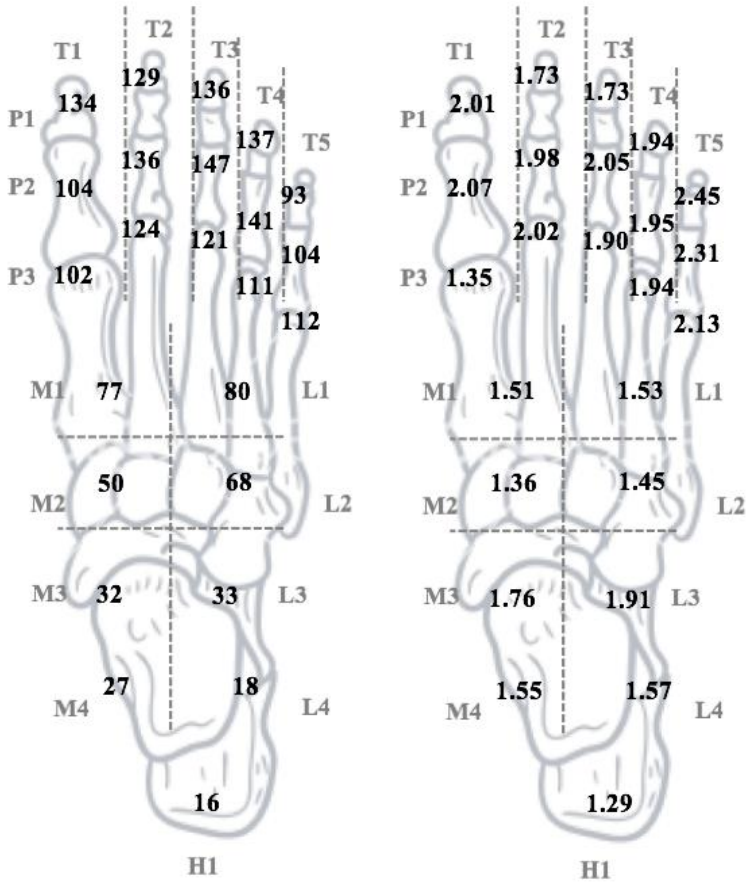

Figure 16 - Average peak FTV frequency (a) and amplitude (b) measured at 24 locations on the foot.

2.4.4 From experimental data to analytical model

In order to simplify and reduce the number of experimental tests required, [53] developed a biomechanical model of the foot and ankle system for evaluating the vibration transmissibility and so dynamic response to vertical vibrations in standing posture.
This model aims not only in reproducing the transmissibility of the foot as a single system. The challenging aspect is to create a model able to reproduce the transmissibility of each segment of the FAS: forefoot, midfoot and rearfoot. This is an innovative solution in the research field of FTV since the existing models deal only with two-degrees of freedom simplifications (Figure 11). This analytical model can be used in different fields, such as isolation strategies and prevent vibration-induced injuries to feet.
The possibility to accurately calculate through a model the transmitted stresses allows to better understand how vibrations are transmitted within the human body, to study different strategies for vibration reduction and to prevent vibration effects on human health. The experimental tests have the fundamental role of providing information on the behaviour of the FAS since, in order to be effective, the identification must be able to synthesize the information contained in the experimental tests. Indeed, the final objective is to implement a mathematical model that in the numerical simulations reflects in the most complete and simplest way the real dynamics of the FAS. Starting from the results presented in the previous paragraph some considerations about how the vibrations are transmitted within the FAS can be done.
The transmissibility response differs for various anatomical locations on the foot, generally:

- at the toes resonance occurred at higher frequencies due to less mass, soft tissue, and weight bearing
- at the ankle resonance is at lower frequencies because of increased mass, soft tissue and weight bearing necessities

These results can be easily compared to HAV exposure measurements, where fingertip resonance occurred at higher frequencies and palm resonance occurred at lower frequencies [48] [47]. As described before, during the experimental tests 24 different anatomic positions were considered but experimental results suggest that a two-dimensional lumped parameter model is a good representation of the FAS system.
In order to develop a two-dimensional lumped parameter model (mass, spring and damper), it has been considered appropriate to study the obtained transmissibility function, both in terms of amplitude and phase, to split the foot in distinct and different macro areas considering the behaviour of the transmissibility functions and to evaluate the mean value

of each foot macro area. Therefore, an average between transmissibility (both for module and phase) of each one of the 5 foot areas was calculated. The transmissibility response of the foot can be qualitatively divided into five different areas based on the obtained magnitudes and phase diagrams, visible in Figure 17:

- toes (hub and tip), whose magnitude is always above 1 and increases for frequency greater than 70 Hz
- midfoot, that takes into consideration metatarsal and cuneiforms, whose magnitude starts from 1, have a peak at around 75 Hz and then starts decreases
- rearfoot, in particular the heel, whose magnitude is about 1 at lower frequencies and the decreases at higher frequencies
- ankle, whose magnitude is higher at lower frequency and then starts to drop

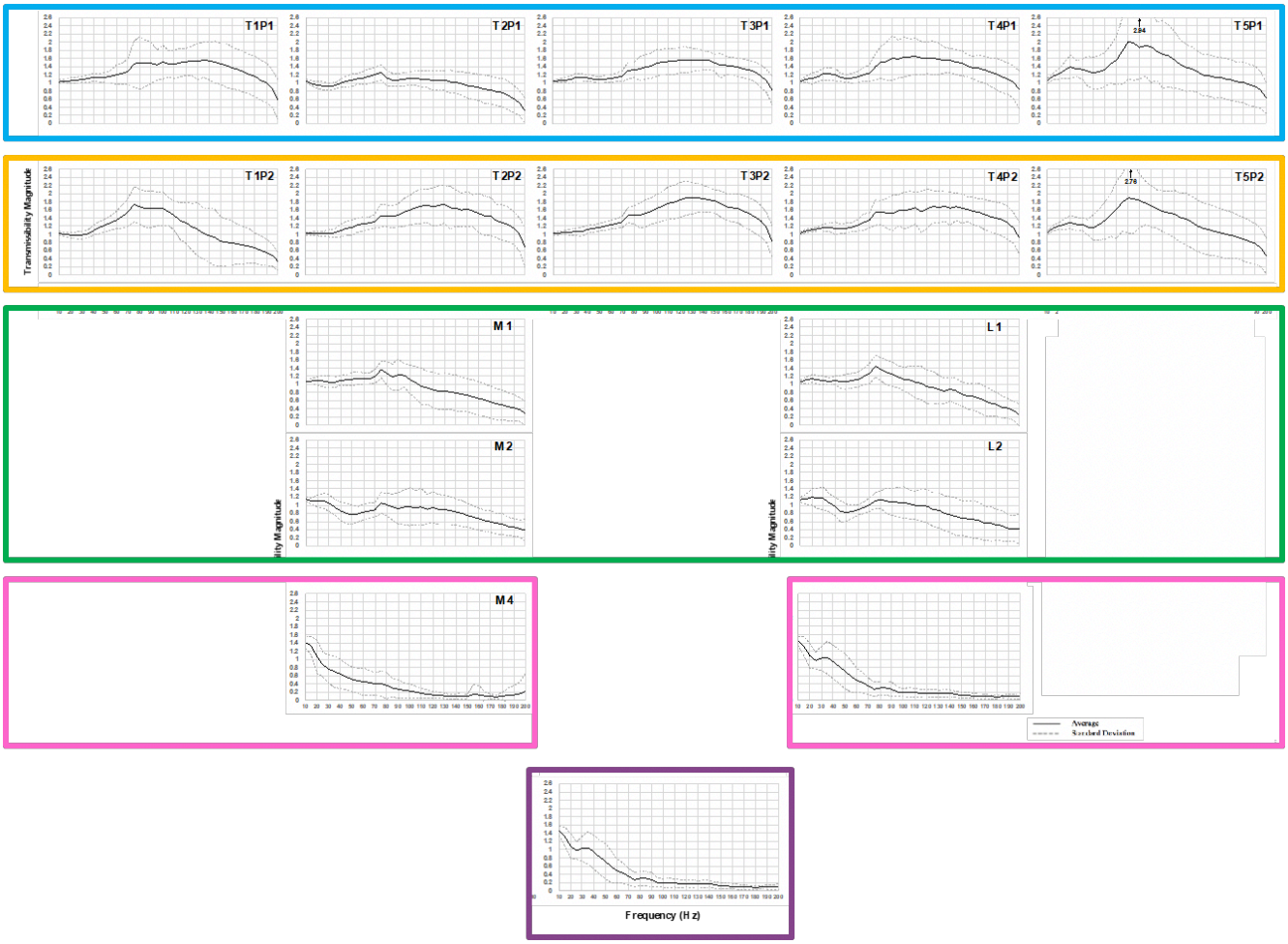

Figure 17 - FTV transmissibility magnitude divided in macro areas based on the similarity of the response. In light blue: tip toes; in yellow: hub toes; in green: midfoot, in pink: ankle and in purple: heel.

From the similarities between transmissibilities in Figure 17 [53] grouped the markers on foot considering as a parameter for optimization the average between the transmissibility of all the markers in that group (Table 2).

Foot part	Markers
Heel	H1
Ankle	M4 L4
Midfoot	L1 L2 M1 M2
Forefoot	T1P3 T2P3 T3P3 T4P3 T5P3
Tip toes	T1P1 T2P1 T3P1 T4P1 T5P1

Table 2 - Foot parts and markers

Vibration transmissibility was amplified:

- at the toes at almost all frequencies between 10-160 Hz;
- at midfoot at frequencies between 10-110Hz;
- at the ankle at frequencies between 10-50Hz. The average (± standard deviation) transmissibility amplitudes are plotted for 24 anatomical locations (see Figure 15 for position and nomenclature).

Across a frequency range of 10-160Hz:

- red, light green and light blue colours indicates the anatomical positions and transmissibility of hub, mid and tip of the toes;
- in yellow is shown the anatomical positions and the transmissibility for the midfoot;
- finally, in purple and dark green are pointed out the anatomical positions and the transmissibility for the ankle and heel respectively.

With the information of [67] [70] [46] and with experimental data acquired before, the final and improved but more complex biomechanical model was developed by Delphine Chadefaux et al. [72]. The model in Figure 18 has 7 degrees of freedom and consists of several lumped masses connected by linear spring and dampers. The analytical model is designed in order to approximate the behaviour of the FAS that undergoes a vertical input vibration in terms of transmissibility.

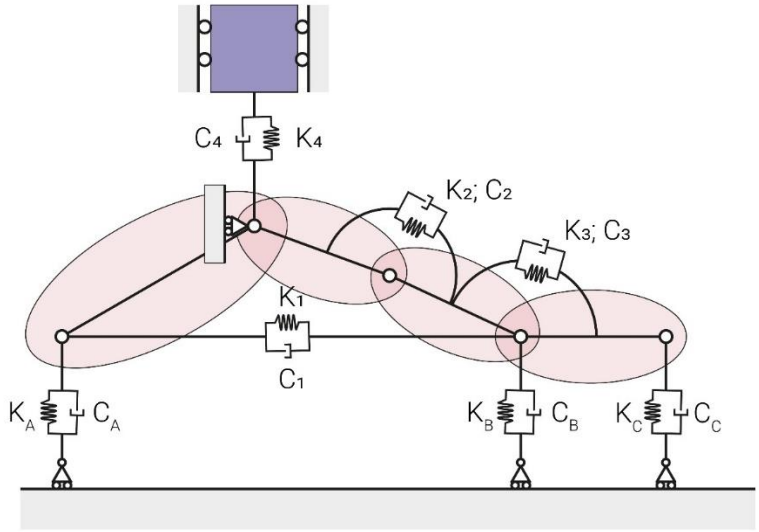

Figure 18 - Designed and developed biomechanical model and its dynamical characteristics

In order to evaluate and validate the lumped parameters of masses, springs and dampers a fitting between the model and measured data was done. Analytical and experimental transmissibility have been compared to obtain an optimization of lumped parameters.
Three different load distributions on the FAS have been considered:

- normal standing position
- backward position, with most of the weight loaded on the rearfoot
- forward position, with the forefoot most loaded

For each of these positions five transmissibility functions have been calculated by the model considering:

- as input the speed of vibrating ground
- as output the speed of five different points belonging to the foot and ankle system

The corresponding transmissibility data measured at the same foot and ankle positions were used to optimize the model parameter. The modelled transmissibility function is then

$$[\tilde{T}] = \frac{r_{dof}}{r_{in}} = \frac{-(-\Omega^2[M_{FC}] + i\Omega[C_{FC}] + [K_{FC}])}{(-\Omega^2[M_{FF}] + i\Omega[C_{FF}] + [K_{FF}])}$$

with Ω is the angular frequency, and $[M_{FF}], [C_{FF}], [K_{FF}], [M_{FC}], [C_{FC}], [K_{FC}],$ free-free and free-constrained components of the global mass, damping, and stiffness matrices, respectively. Matrices $[M_{FF}], [C_{FF}], [K_{FF}], [M_{FC}], [C_{FC}], [K_{FC}]$ were composed of the geometrical and inertial characteristic in Table 3, a total mass of the body equal to the average mass of 70kg but also from $K_{a\ldots g}$ and $C_{a\ldots g}$ so the stiffness and damping parameters are the only variable that are

optimized. Therefore, the modal parameters were computed by optimizing the authorized degrees of freedom in order to fit the experimental results by making a least square root optimization.

COP Location	$\theta_1\ [Deg]$	$\theta_2\ [Deg]$	$\theta_3\ [Deg]$
Backward position	45	66	80
Neutral position	49	69	82
Forward position	52	74	85

Table 3 - Geometrical properties of the modelled foot with respect to the three investigated centre of pressure location (forward, neutral [73] and backward)

	Segment I	Segment II	Segment III	Segment IV
m $[kg]$	0,294	0,294	0,196	0,098
L $[m]$	0,046	0,085	0,07	0,06
I $[kg \cdot m^2]$	$28 \cdot 10^{-5}$	$10 \cdot 10^{-7}$	$14 \cdot 10^{-6}$	$15 \cdot 10^{-7}$

Table 4 - Geometrical and inertial characteristics of the four segments composing the foot [74] [75] [18]

Similarly, to some of the whole-body vibration studies, the transmissibilities from the driving point to the different areas of the foot were measured using the vertical sinusoidal vibration input.

The estimation of $K_{a\ldots g}$ and $C_{a\ldots g}$ was performed with the same procedure adopted in [73] based on a nonlinear curve-fitting in least-squares sense (lsqcurvefit function implemented in Matlab R2018a software) with respect to the experimentally measured transmissibility functions, averaged in all the subjects. The initial guess values K_0 and C_0 provided to the solver were chosen as the parameters estimated in neutral position (Table 5).

	a	b	c	d	e	f	g
K_0	228,0	52,81	7,590	3498	13650	147400	536,1
C_0	0,2449	0,1523	0,3750	48,22	70,96	0,006776	123,9

Table 5 - Initial guess for estimation of the modal parameters

Further, the intervals to look for the optimal stiffness and damping parameters were defined as [0.5 K_0; 1.5 K_0] and [0.5 C_0 ; 1.5 C_0]. To evaluate the optimization process, the reconstruction quadratic error was systematically computed as

$$\varepsilon = \sqrt{\frac{1}{N}\sum_{f=10}^{100} |\tilde{T}(f) - T(f)|^2}$$

Where f is the frequency vector, and $\tilde{T}(f)$ and $T(f)$ are respectively the modelled and the targeted transmissibility functions, and N is the length of the discrete transmissibility function vectors. This process is repeated with the data acquired standing with body weight leaning backward, standing in a neutral position, and standing with the body weight leaning forward.

2.4.5 Effect of the frequency boundary on the model

The model was developed to evaluate how the human body responds to a vibration with frequency from 10 to 100 Hz because the at higher frequencies the dynamic behaviour of the foot is heavily affected by the one of the soft tissues covering the upper part of the foot, that at the moment were not included in the proposed model. As the model parameters are computed by an optimization on the transmissibility function (that is a frequency response function), the purpose of this chapter is to understand if optimizing in a smaller frequency bound the model becomes more performing for the lower frequencies. In Figure 19 is possible to see an example of the results: there are plotted the transmissibility function computed analytically with a frequency bound of both 10-100Hz and 10-50Hz compared to the averaged experimental transmissibility function. The other transmissibility functions computed are shown in Appendix A. The least square error ε is to be computed both in the range of 10-100Hz and in the range of 10-50 Hz.

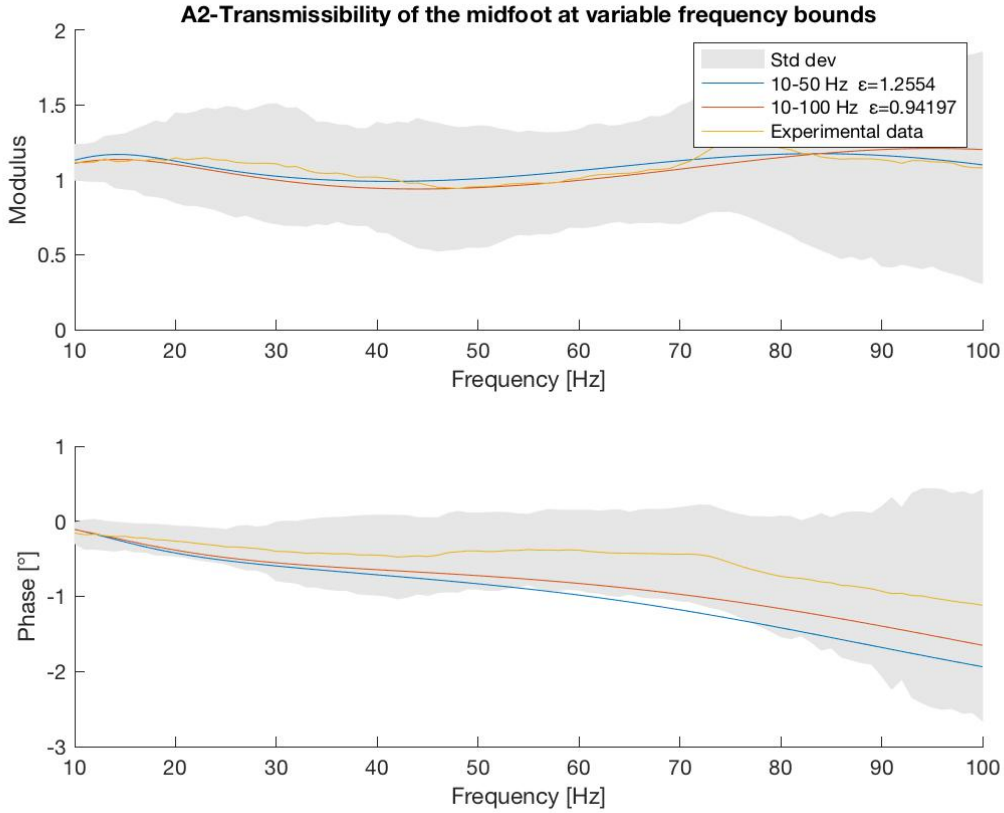

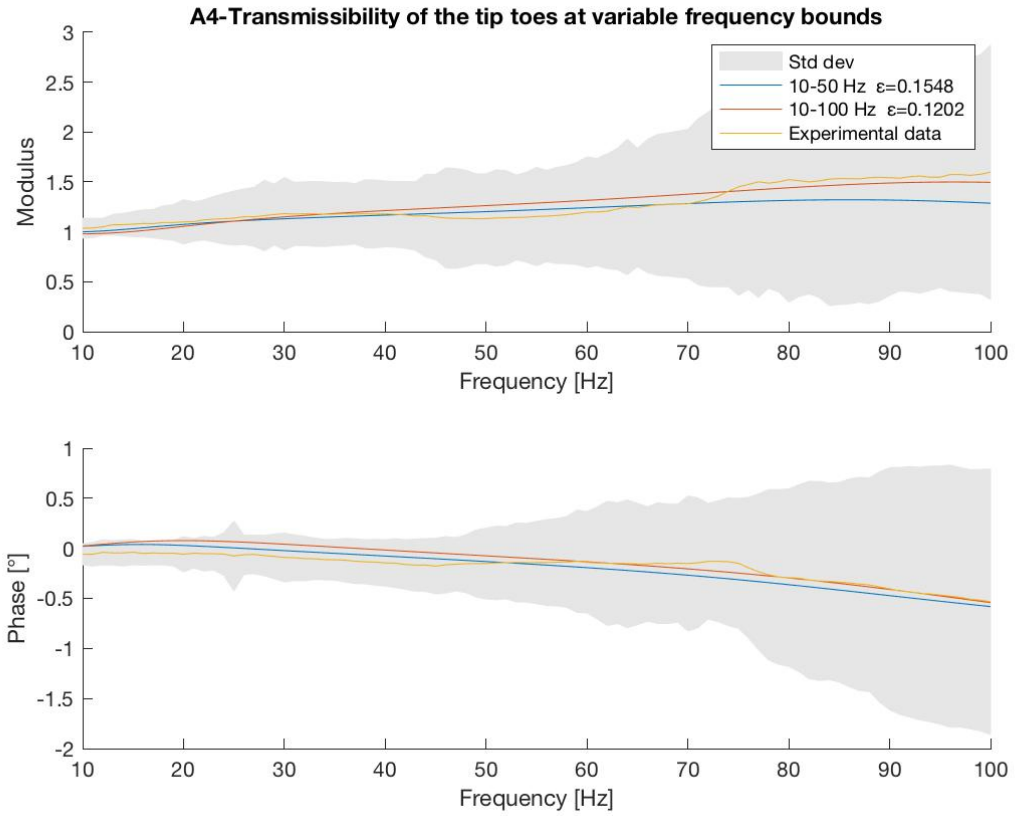

Figure 19 - Comparison between transmissibility functions computed with a frequency bound of 10-50Hz or 10-100Hz

In Table 6 are resumed the least square errors with the three different frequency boundaries.

	Average mean square error evaluated locally (10-50Hz)	Average mean square error evaluated on (10-100Hz)	Average mean square error evaluated globally (10-200Hz)
10-50Hz	0,00386	0,00780	0,0290
10-100Hz	0,00482	0,00426	0,147
10-200Hz	0,00520	0,00570	0,00580

Table 6 - Comparison between least square errors of the optimized transmissibility computed with the range of frequencies 10-50Hz, 10-100Hz and 10-200Hz (rows). Then, the error is computed on both the intervals of frequency to understand the performance locally (10-50Hz) and globally (10-100Hz)

As can be seen from the table, the lowest value of mean square error of each frequency boundary is obtained in the diagonal, so evaluating the error of the curve in the same frequency domain. Globally the lowest value is in the interval of 10-50Hz, that means that if the interested frequency is from 10Hz to 50Hz, the model is more performing if the higher frequencies are excluded. This improvement with reduction of frequency bounds is probably linked to the fact that a concentrated linear lumped parameters model can be too simple, to model the response at high frequency. Moreover, at frequencies around 200Hz the vibration is limited to the first layers of the skin.

In any case in Table 6 is possible to note that the errors are small and that they don't change so much, neither the modal parameters in Table 7. This means that results are robust to the frequency boundary. Following in Table 7 is possible to compare the values of the modal parameters evaluated on the three intervals.

	10-50Hz	10-100Hz	10-200Hz	Description
$K_a \left[N/m\right]$	114,0	114,0	114,0	stiffness of the ankle/body joint
$K_b \left[N/m\right]$	44,35	52,08	43,43	stiffness of the segments II/III joint
$K_c \left[N/m\right]$	11,38	5,730	3,800	stiffness of the segments III/IV joint
$K_d \left[N/m\right]$	3975	4192	3989	stiffness of the plantar aponeurosis
$K_e \left[N/m\right]$	20210	14360	16880	stiffness of the rearfoot sole
$K_f \left[N/m\right]$	143300	174200	217300	stiffness of the forefoot sole
$K_e \left[N/m\right]$	268,0	268,0	268,1	stiffness of the toes sole
$C_a \left[N/m \cdot s\right]$	0,12	0,12	0,12	damping of the ankle/body joint
$C_b \left[N/m \cdot s\right]$	0,10	0,12	0,08	damping of the segments II/III joint
$C_c \left[N/m \cdot s\right]$	0,19	0,32	0,32	damping of the segments III/IV joint
$C_d \left[N/m \cdot s\right]$	58,02	72,33	72,33	damping of the plantar aponeurosis
$C_e \left[N/m \cdot s\right]$	106,4	106,4	106,5	damping of the rearfoot sole
$C_f \left[N/m \cdot s\right]$	0,010	0,0034	0,0033	damping of the forefoot sole
$C_g \left[N/m \cdot s\right]$	112,35	108,01	84,85	damping of the toes sole

Table 7 - Comparison between modal parameters of the frequency bounds of 10-50Hz and 10-100Hz

These results show that the values of stiffness of the A and E segments are completely independent from the frequency boundary, and that in general the values of damping are less affected than the stiffness ones by this kind of variation.

2.4.6 Effect of the optimization maximum and minimum range

In the concentrated parameters model considered, and in the State of the Art, the modal parameters are computed by a least square optimization. In mathematics, computer science and operations research, mathematical optimization or mathematical programming is the selection of a best element (with regard to some criterion) from some set of available alternatives. In the simplest case, an optimization problem consists of maximizing or minimizing a real function by systematically choosing input values from within an allowed set and computing the value of the function. The generalization of optimization theory and techniques to other formulations constitutes a large area of applied mathematics. More generally, optimization includes finding "best available" values of some objective function given a defined domain (or input), including a variety of different types of objective functions and different types of domains. Optimization problems are often multi-modal; that is, they possess multiple good solutions. They could all be globally good (same cost function value) or there could be a mix of globally good and locally good solutions. Obtaining all (or at least some of) the multiple solutions is the goal of a multi-modal optimizer. Classical optimization techniques due to their iterative approach do not perform satisfactorily when they are used to obtain multiple solutions, since it is not guaranteed that different solutions will be obtained even with different starting points in multiple runs of the algorithm.

For the optimization are necessary some higher and lower boundaries as constraints in order to stop the optimization if some parameter exceed the highest or lower value possible and therefore to keep the values stick to the reality. The objective is to evaluate the effect of this upper and lower boundaries on the resulting modal parameters and transmissibility function. In the state of the art the boundaries are linear function of the initial values, so they change during the optimization at every step. In particular they are:

$$V_{min} = \frac{1}{2} \cdot V_0 \qquad\qquad V_{max} = \frac{3}{2} \cdot V_0$$

Where V_{min} and V_{max} are respectively the minimum and maximum value that a parameter can assume and V_0 is the initial value considered for that modal parameter (see Table 5).
The optimized value of each modal parameter is given by the optimization of the averaged response of all the 21 subjects. But computing the optimal values for each subject is possible to note that the values are often divided in two groups.
This lead to think about a systematical error and it could be related to the restricted boundary constraint of the optimization procedure. Therefore, it's interesting to evaluate

the robustness of the model to the optimization boundary constraints. The following analysis in made by gradually increasing the range of boundary constraints changing the parameter n from 0,5 to 10 in the following new expression of the boundary constraints:

$$V_{min} = \frac{V_0}{n} \qquad\qquad V_{max} = \mathrm{n} \cdot V_0$$

Plotting the resulting transmissibilities (Figure 20) is possible to notice that overcoming a certain boundary amplitude the results are stable on a value. Stable results are more eligible, and with this consideration the parameter presented before assumes different values for each subject.

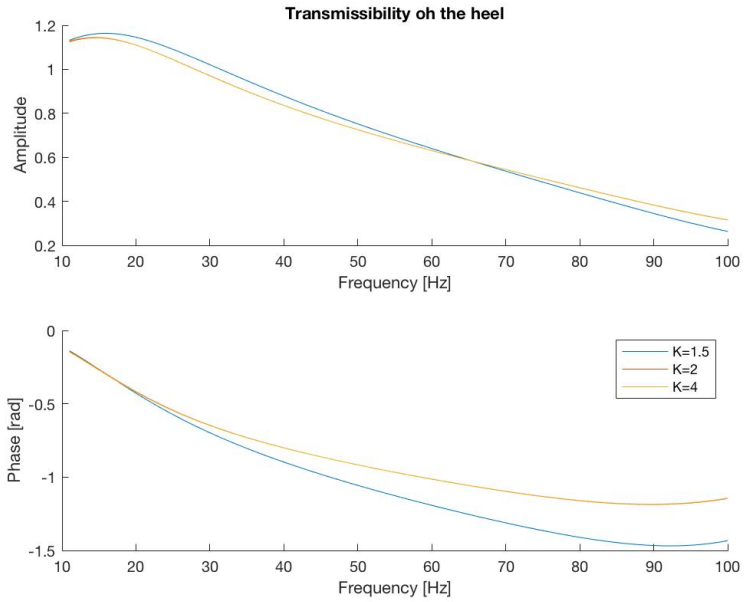

Figure 20 - Transmissibility curve at variable optimization boundary range, the curves with a boundary factor higher than 2 completely overlap themselves

2.5 Dynamic model

Another objective of this thesis work is to evaluate if the model presented in the previous chapters can describe the apparent mass response and, if not, to improve the model. Linear lumped parameter models of the apparent masses of human subjects in standing positions when exposed to vertical whole-body vibration have been developed yet.
The model presented until now does not consider the apparent mass, in the next pages are shown the results with the respect to apparent mass. In order to compute the apparent mass of the foot and ankle system, is necessary to pay more attention to the movement of the part of the foot that is in contact with the vibrating plate. Indeed, especially in that points are exchanged the forces between the vibrating plate and the foot. The model has 7 degrees of freedom (Figure 21 Figure 22) and they can be resumed in the vector x

$$x = [y_1, \quad y_2, \quad \vartheta_1, \quad \vartheta_2, \quad \vartheta_3, \quad \vartheta_4, \quad x_c]$$

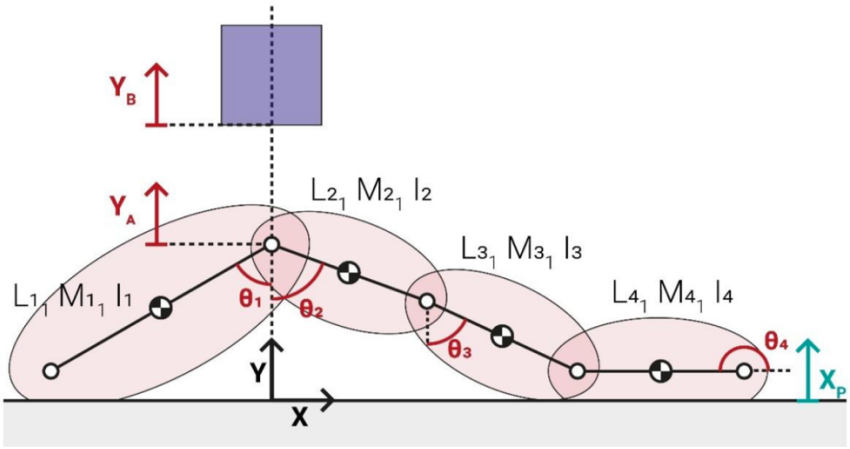

Figure 21 - 7 d.o.f. model: masses and length

Where x_c is the motion of the constraint, and the other variables are the degrees of freedom of the concentrated parameter system that are shown in Figure 21. Once computed the variable x at each frequency, by simple geometrical correlations is possible to find the movement of the contact points

$$y_1 = a - l_1 \cos\vartheta_1$$
$$y_3 = a - l_2 \cos\vartheta_2 - l_3 \cos\vartheta_3$$
$$y_4 = a - l_2 \cos\vartheta_2 - l_3 \cos\vartheta_3 - l_4 \sin\vartheta_4$$

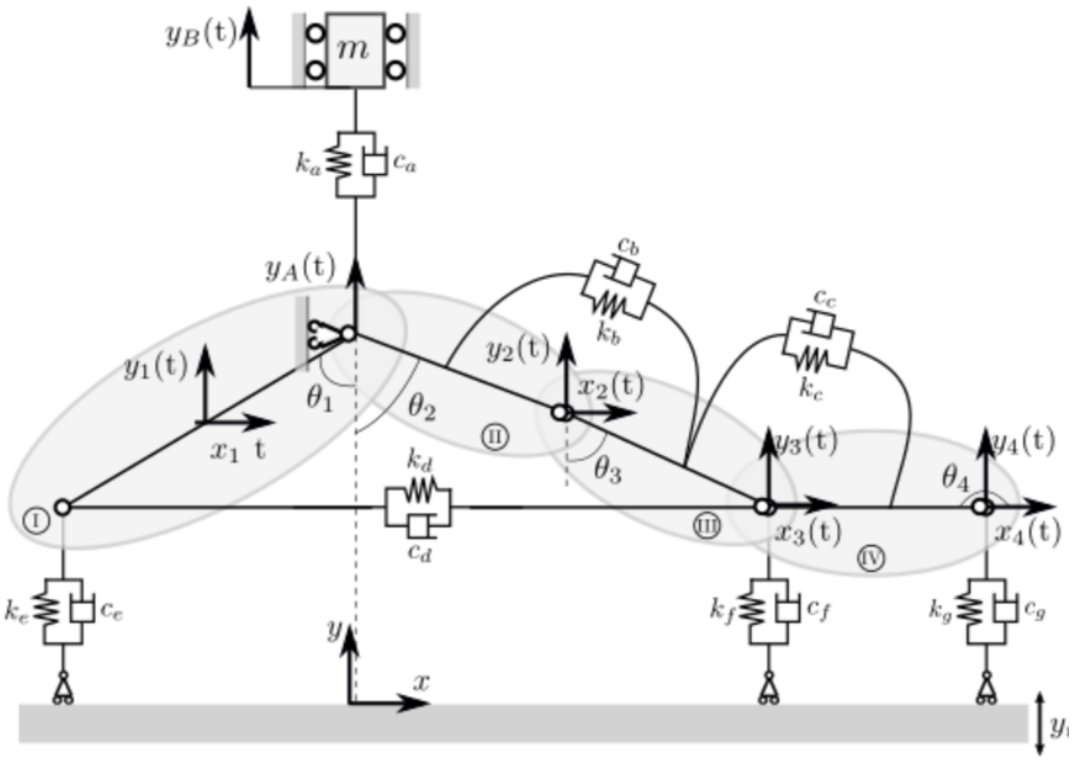

Figure 22 - 7 d.o.f. model: Degrees of freedom and modal parameters

Given this model, is possible to compute with numerical analysis F_1 F_2 F_3 that are the forces exchanged between the vibrating plate and the foot, therefore the total force F_{tot} is the sum of the three contact forces.

$$F_1 = (K_e + c_e J\omega) \cdot (y_1 - y_{in})$$
$$F_3 = (K_f + c_f J\omega) \cdot (y_3 - y_{in})$$
$$F_4 = (K_g + c_g J\omega) \cdot (y_4 - y_{in})$$

$$F_{tot} = F_1 + F_3 + F_4$$

Being the total force the product of mass and acceleration,

$$F = m\ddot{x}$$

The resulting normalized apparent mass is

$$m_{apparent} = \frac{F_{tot}}{\ddot{x}_c} = \frac{F_{tot}}{-\omega^2 x_c M}$$

As the optimization doesn't take in account the apparent mass the results are significantly different from the experimental data.

In Figure 23 is possible to compare different optimization results in terms of apparent mass. The purple line, represents the experimental data of [56], and is possible to note that the curve that optimize just the apparent mass (blue line) is the one that fits better experimental data. Instead the previous modal parameters, that were built just optimizing transmissibility (red line) are completely not able to fit apparent mass curve. Finally, yellow line is the one made by running optimization on both apparent mass and transmissibility is not able to give successful results: the apparent mass is increased tenfold on the resonant frequency.

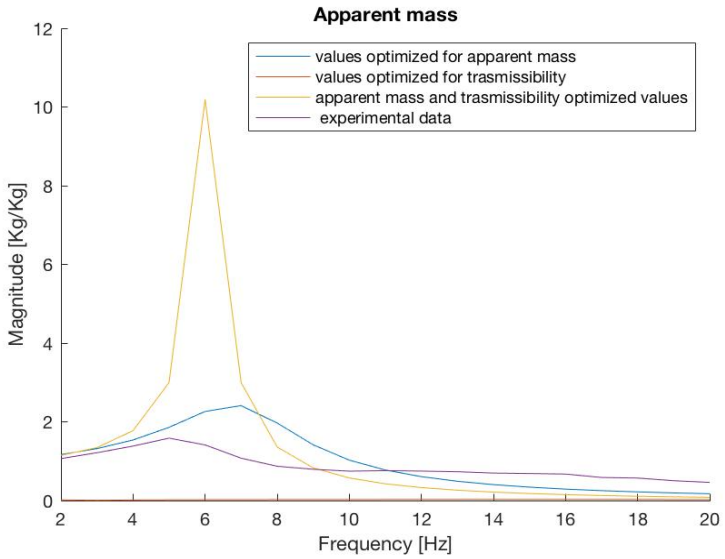

Figure 23 - Apparent mass: comparison between different optimizations

From Figure 24 instead, is possible to see what happens in terms of transmissibility. In this figure is possible to see the weakness of the single apparent mass optimization: the blue curve completely not fit the transmissibility plot. Also, the yellow line, the values obtained optimizing both apparent mass and transmissibility are not consistent.

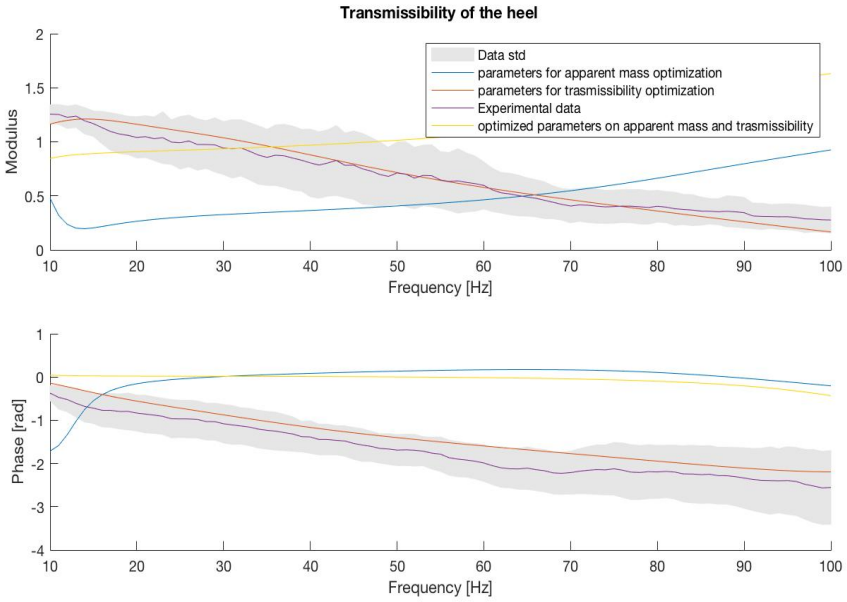

Figure 24 - Transmissibility: comparison between different optimizations

Comparing Figure 23 and Figure 24 is possible to realize that the model presented until now and in [53] is not able to fit both apparent mass and transmissibility, even if changing the parameters in a way that tries to optimize both.

2.6 A new multi-objective model with eight degrees of freedom

As mentioned before, the 7 d.o.f. model is not able to model both apparent mass and transmissibility response.

Matsumoto and Griffin studied different mathematical models for the apparent masses of standing subjects exposed to vertical whole-body vibration [76]. They evaluated the differences between different lumped parameters models of the foot. In order to assist practical applications [76] considered simple linear lumped parameter models with a particular attention to apparent mass. Their intention was not to model the internal movements of the body responsible for the observed characteristics of the apparent mass, such models are much more complex than is necessary for predicting the driving-point apparent mass of the human body. In [76] Matsumoto and Griffin developed mathematical models of the vertical apparent mass of the seated human body. They previously reported the optimum parameters of four models (two single-degree-of-freedom models and two two-degree-of-freedom models) are derived from the mean measured apparent masses of 60 subjects (24 men, 24 women, 12 children). The best fits were obtained by fitting the phase data with single-degree-of-freedom and two-degree-of-freedom models having rigid support structures. For these two models, curve fitting was performed on each of the 60 subjects (so as to obtain optimum model parameters for each subject), for the averages of each of the three groups of subjects, and for the entire group of subjects.

The use of a two-degree-of-freedom model provided a better fit to the phase of the apparent mass at frequencies greater than about 8 Hz and an improved fit to the modulus of the apparent mass at frequencies around 5 Hz. It is concluded that the two-degree-of-freedom model provides an apparent mass similar to that of the human body. [54] [77].

2.6.1 Equation of motion

Matsumoto and Griffin [76] evaluated the difference between different kind of models. They showed that a model with two d. o. f. fitted experimental data better than the single d. o. f. models.
The two degrees of freedom model with a massless structure and two mass-spring-damper systems in series (Model 2a) showed a better agreement with experimental data than those with support having a mass, especially in the range between 10 and 20 Hz.

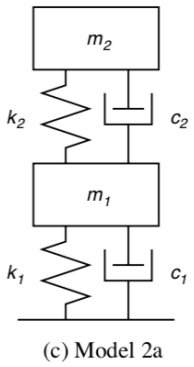

Figure 25 - Matsumoto and Griffin [61] model 2a of the FAS that optimize apparent mass

With this model the apparent mass is computed by the following formula

$$M_{2a}(i\omega) = \frac{(ic_1\omega + k_1)\{m_1(-m_2\omega^2 + ic_2\omega + k_2) + m_2(ic_2\omega + k_2)\}}{\{-m_1\omega^2 + i(c_1 + c_2)\omega + (k_1 + k_2)\}(-m_2\omega^2 + ic_2\omega + k_2) - (ic_2\omega + k_2)^2}$$

The parameter identification is made minimizing the cost function:

$$err = \sum |M_m(n\Delta f) - M_c(n\Delta f)|^2$$

Where $M_m$is the measured apparent mass using complex numbers, M_c is the calculated apparent mass using complex numbers and Δf is the frequency resolution of the measured data (0,25 Hz). The results obtained from Matsumoto and Griffith are shown in Figure 26: the analytical apparent mass curve (the dotted line) follows the experimental data (black line) almost perfectly.

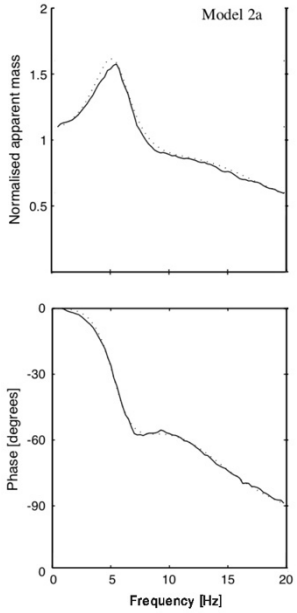

Figure 26 - Mathematical model 2a of Matsumoto and Griffin [76] results in terms of apparent mass

The new model in Figure 27 takes in consideration the necessity of a two mass-spring-damper system on the ankle in order to narrowly model the apparent mass. Therefore, the mass of 35kg in the previous model [53] is substituted with a two mass-spring-damper system with the parameters in
Table 8 [76].

Stiffness $[^{N}/_{m \cdot kg}]$		Damping $[^{Ns}/_{m \cdot kg}]$		Mass $[^{kg}/_{kg}]$	
k_1	k_2	c_1	c_2	m_1	m_2
4390	553	37,1	11,8	0,574	0,394

Table 8 - Optimized model parameters of model 2a, for the mean normalized apparent masses of 12 subjects in a normal standing posture

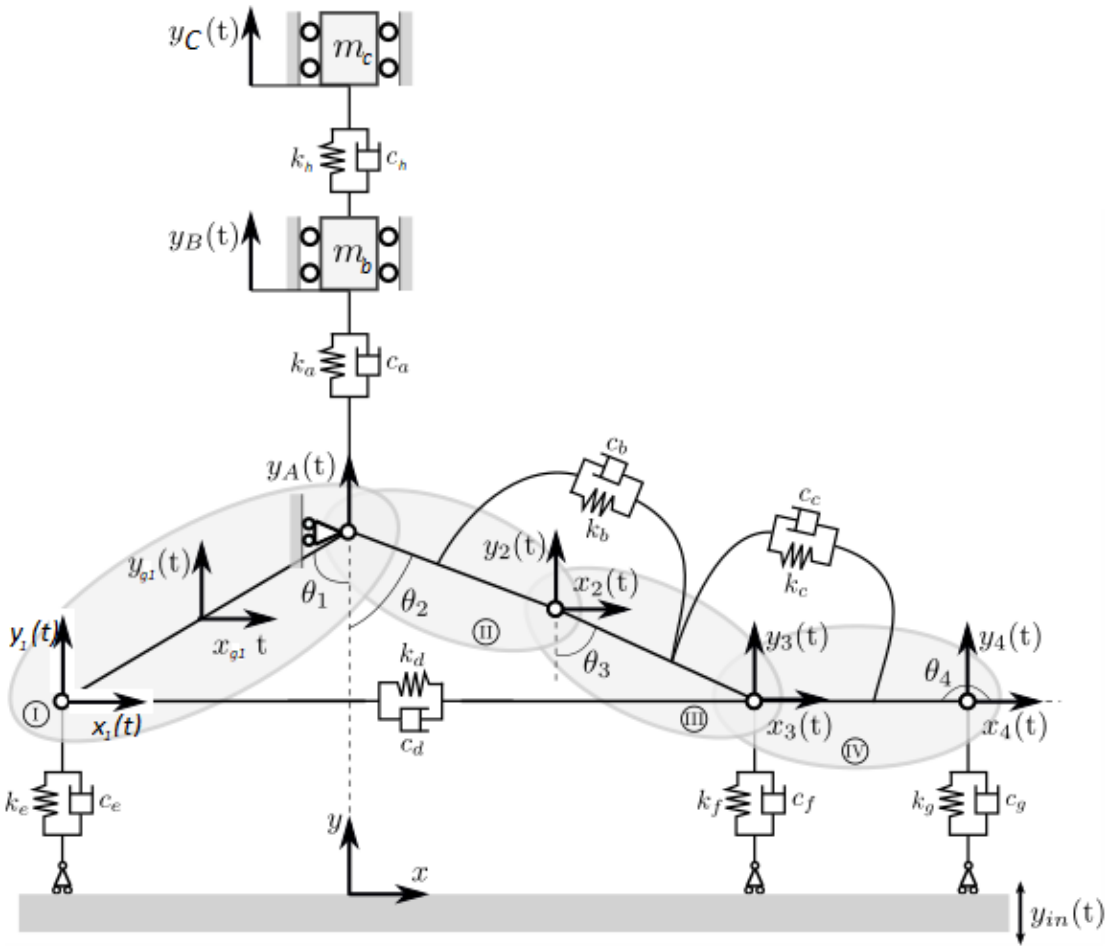

Figure 27 - New 8 d. o. f. model for transmissibility and apparent mass modelling

The model in Figure 27 is therefore made by the union between two mayor studies: [53] for the kinematic behaviour and [76] for the dynamic one. The resulting model have one more d.o.f. with the respect of the one in [53], so it has got a new equation of motion.
In particular the vector containing all the degrees of freedom is

$$x = \begin{bmatrix} y_A \\ y_B \\ y_C \\ \vartheta_1 \\ \vartheta_2 \\ \vartheta_3 \\ \vartheta_4 \\ x_c \end{bmatrix}$$

The cinematic bonds are resumed in Table 9 the positions of centre of mass are in Table 10.

Point 1	$x_{p1} = 0$	$y_{p1} = y_B$
Point 2	$x_{p2} = L_2 \sin\vartheta_2$	$y_{p2} = y_A - L_2 \cos\vartheta_2$
Point C	$x_{pC} = 0$	$y_{pC} = y_C$
Point 3	$x_{p3} = L_2 \sin\vartheta_2 + L_3 \sin\vartheta_3$	$y_{p3} = y_A - L_2 \cos\vartheta_2 - L_3 \cos\vartheta_3$
Point 4	$x_{p4} = -L_1 \sin\vartheta_1$	$y_{p4} = y_A - L_1 \cos\vartheta_1$
Point 5	$x_{p5} = L_2 \sin\vartheta_2 + L_3 \sin\vartheta_3 + L_4 \cos\vartheta_4$	$y_{p5} = y_A - L_2 \cos\vartheta_2 - L_3 \cos\vartheta_3 + L_4 \sin\vartheta_4$
Point 6	$x_{p6} = 0$	$y_{p6} = y_A$

Table 9 - Cinematic bonds of the 8 d. o. f. model

Point G1	$x_{G1} = -\frac{L_1}{2\sin\vartheta_1}$	$y_{G1} = y_A - \frac{L_1}{2\cos\vartheta_1}$
Point G2	$x_{G2} = \frac{L_2}{2\sin\vartheta_2}$	$y_{G2} = y_A - \frac{L_2}{2\cos\vartheta_2}$
Point G3	$x_{G3} = L_2 \sin\vartheta_2 + \frac{L_3}{2\sin\vartheta_3}$	$y_{G3} = y_A - L_2 \cos\vartheta_2 - \frac{L_3}{2\cos\vartheta_3}$

Table 10 - Position of centre of mass in the 8 d. o. f. model

With the Lagrange equation in matrix form, the linearized mass matrix is:

$$M_f = \begin{bmatrix} m_B & 0 & 0 & 0 & 0 & 0 & 0 & 0 & 0 & 0 & 0 & 0 & 0 & 0 & 0 & 0 \\ 0 & m_B & 0 & 0 & 0 & 0 & 0 & 0 & 0 & 0 & 0 & 0 & 0 & 0 & 0 & 0 \\ 0 & 0 & m_C & 0 & 0 & 0 & 0 & 0 & 0 & 0 & 0 & 0 & 0 & 0 & 0 & 0 \\ 0 & 0 & 0 & m_C & 0 & 0 & 0 & 0 & 0 & 0 & 0 & 0 & 0 & 0 & 0 & 0 \\ 0 & 0 & 0 & 0 & m_1 & 0 & 0 & 0 & 0 & 0 & 0 & 0 & 0 & 0 & 0 & 0 \\ 0 & 0 & 0 & 0 & 0 & m_1 & 0 & 0 & 0 & 0 & 0 & 0 & 0 & 0 & 0 & 0 \\ 0 & 0 & 0 & 0 & 0 & 0 & J_1 & 0 & 0 & 0 & 0 & 0 & 0 & 0 & 0 & 0 \\ 0 & 0 & 0 & 0 & 0 & 0 & 0 & m_2 & 0 & 0 & 0 & 0 & 0 & 0 & 0 & 0 \\ 0 & 0 & 0 & 0 & 0 & 0 & 0 & 0 & m_2 & 0 & 0 & 0 & 0 & 0 & 0 & 0 \\ 0 & 0 & 0 & 0 & 0 & 0 & 0 & 0 & 0 & J_2 & 0 & 0 & 0 & 0 & 0 & 0 \\ 0 & 0 & 0 & 0 & 0 & 0 & 0 & 0 & 0 & 0 & m_3 & 0 & 0 & 0 & 0 & 0 \\ 0 & 0 & 0 & 0 & 0 & 0 & 0 & 0 & 0 & 0 & 0 & m_3 & 0 & 0 & 0 & 0 \\ 0 & 0 & 0 & 0 & 0 & 0 & 0 & 0 & 0 & 0 & 0 & 0 & J_3 & 0 & 0 & 0 \\ 0 & 0 & 0 & 0 & 0 & 0 & 0 & 0 & 0 & 0 & 0 & 0 & 0 & m_4 & 0 & 0 \\ 0 & 0 & 0 & 0 & 0 & 0 & 0 & 0 & 0 & 0 & 0 & 0 & 0 & 0 & m_4 & 0 \\ 0 & 0 & 0 & 0 & 0 & 0 & 0 & 0 & 0 & 0 & 0 & 0 & 0 & 0 & 0 & J_4 \end{bmatrix} \quad Jc = \begin{bmatrix} dx_{p1} \\ dy_{p1} \\ dx_{pC} \\ dy_{pC} \\ dx_{G1} \\ dy_{G1} \\ J\vartheta_1 \\ dx_{G2} \\ dy_{G2} \\ J\vartheta_2 \\ dx_{G3} \\ dy_{G3} \\ J\vartheta_3 \\ dx_{G4} \\ dy_{G4} \\ J\vartheta_4 \end{bmatrix}$$

$$M = {J_C}^T \cdot m_f \cdot J_C$$

Matrix M has been linearized around the initial condition for each dof, using the Taylor series. The elements with order higher than one have been neglected. The same linearization has been applied to damping and stiffness matrices.

Following the damping matrix:

$$C_f = \begin{bmatrix} c_D & 0 & 0 & 0 & 0 & 0 & 0 & 0 \\ 0 & c_B & 0 & 0 & 0 & 0 & 0 & 0 \\ 0 & 0 & c_C & 0 & 0 & 0 & 0 & 0 \\ 0 & 0 & 0 & c_A & 0 & 0 & 0 & 0 \\ 0 & 0 & 0 & 0 & c_E & 0 & 0 & 0 \\ 0 & 0 & 0 & 0 & 0 & c_F & 0 & 0 \\ 0 & 0 & 0 & 0 & 0 & 0 & c_g & 0 \\ 0 & 0 & 0 & 0 & 0 & 0 & 0 & c_H \end{bmatrix} \qquad \Delta_L = \begin{bmatrix} d\Delta_{L\_D} \\ d\Delta_{L\_B} \\ d\Delta_{L\_C} \\ d\Delta_{L\_A} \\ d\Delta_{L\_E} \\ d\Delta_{L\_F} \\ d\Delta_{L\_G} \\ d\Delta_{L\_H} \end{bmatrix}$$

$$C = J\Delta_L{}^T \cdot K_f \cdot J\Delta_L$$

And finally, the stiffness matrix:

$$K_f = \begin{bmatrix} k_D & 0 & 0 & 0 & 0 & 0 & 0 & 0 \\ 0 & k_B & 0 & 0 & 0 & 0 & 0 & 0 \\ 0 & 0 & k_C & 0 & 0 & 0 & 0 & 0 \\ 0 & 0 & 0 & k_A & 0 & 0 & 0 & 0 \\ 0 & 0 & 0 & 0 & k_E & 0 & 0 & 0 \\ 0 & 0 & 0 & 0 & 0 & k_F & 0 & 0 \\ 0 & 0 & 0 & 0 & 0 & 0 & k_g & 0 \\ 0 & 0 & 0 & 0 & 0 & 0 & 0 & k_H \end{bmatrix} \qquad J\Delta_L = \begin{bmatrix} d\Delta_{L\_D} \\ d\Delta_{L\_B} \\ d\Delta_{L\_C} \\ d\Delta_{L\_A} \\ d\Delta_{L\_E} \\ d\Delta_{L\_F} \\ d\Delta_{L\_G} \\ d\Delta_{L\_H} \end{bmatrix}$$

$$K = J\Delta_L{}^T \cdot K_f \cdot J\Delta_L$$

Then, matrixes are divided it their components free and constrained:

$$M = \begin{bmatrix} M_{FF} & M_{FC} \\ M_{CF} & M_{CC} \end{bmatrix} \qquad C = \begin{bmatrix} C_{FF} & C_{FC} \\ C_{CF} & C_{CC} \end{bmatrix} \qquad K = \begin{bmatrix} K_{FF} & K_{FC} \\ K_{CF} & K_{CC} \end{bmatrix}$$

The equation of motion is:

$$\begin{bmatrix} M_{FF} & M_{FC} \\ M_{CF} & M_{CC} \end{bmatrix} \begin{bmatrix} \ddot{x_F} \\ \ddot{x_C} \end{bmatrix} + \begin{bmatrix} C_{FF} & C_{FC} \\ C_{CF} & C_{CC} \end{bmatrix} \begin{bmatrix} \dot{x_F} \\ \dot{x_C} \end{bmatrix} + \begin{bmatrix} K_{FF} & K_{FC} \\ K_{CF} & K_{CC} \end{bmatrix} \begin{bmatrix} x_F \\ x_C \end{bmatrix} = \begin{bmatrix} 0 \\ F_C \end{bmatrix}$$

$$\left(- \begin{bmatrix} M_{FF} & M_{FC} \\ M_{CF} & M_{CC} \end{bmatrix} j\omega^2 + \begin{bmatrix} C_{FF} & C_{FC} \\ C_{CF} & C_{CC} \end{bmatrix} j\omega + \begin{bmatrix} K_{FF} & K_{FC} \\ K_{CF} & K_{CC} \end{bmatrix} \right) \begin{bmatrix} x_F \\ x_C \end{bmatrix} = \begin{bmatrix} 0 \\ F_C \end{bmatrix}$$

$$\begin{bmatrix} x_F \\ x_C \end{bmatrix} = \left(- \begin{bmatrix} M_{FF} & M_{FC} \\ M_{CF} & M_{CC} \end{bmatrix} j\omega^2 + \begin{bmatrix} C_{FF} & C_{FC} \\ C_{CF} & C_{CC} \end{bmatrix} j\omega + \begin{bmatrix} K_{FF} & K_{FC} \\ K_{CF} & K_{CC} \end{bmatrix} \right)^{-1} \begin{bmatrix} 0 \\ F_C \end{bmatrix}$$

2.6.1 Single subject optimization

As mentioned before, the previous knowledge about the topic of FTV was made by a group of researchers of Politecnico di Milano [53] on a group of 21 subjects, computing the average transmissibility to vibration of the FAS of all the subjects. The estimation of $K_{a\ldots g}$ and $C_{a\ldots g}$ was performed with the same procedure adopted in [73] based on a nonlinear curve-fitting in least-squares sense (lsqcurvefit function implemented in Matlab R2018a software) with respect to the experimentally measured transmissibility functions, averaged in all the subjects. Researchers averaged each transmissibility curve obtained from experimental activities in order to neglect all the person-to-person variability.

The aim of this chapter is to compare the previous results with a more specific analysis, made on each single subject to evaluate if using the average mass of the body of 70kg together with the averaged foot response, can be considered more an approximation than an error cancellation. The great advantage of single subject optimization is the fact that is possible to use right mass of the subject instead of the averaged one, moreover, is possible to optimize the response of the specific subject. In this way, instead of computing the modal parameters by fitting the average and analytical response, is possible to fit the response of each single subject with the analytical response, with in addition the right mass of the subject (and not the averaged one). The results are in chapter 3.2.

2.7 Insoles

As already mentioned, if vibration is transmitted through the foot it can lead to a series of injuries like vibration white feet resulting in blanching of the toes and disruption of blood circulation. Until now, there is a lack of studies identifying industrial boot characteristics effective at attenuating the vibration exposures but materials capable of attenuating FTV to the toes in the 30-40 Hz range are anyway needed. In this chapter the aim is to evaluate vibration transmissibility to the foot when standing on four different outsole and three different insole materials [78]. A group of researchers of Politecnico di Milano made an experimental test about this topic [78]. Twenty-one participants randomly stood on different materials placed on the vibrating plate (Figure 28).

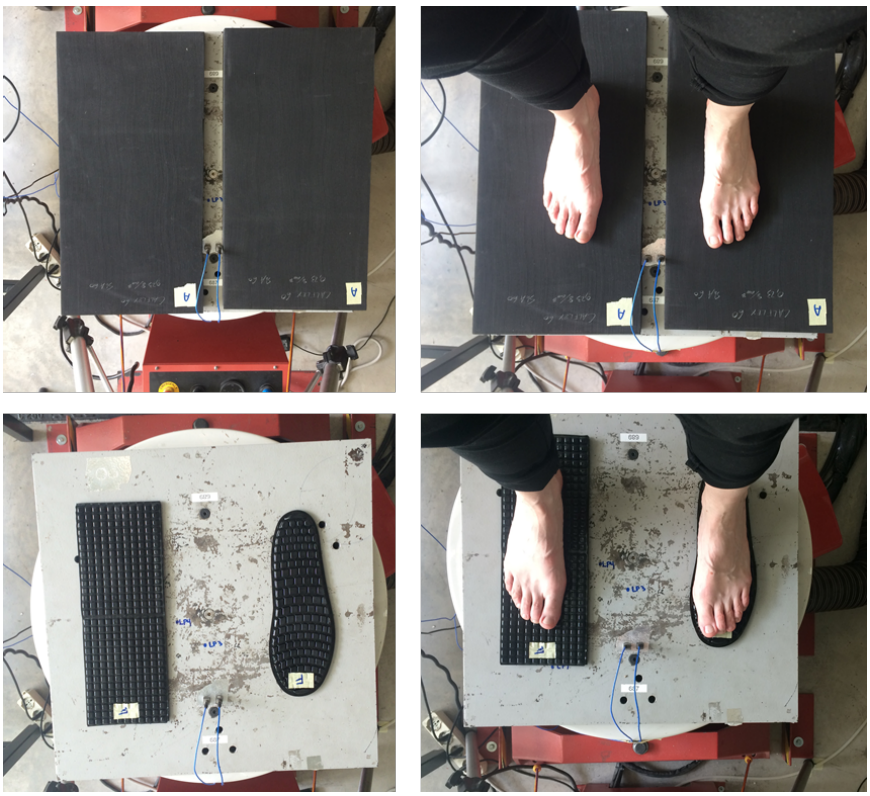

Figure 28 - Example outsole material evaluated (top left) and participant standing on the shaker and outsole material (top right). An example of insole material evaluated (bottom left) and participant standing on the insole material (bottom right) is also shown.

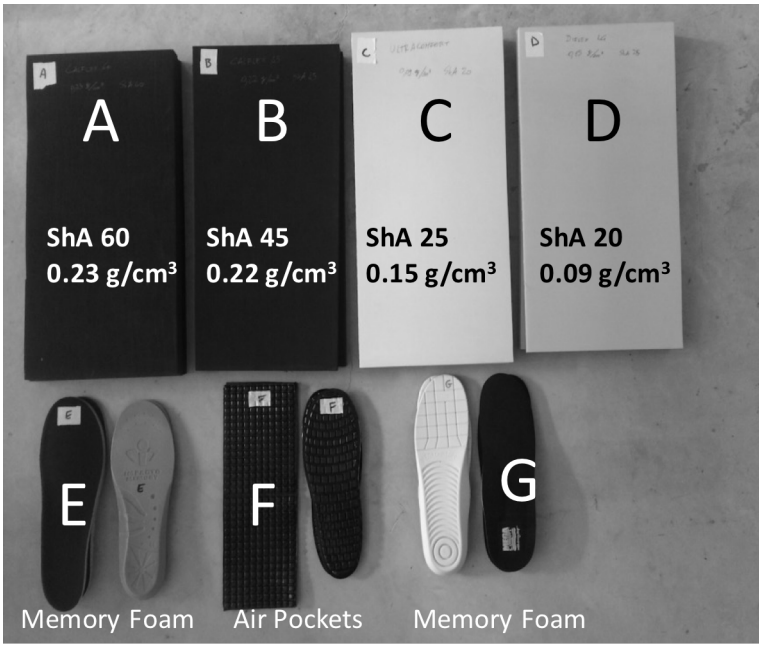

Figure 29 - Materials and insoles that were used in the tests described in this paper. Upper row: midsole materials; lower row: insoles.

The different materials interposed between the feet and the vibrating plate are shown in Figure 29 along with a description of their characteristics. They were labelled with letters from A to G: the first four were foams typically used for manufacturing shoe midsole (Shore hardness from 20 to 60, density from 0.09 to 0.23 g/cm^3), while two of the insoles were commercially available and one was a proto-type (F). The material was interposed between both feet when the participants were standing on the vibrating platform. In that research not only was measured the transmissibility through the materials in 10 locations of the foot across the frequency range 10-200Hz but also were used questionnaires to evaluate the comfort of each material. Results of tests described in that paper evidenced that the subjective evaluation of comfort is not adequate to assess the efficiency of working shoes in reducing the vibration at the toes. Since most of the tested materials worsen the toes vibration exposure with respect to the barefoot conditions in the frequency region (90-150Hz) where the toes resonance occur, it is important to develop an insole or a shoe able to reduce vibration in this range of frequency. In order to do this, a model of the FAS that includes also an insole can be useful.

2.7.1 FAS model with insole

Until now, the bio-mechanical model presented, was neglecting the presence of insoles. Once defined the model of the FAS, is possible to add the insole to the model, with the application under each contact point between foot and vibrating plate of a Kelvin-Voigt system. In Figure 30 is possible to see that the new kelvin-Voigt systems under the FAS ($k_1c_1k_2c_2k_3c_3$), are positioned in series with the respect to the foot sole systems ($k_ec_ek_fc_fk_gc_g$).

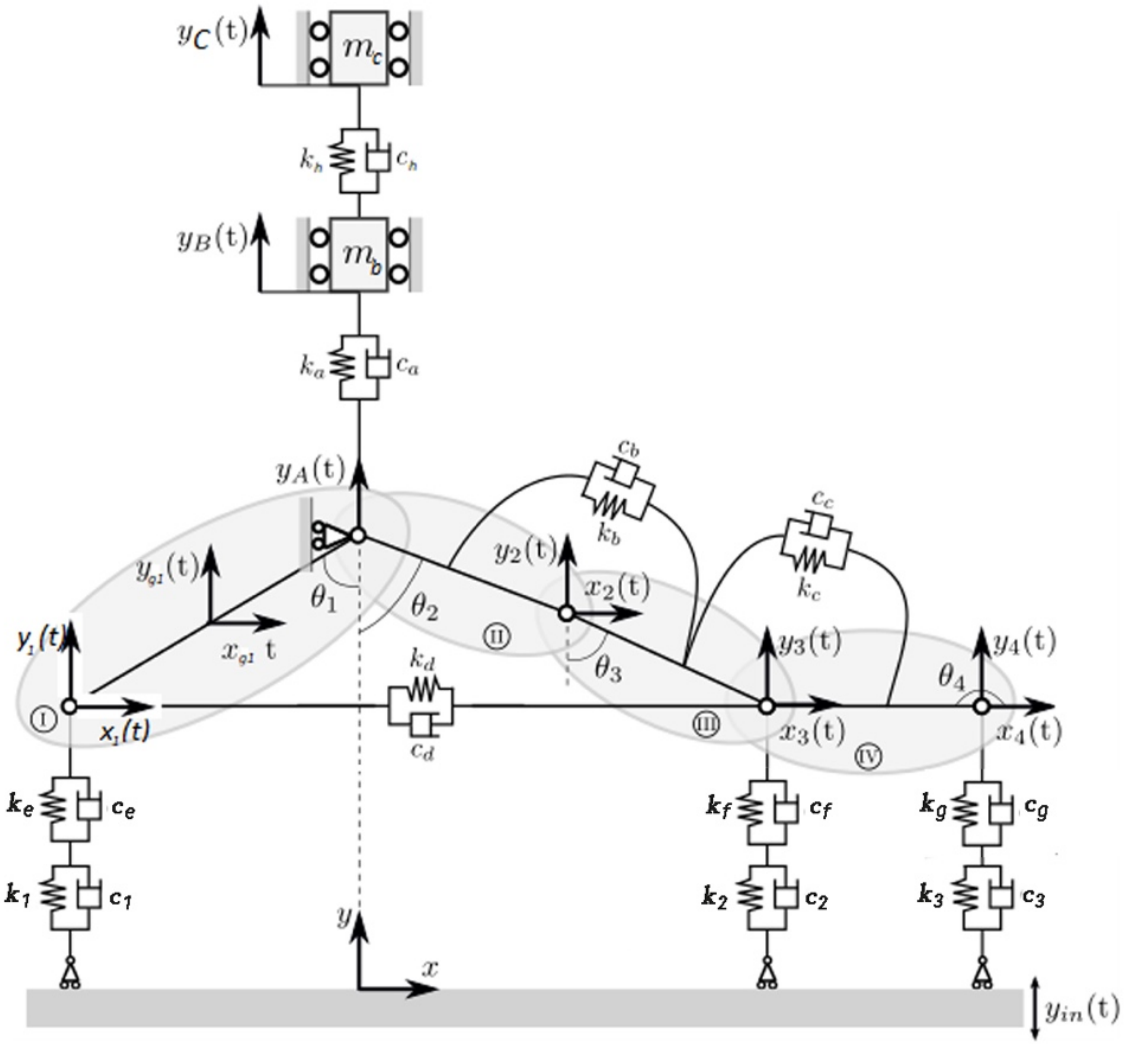

Figure 30 - Model of the FAS including an insole

With this kind of modification of the model is not necessary to insert any new degree of freedom, this because is possible to write the equivalent stiffness and damping (like shown in Figure 31) of two stiffnesses and damping placed in series with the following formula.

$$\frac{1}{k_{eq}} = \frac{1}{k_i} + \frac{1}{k_n}$$
$$\frac{1}{c_{eq}} = \frac{1}{c_i} + \frac{1}{c_n}$$

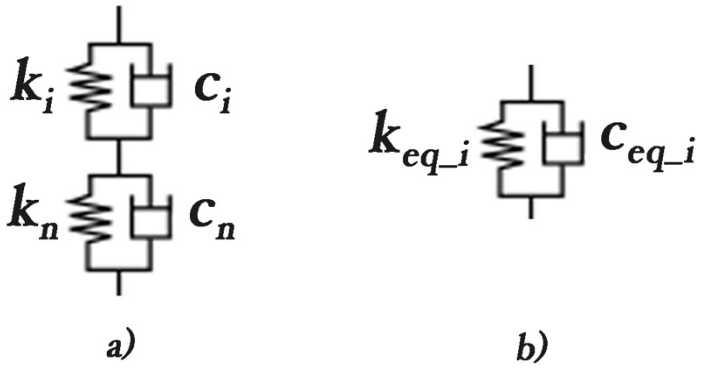

Figure 31 - equivalent stiffness and damping of two Kelvin-Voigt models in series

Where the subscript i indicates the equivalent dynamic characteristic of soft tissue and fat pad of foot sole, and the subscript n instead represents the modal parameters of the rubber insole. The equivalent parameters are computed through a linear multi objective optimization that fits both the curve of apparent mass (neutral position, barefoot) and average transmissibility with insole. The only parameters that are free to change during the optimization are the ones that change between the model with and without the insole. Therefore, they are the one that represents the equivalent stiffness/damping of the system foot pad-insole ($k_{eq1}c_{eq1}k_{eq2}c_{eq2}k_{eq3}c_{eq3}$). With the resulting dynamic characteristics is possible to find the damping and stiffness coefficient of the insole when compressed by the subject's weight and with a vertical vibration input. This is made running the model as it was, and computing the insole parameters through the following inverse formula:

$$\frac{1}{k_n} = \frac{1}{k_{eq}} - \frac{1}{k_i} = \frac{k_i - k_{eq}}{k_{eq}k_i}$$

$$k_n = \frac{k_{eq}k_i}{k_i - k_{eq}} \qquad c_n = \frac{c_{eq}c_i}{c_i - c_{eq}}$$

The first trial gave results with no physical meaning, in particular we obtained negative stiffness and damping coefficients, with some parameters that didn't change as well when passing from foot pad and equivalent foot-pad/insole, therefore creating values of stiffness and damping of the insole very high with respect to what they are in reality. In order to get some reliable output values, the increase of values is blocked, in this way values can only decrease like the model series of springs and dampers impose.

Then with the model will be possible to compute the stiffness and damping values that would reduce vibration amplitude.

3 Results

All the results of the model threated in the previous chapters are shown in the following pages.

3.1 Results of the 8 d.o.f. multi objective optimization model

Figure 32 compares the results of the 7 degrees of freedom model and the 8 d.o.f. model in terms of apparent mass. The 8 d.o.f. model follows evidently better the apparent mass path with the respect to the 7 d.o.f one. Indeed, the average least square error ε of the 7 d.o.f. model is three times greater than the one with 8 d.o.f.

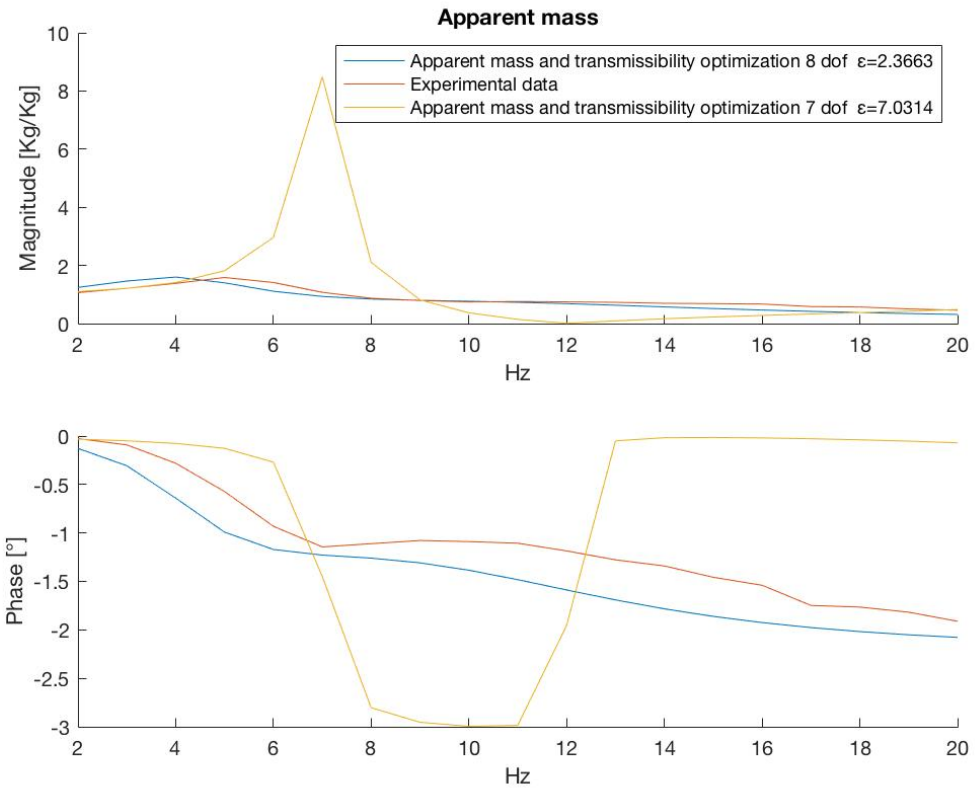

Figure 32 - Apparent mass results with 8 d. o. f.

Moreover, in Figure 33 are shown the transmissibility results with both apparent mass and transmissibility optimization computed by the 8 d.o.f. model, compared to experimental averaged transmissibility.

Since the least square error is significantly higher in the 8 d.o.f. model, is possible to understand that the new model presented in this chapter is definitely more reliable in terms

of both transmissibility and apparent mass. As can be seen in Figure 33 the model creates some problem in the transmissibility of the heel and ankle at low frequencies, even if evaluating the whole frequency range, the error of the curves is considerable quite small. In Table 11 are listed the least square errors that can help in the comparison between the two models with the respect to the 7 and 8 d.o.f. model. In particular from Table 11 is evident that both in general and in each single curve except the tip toes transmissibility, the 8 d.o.f. model is more capable to describe the kinematic and dynamic behaviour of the FAS subject to vertical vibration in neutral position.

Least square error ε							
	Heel	Forefoot	Tip toes	Midfoot	Ankle	Apparent mass	Average
7 d.o.f. model	2,93	1,94	0,51	2,32	2,44	7,03	2,86
8 d.o.f. model	0,17	1,09	0,95	0,95	0,23	2,37	0,96

Table 11 - Least square errors of the 8 d.o.f. model compared to 7 d.o.f. model

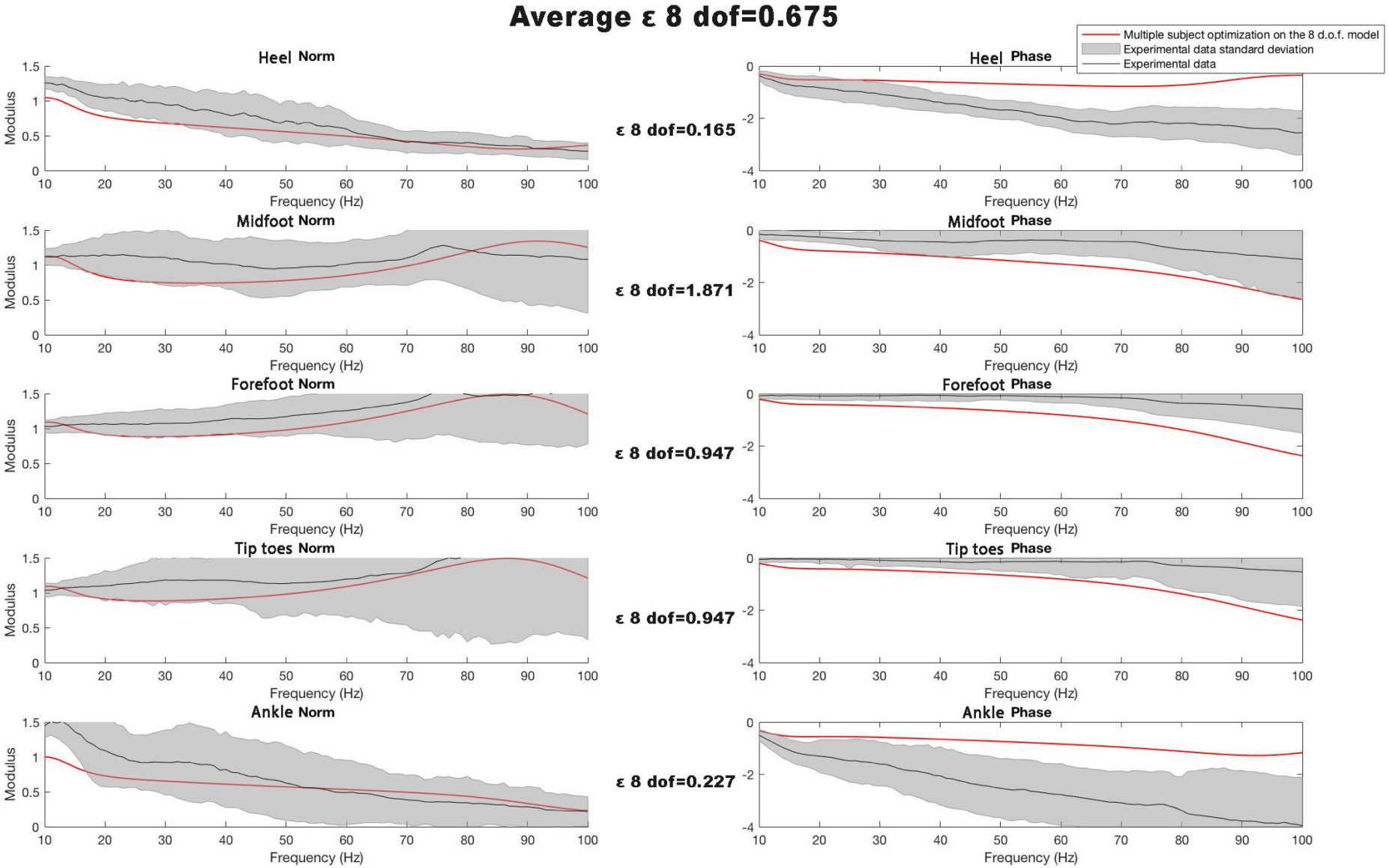

Figure 33 - Transmissibility results with 8 d.o.f.

The modal parameters are in Table 12, the values of Ka, Ca, Kh and Ch are the ones computed by Matsumoto and Griffin [76] for the model 2a, the other parameters are optimized for both transmissibility and apparent mass.

	7 d.o.f.	8 d.o.f.	Variation %	Description
$K_a \left[N/m\right]$	57000	153700	170%	stiffness of the ankle/body joint
$K_b \left[N/m\right]$	212,0	212,0	0%	stiffness of the segments II/III joint
$K_c \left[N/m\right]$	32,00	2,00	-94%	stiffness of the segments III/IV joint
$K_d \left[N/m\right]$	10000	10000	0%	stiffness of the plantar aponeurosis
$K_e \left[N/m\right]$	400000	294000	-26%	stiffness of the rearfoot sole
$K_f \left[N/m\right]$	546300	111500	-80%	stiffness of the forefoot sole
$K_g \left[N/m\right]$	57000	134	-100%	stiffness of the toes sole
$K_h \left[N/m\right]$	-	1,60	-	stiffness of the ankle-body joint
$C_a \left[N/m \cdot s\right]$	11280	11280	0%	damping of the ankle/body joint
$C_b \left[N/m \cdot s\right]$	0,05	0,24	380%	damping of the segments II/III joint
$C_c \left[N/m \cdot s\right]$	2144	19360	803%	damping of the segments III/IV joint
$C_d \left[N/m \cdot s\right]$	0,05	1299	2596900%	damping of the plantar aponeurosis
$C_e \left[N/m \cdot s\right]$	284	284	0%	damping of the rearfoot sole
$C_f \left[N/m \cdot s\right]$	0	0	0%	damping of the forefoot sole
$C_g \left[N/m \cdot s\right]$	30,98	30,98	0%	damping of the toes sole
$C_h \left[N/m\right]$	-	413,0	-	Damping of the ankle-body joint

Table 12 - Modal parameters of 7 d.o.f. model and 8 d.o.f. model

In general analysing Table 12, is possible to note that the introduction of a new d.o.f. in the model creates a series of great changes in the modal parameters, that have to adapt to the new condition. The most important variations from the two models are in the stiffness-damping between the foot and the vibrating plate. This can be related to the fact that apparent mass is function of the contact force between the foot and the vibrating plate.

3.2 Single subject optimization

This chapter shows the results of the dingle subject optimization, compared to the ones of the multiple subject shown in the previous paragraph. Computing through a multi objective optimization for transmissibility and apparent mass, the modal parameters of each subject is possible to obtain a matrix 21x16 parameters. Therefore 21 different models are obtained: one for each subject. Following, in Table 13 are listed the parameters computed by the multiple subject optimization (average response, average mass, mathematical 8 d.o.f. model) and the average-standard deviation of the modal parameters by the single subject optimization (single subject response, single subject mass, mathematical 8 d.o.f. model) for the neutral position.

	multiple subject optimization	Mean single subject optimization	Standard deviation single subject	**Description**
$K_a\ [N/m]$	153600	156000	30630	stiffness of the ankle/body joint
$K_b\ [N/m]$	212	106	0	stiffness of the segments II/III joint
$K_c\ [N/m]$	2,00	4,20	0,86	stiffness of the segments III/IV joint
$K_d\ [N/m]$	10000	23480	13760	stiffness of the plantar aponeurosis
$K_e\ [N/m]$	294000	125300	25670	stiffness of the rearfoot sole
$K_f\ [N/m]$	111500	77870	6029	stiffness of the forefoot sole
$K_g\ [N/m]$	134	602,5	402,7	stiffness of the toes sole
$K_h\ [N/m]$	1,60	19660	3859	stiffness of the ankle-body joint
$C_a\ [N/m \cdot s]$	11280	5613	119,1	damping of the ankle/body joint
$C_b\ [N/m \cdot s]$	0,24	0,35	0,10	damping of the segments II/III joint
$C_c\ [N/m \cdot s]$	19360	0,25	0,17	damping of the segments III/IV joint
$C_d\ [N/m \cdot s]$	1298	1319	258,9	damping of the plantar aponeurosis
$C_e\ [N/m \cdot s]$	284	116	45,43	damping of the rearfoot sole
$C_f\ [N/m \cdot s]$	0	0	0	damping of the forefoot sole
$C_g\ [N/m \cdot s]$	30,98	62	0,22	damping of the toes sole
$C_h\ [N/m \cdot s]$	413	419,5	82,34	Damping of the ankle-body joint

Table 13 - Comparison of modal parameters computed between the averaged response with average mass and the average parameters computed by single subject response on the multi objective cost function that optimize both transmissibility and apparent mass

The resulting analytical transmissibility functions shown in Figure 34 are computed by using the concentrated parameter model, using once the optimized parameters on the averaged response, and once the average of the modal parameters computed on the single subject response.
In black colour is possible to see the average transmissibility response, in order to evaluate if the model can perform a result similar to the reality. For this reason, is provided also a grey standard deviation curve.

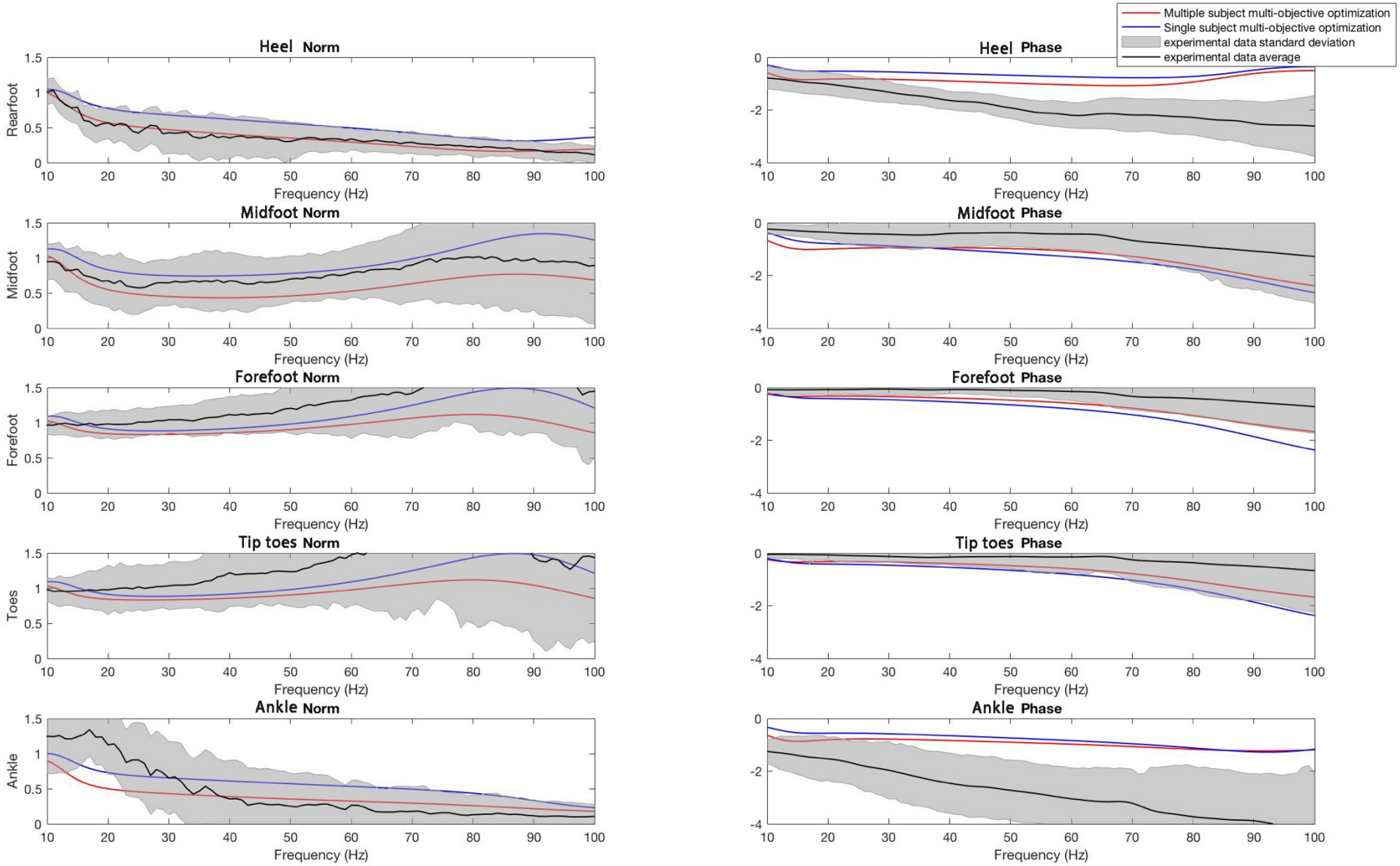

Figure 34 - analytical transmissibility functions computed with optimized parameters in comparison with averaged transmissibility response

Moreover, in Figure 35 are shown the different results in terms of apparent mass. As told before, the 7 d.o.f. model presented in the state of the art is not able to attend reliable results for apparent mass. In this case is possible to note that the results obtained with the single subject optimization are less accurate than the ones obtained with the multiple subject average. This is probably related to the fact that the apparent mass curve from experimental data is an averaged curve, computed on the apparent mass response of multiple subjects, and from the data that we have got is not possible to apply the single subject optimization also on the apparent mass curve.

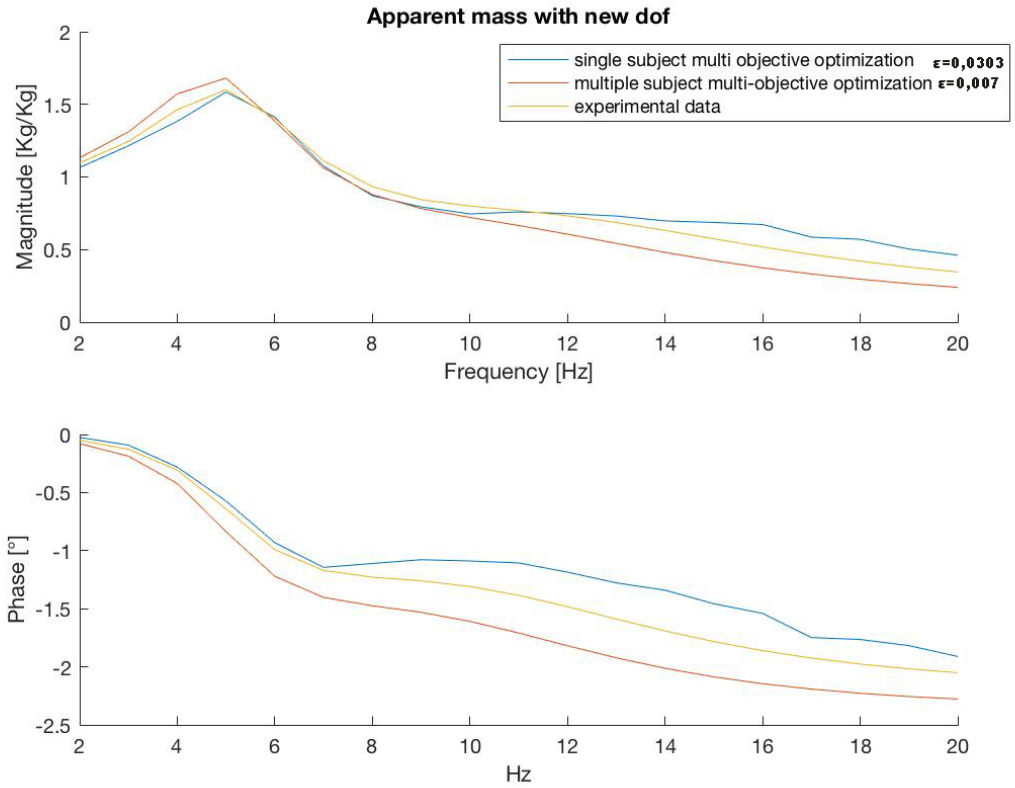

Figure 35 -analytical apparent mass functions computed with optimized parameters in comparison with averaged apparent mass from experimental data

In order to compare the results, is possible to compute the least square error of both the methods and the error if the multi objective optimization is run on the previous 7 d.o.f. model. The results are listed in Table 14.

Least square error ε							
	Heel	Forefoot	Tip toes	Midfoot	Ankle	Apparent mass	Average
single subject 8 d.o.f. model	0,060	0,102	0,227	0,227	0,068	0,030	0,119
multiple subject 8 d.o.f. model	0,011	0,301	0,453	0,453	0,017	0,007	0,207

Table 14 - Least square error comparison between the two-way computing the modal parameters

In the first row of Table 14 there are the least square errors computed using the method presented in this chapter, so averaging the parameters gotten from the optimization of each single subject. In the second row instead, there are the least square errors of the results with the method used in the state of the art, so making the optimization on averaged response and mass. Finally, in order to make a comparison, the third row is about the results of the state of the art FAS model with 7 d.o.f. used in the multi objective optimization that takes into consideration not only transmissibility but also apparent mass. As can be seen from the result, the second method is more performing not only for the apparent mass but also for the transmissibilities of heel. Anyway, the average least square error is significantly less in the single subject optimization. Therefore, is possible to say that even if both the analysis are reliable, the method that uses single subject optimization is able to perform a smaller least square error, it is so the most accurate.

3.3 Response of the model to other two body positions: leaning backward and leaning forward

In [53] Tarabini et al. studied the effect of the position of the body on the transmissibility response in order to understand if maintaining a particular position could attenuate the vibration transmitted to the body. The objective is to study how the geometry and stiffness/damping coefficients of the FAS model vary by varying the weight distribution.
In particular three different load distributions on the FAS have been considered:

- normal standing position
- backward position, with most of the weight loaded on the rearfoot
- forward position, with the forefoot most loaded

Since the experimental data are available for different positions of the human body, it is possible to repeat the modelling and optimization procedure on different position of the body with respect to the FAS system. The starting two-dimensional lumped parameter model is the one described before. Some slight changes have been implemented to reflect the different load distribution: the mass of the body is no more centred on the ankle but is shifted on the forefoot. The springs and dampers remain in the same positions. This change is made by a modification of the geometrical properties as the angle between foot bones, that are listed in Table 15.

COP Location	$\theta_1\ [Deg]$	$\theta_2\ [Deg]$	$\theta_3\ [Deg]$
Backward position	45	66	80
Neutral position	49	69	82
Forward position	52	74	85

Table 15 - Geometrical properties of the modelled foot with respect to the three investigated centre of pressure location (forward, neutral and backward)

In this chapter are shown the results of the application of apply the new 8 d.o.f. kinematic and dynamic model to these two positions in order to investigate if the 8 d.o.f. model created is able or not to perform a good mathematical model of the reality. In Table 16 are resumed the least square error averaged on all the transmissibility and apparent mass of the three methods of analysis and in the three positions. Looking at Table 16 is possible to see that in general, the errors of the leaning backward and forward positions are higher than the errors in the neutral position. This increase of the least square error can be related to two problems:

the apparent mass data availability and the position of the mass of the body. With respect to the apparent mass data availability we have to say that the apparent mass curve used for the optimization is the same curve for all neutral backward and forward position. This can be a good theme for future research.
Regarding the position of the mass, we have to say that in the considered model the position of the mass of the body is not able to be changed horizontally but only vertically, and this is a great constraint of the model that creates error when the position of the mass in the reality is changed. Indeed, in the model, even if in the forward and backward position model the mass is shifted forward or backward, it can slide just vertically and not inclined.
Form Table 16 is possible to note that the leaning backward position is not so well modelled with respect to the other two, in Figure 37 is possible to see the mayor error on the heel.
In general, the model works better in the neutral position.

Average least square error ε			
	Neutral position	Leaning forward	Leaning backward
single subject 8 d.o.f. model	0,119	0,136	0,318
multiple subject 8 d.o.f. model	0,207	0,257	0,244

Table 16 - Mean least square error for neutral-forward-backward position

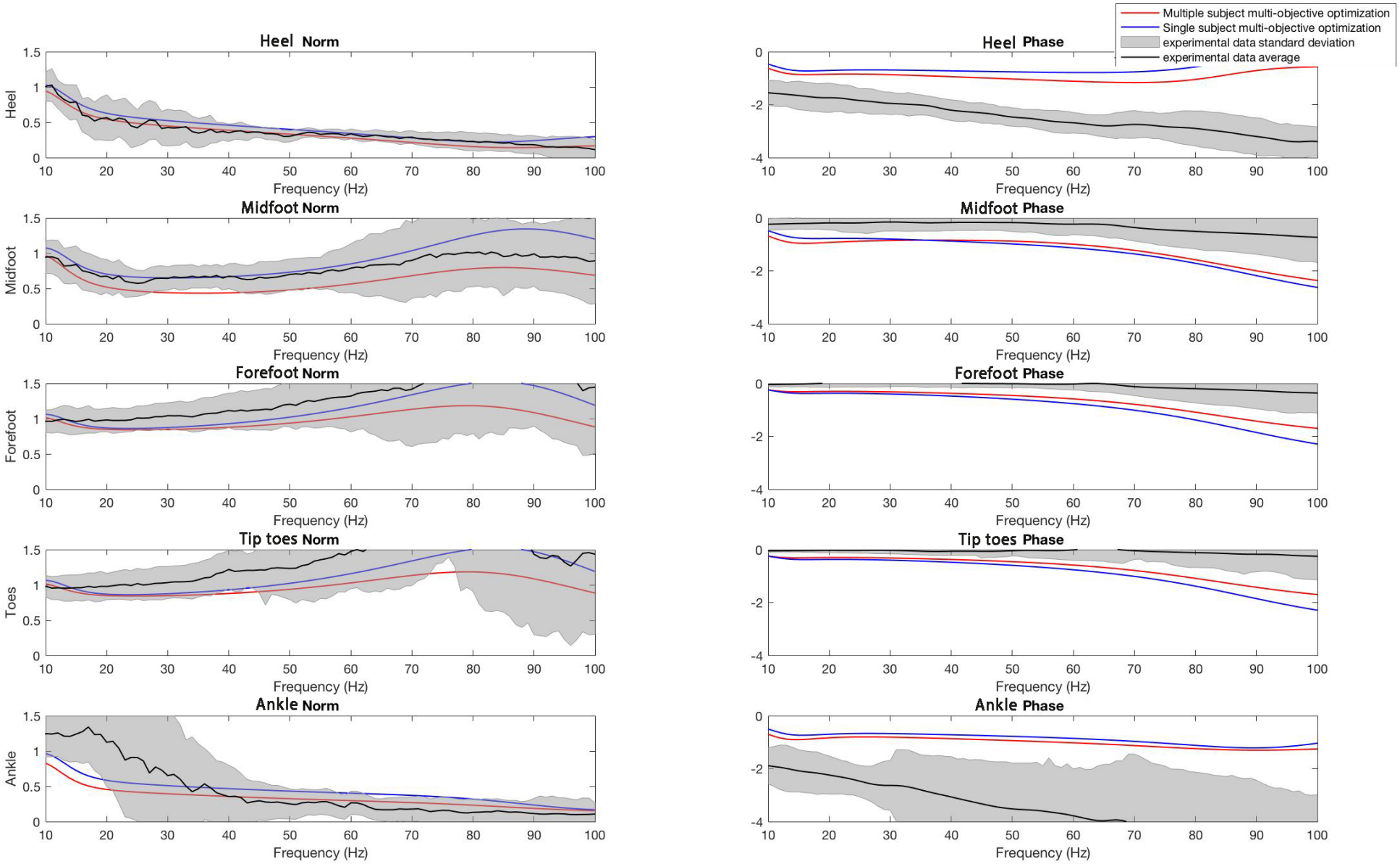

Figure 36 - Analytical transmissibility function of the FAS in leaning forward position of the body

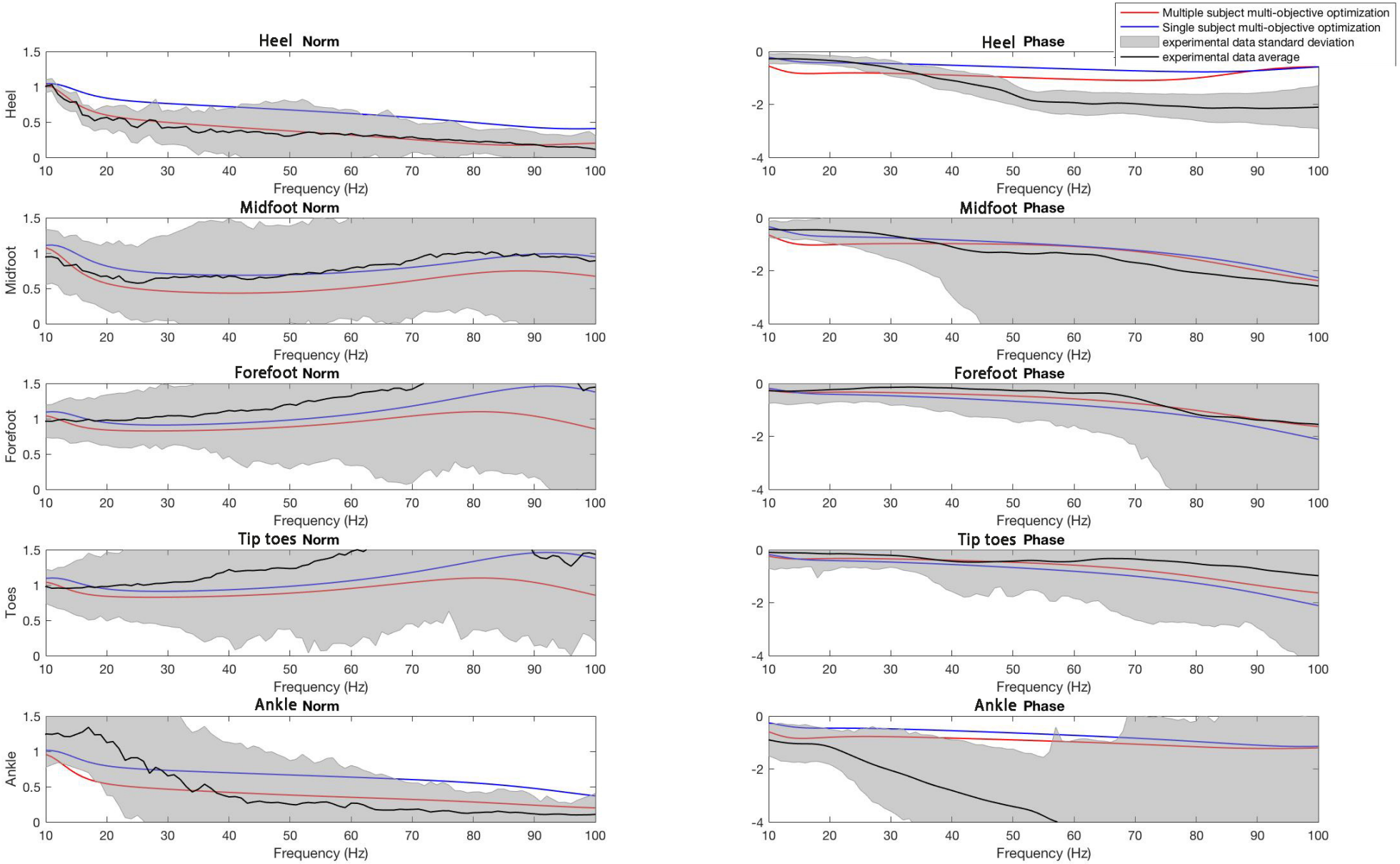

Figure 37 - Analytical transmissibility function of the FAS in leaning backward position of the body

In Table 17 is possible to observe how the modal parameters of the FAS vary when the position of the body is changed. It's important to underline that the values of the stiffness and damping K_d K_h C_d C_h are fixed values because they are the one studied by Griffin and Matsumoto in [76].

Consistently with reality the value of K_g that is the stiffness of the foot sole in the forefoot, in forward position increases of 33%, and decreases in backward position.

Meanwhile, the value of K_e that is the stiffness of the foot sole under the heel, increases in backward position and decreases in forward one. Is possible to deeply understand these results thinking about how the mass of the body is distributed on the foot sole during backward and forward position. In backward position a great part of the mass of the body is concentrated in the back part of the foot, and therefore the values of stiffness of the foot back increase and the ones of the forefoot decrease. Meanwhile, for the forward position.

From the results it doesn't seems that the damping has the same behaviour of the stiffness indeed it doesn't change so much with body position. With respect to the damping the value that changes the most is C_c so the damping of tip toes- forefoot joint, in the forefoot position, it decreases 35,1 %. This result is interesting because it shows that if most of the mass is concentrated on the forefoot the capability to attenuate vibration of that part of the foot is decreased. Thinking about what happen when the position of our body in leaning forward, the joint between the tip toes and the forefoot becomes less free to move, because a series of muscles are activated in order to carry the body weight and to keep us in equilibrium.

	Description	Neutral	Forward	Variation % w.r.t. neutral	Backward	Variation % w.r.t. neutral
$K_a \left[N/m\right]$	stiffness of ankle/body joint	156000	156000	0,00%	156000	0,00%
$K_b \left[N/m\right]$	stiffness of the segments II/III joint	106	106	0,00%	105,9	-0,13%
$K_c \left[N/m\right]$	stiffness of the segments III/IV joint	4,52	4,20	-7,14%	4,02	-11,12%
$K_d \left[N/m\right]$	stiffness of the plantar aponeurosis	20760	23480	13,09%	20300	-2,22%
$K_e \left[N/m\right]$	stiffness of the rearfoot sole	133300	125300	-6,00%	144900	8,70%
$K_f \left[N/m\right]$	stiffness of the forefoot sole	94590	77870	-17,67%	102800	8,63%
$K_g \left[N/m\right]$	stiffness of the toes sole	453	602,4	32,98%	424,4	-6,32%
$K_h \left[N/m\right]$	stiffness of the ankle-body joint	19660	19660	0,00%	19660	0,00%
$C_a \left[N/m \cdot s\right]$	damping of the ankle/body joint	1319	1319	0,00%	1319	0,00%
$C_b \left[N/m \cdot s\right]$	damping of the segments II/III joint	0,33	0,35	7,62%	0,33	-0,15%
$C_c \left[N/m \cdot s\right]$	damping of the segments III/IV joint	0,39	0,25	-35,15%	0,42	7,18%
$C_d \left[N/m \cdot s\right]$	damping of the plantar aponeurosis	5608	5612	0,07%	5594	-0,26%
$C_e \left[N/m \cdot s\right]$	damping of the rearfoot sole	135,5	116	-14,43%	132,8	-2,04%
$C_f \left[N/m \cdot s\right]$	damping of the forefoot sole	0	0	0,00%	0	0,00%
$C_g \left[N/m \cdot s\right]$	damping of the toes sole	62,34	62,00	-0,55%	62,09	-0,40%
$C_h \left[N/m\right]$	Damping of the ankle-body joint	419,5	419,5	0,00%	419,5	0,00%

Table 17 - Average of the optimized parameter by single subject multi objective optimization in neutral, forward e backward positions

3.4 Insoles

As the harmful effects of vibration to the human body are transmitted to the body through the FAS, it is very important to improve technology in order to reduce the transmission of the vibration.

In this chapter are shown the results obtained with the application under the FAS of 7 different rubber soles. In general, looking at the transmissibility function obtained experimentally with and without the insole, is possible to observe that the amplitude of the transmitted vibration is reduced with almost all the insoles. Vibration transmissibility to the 10 measurement locations on the foot also varied across the vibration exposure frequencies for the seven materials tested (Figure 38). But the transmissibility at the toes, independently from the material, was very close to the one measured in barefoot, apart from the prototype F that increased the transmissibility at high frequencies. The transmissibility at the heel was lower 0.3 above 100 Hz and the differences between the foams was always lower than 20%; this indicates the marginal effect of the tested materials in reducing the vibration transmitted to the upper body. The materials were less effective at attenuating vibration transmitted to the tip toe region of the foot then the heel. The transmissibility to the heel reached a high of 1 between 10-20Hz and a low of 0.3 between 150-200Hz. Between 10-20 Hz all outsoles resulted in an average transmissibility of 0.9 and all insoles 0.8 with the greatest transmissibility reduction occurring between 20-50Hz when standing on an air insole. The average transmissibility for the first toe was 1 between 10-50 Hz and increased to 1.4 between 100-150 Hz [78]. For example, Figure 38 shows the effects of the insoles. On first a slight reduction of the modulus amplitude of the transmissibility function and an increased phase signal, therefore the response is anticipated with respect to the input signal with a single exception of the heel phase which response is delayed from the insole.

Regarding the dynamic behaviour, research confirm that a different shoes compliance does not modify the apparent mass measured at the driving point (Tarabini, Saggin, Scaccabarozzi, Gaviraghi, & Moschioni, 2013).

Goggins and colleagues [37] also observed a difference in vibration transmissibility over a 25-50 Hz exposure frequency with the greatest magnitude of transmissibility occurring at 25-30Hz for the ankle and 50Hz for the first toe.

Now, it is interesting to evaluate how the modal parameters of the equivalent Kelvin-Voigt systems foot sole-insole change. In Table 18 is possible to see the difference of the modal parameters obtained with the barefoot foot and with the insole, and the analytically computed insole.

	Barefoot	Equivalent insole-foot fat pad (average)	insole
$K_e \left[N/m\right]$	156000	156000	4,63E+11
$K_f \left[N/m\right]$	133300	151600	5,36E+11
$K_g \left[N/m\right]$	94590	50030	214000
$C_e \left[N/m \cdot s\right]$	135,6	68	132,4
$C_f \left[N/m \cdot s\right]$	0	0	0
$C_g \left[N/m \cdot s\right]$	62,34	31	63,58

Table 18 - Comparison between the parameters of the barefoot foot, the foot with insoles and the insole parameters computed analytically

Insole							
Parameter	A	B	C	D	E	F	G
$K_e \left[N/m\right]$	4,63E+11	4,63E+11	4,63E+11	4,63E+11	4,63E+11	4,63E+11	4,63E+11
$K_f \left[N/m\right]$	5,36E+11	5,36E+11	5,36E+11	5,36E+11	5,36E+11	5,36E+11	5,36E+11
$K_g \left[N/m\right]$	212100	210400	209800	211100	213093,76	231000	211000
$C_e \left[N/m \cdot s\right]$	132,5	132,5	132,5	132,5	132,5	132,5	132,5
$C_f \left[N/m \cdot s\right]$	0	0	0	0	0	0	0
$C_g \left[N/m \cdot s\right]$	63,30	63,01	63,03	63,06	64,22	65,00	63,44

Table 19 - Parameters of the insole, computed with the model

In Table 19 are listed the resulting modal parameters of each insole tested, as can be seen they are similar each other, between one insole and the other, but changes the value between the heel, midfoot and forefoot. This phenomenon can be related to the mass distribution, that compress the rubber and changes its dynamical characteristics.

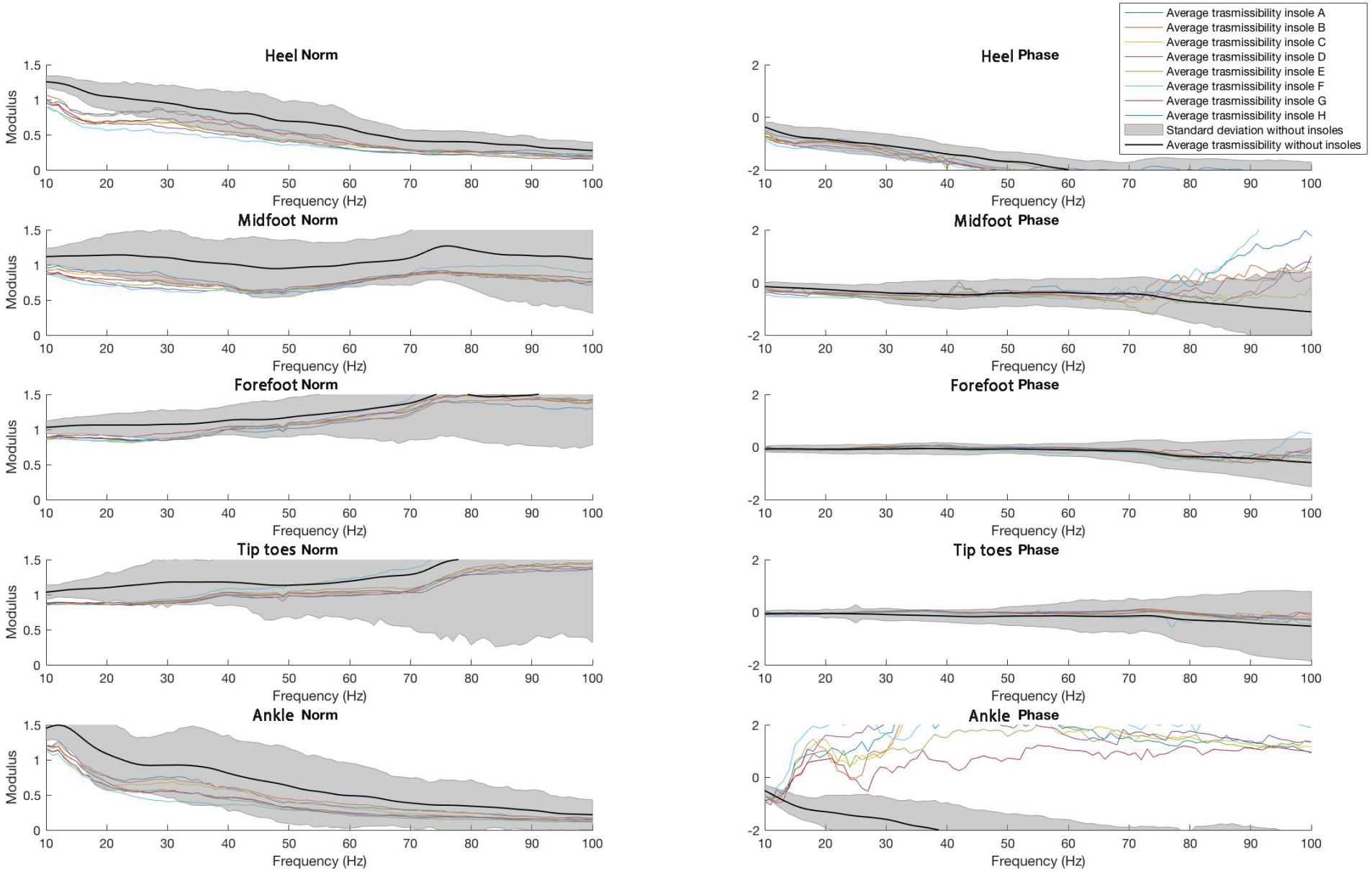

Figure 38 - Experimental transmissibility functions obtained with the different insoles compared to the average +- standard deviation barefoot transmissibility

In Table 20 there are the results obtained from the optimization of the parameters with the insoles. These results are obtained fixing the internal values of the foot. Therefore, it is normal to have higher errors. Except for the insole B, C, and D the model is able to perform a good representation of reality.

	A	B	C	D	E	F	G
Heel	0,19	0,18	0,15	0,15	0,14	0,17	0,19
Midfoot	2,59	2,60	2,65	2,63	2,82	2,63	2,59
Forefoot	1,44	1,55	1,58	1,62	2,11	1,59	1,44
Ankle	1,41	1,52	1,46	1,52	2,42	1,48	1,41
Tip toes	0,16	0,16	0,14	0,12	0,11	0,12	0,16
Apparent mass	0,61	0,61	0,61	0,61	0,61	0,61	0,61
Average	1,07	1,10	1,10	1,11	1,37	1,10	1,07

Table 20 - Least square errors of the optimized transmissibility and apparent mass with insoles

With the model, it would be possible to compute the modal parameters of the insole in order to get a specific transmissibility function.

An interesting future research would be the creation of an insole with dynamic characteristics matching the model presented in this thesis. It would be interesting to evaluate if the obtained experimental transmissibility values are correlated to the analytical ones.

Conclusions

We improved an existing FAS model to better understand the effect of WBV and FTV. The dynamic response of the FAS under vertical vibration was modelled with a 8 DOF system. The vibration transmissibility (modulus and phase) measured at 24 anatomical locations was summarized to reproduce a 2D model that includes the heel, ankle, midfoot, hub and tip toes. We modified the original model [72], consisting of five-rigid bodies including a lumped mass, and viscoelastic parts, that are ligaments, tendons and soft tissues, with the introduction of the lumped parameter model of standing subjects proposed by Matsumoto and Griffin [76].

The forefoot in the medial arch was expressed with three-rigid bodies, the metatarsals, the cuneiforms, the navicular, and the toe. The hindfoot consisting of the talus and calcaneus was modelled a rigid body. The joints between rigid bodies were represented by the viscoelastic Kelvin-Voigt model. The viscoelastic model of the plantar aponeurosis, fat pad of foot, and talus joint were also included in the five-rigid body model. Lagrange's equation was utilized to derive the equations of motion for the model. The derived equation was linearized with Taylor series expansion.

The system identification is based on grey box modes and it was utilized to understand the dynamic characteristics of the foot and ankle system. The modal dynamic parameters are computed trough linear quadratic optimization that fits experimental data and analytical modelled results.

The model parameters were computed to fit the experimental responses in a least square sense. Experimental data were the ones published in the literature.

The robustness of the solution was checked by comparing the parameters obtained (i) fitting a single experimental curve, that is the average of the responses of single subjects and (ii) averaging the parameters obtained by fitting the response of each subject that underwent the tests. Results showed little differences in comparison with the inter- and intra-subject variability.

The model was used to predict the response under three body postures. i.e. neutral standing, leaning forward and leaning backward. The neutral position gave a smaller least square error with respect to leaning forward and leaning backward, this increase of the error can be related to the position of the mass of the body, that is not able to move forward or backward bun only in the vertical plane.

The model was also modified to include the effect of the shoes, that globally reduce the transmissibility of the vibration; results also in this case were consistent with the model prediction. Future researches are needed in order to deepen the knowledge about apparent mass distribution in different postures, this will lead to a more accurate model. Forthcoming studies will focus on the identification of the best shoe performances to reduce the vibration to specific body parts.

4 Bibliography

[1] M. Bovenzi, "Exposure-response relationship in the hand-arm vibration syndrome: an overview of current epidemiology research," *International Archives of Occupational and Environmental Health, 71, 509-519*, 1998.

[2] Bruce P. Bernard Snippet., "Musculoskeletal Disorders and Workplace Factors: A Critical Review of Health and Human Services," *U.S. Dept. Public Health Service, Centers for Disease Control and Prevention, National Institute for Occupational Safety and Health*, 1997.

[3] M., Conrad, L., Jack, R., Dickey, J., & Eger, T. Oliver, "Comfort based seat selection to minimize 6 DOF whole-body vibration in integrated steel manufacturing mobile machinery," *3rd American Conference on Human Vibration, Iowa City Iowa, June 1-4*, 2010.

[4] J., Eger, T., Oliver, M., Boileau, P-E., & Grenier, S. Dickey, "The nature of multiaxis6 degree of freedom vehicle vibrations in forestry, mining and construction heavy equipment," *2nd American Conference on Human Vibration, Chicago, IL, 4 – 6 June*, 2008.

[5] J., Eger, T., & Olivier, M. Dickey, "A systematic approach for studying occupational whole-body vibration. A combined field- and laboratory-based approach," *Work 35,15-26*, 2010.

[6] M. J. Griffin, "Handbook of Human Vibration," *London: Academic Press.*, 1990.

[7] N. Mansfield, "Human Response to Vibration," *New York: CRC, Press*, 2005.

[8] F., Attivissimo, F., Lanzolla, A.M.L., Saponaro, F., and Cervellera, V. Adamo, "Assessment of the uncertainty in human exposure to vibration: An experimental study," *Sensors Journal, 14(2), 474-481. DOI: 10.1109/JSEN.2013.2284257*, 2014.

[9] P.-E., Rakheja, S. Boileau, "Whole-body vertical biodynamic response characteristics of the seated vehicle driver: measurement and model development," *International Journal of Industrial Ergonomics 22, 449–472*, 1998.

[10] Paolo Capodaglio, Cristina Ferrario, Marco Tarabini, Manuela Galli Matteo Zago, "Whole-body vibration training in obese subjects: A systematic review ," *PLoS one*, 2018.

[11] European Parliament, "Directive 2002/44/EC - vibration," *2002*.

[12] M.H., Wilder, D.G., and Magnusson, M.L. Pope, "A review of studies on seated whole-body vibration and low back pain," *Proc Instn Mech Engrs* , pp. Vol 213 Part H, 435-446., 1998.

[13] G.P. et al. Slota, "Effects of seated whole-body vibration on postural control of the trunk during unstable seated balance," *Clinical Biomechanics*, pp. 23:381- 386., 2007.

[14] Jobes CC, Miller RE. Mayton AG, "Comparison of whole-body vibration exposures on older and newer haulage trucks at an aggregate stone quarry operation," *Proceedings of the 2008 ASME Design Engineering Technical Conference & Computers and Information in Engineering Conference; New York City, NY. 2008. p. 7*, 2008.

[15] Malcolm & Wilder, David & Magnusson, Marianne Pope, "A review of studies on seated whole-body vibration and low back pain," *Proceedings of the Institution of Mechanical Engineers. Part H, Journal of engineering in medicine. 213. 435-46. 10.1243/0954411991535040*, 1999.

[16] H. & Heide, R. Seidel, "Long-term effects of whole body vibration: a critical survey of the literature," *International Archives of Occupational and Environmental Health*, pp. 58:1-26., 1986.

[17] M. Bovenzi, "A follow up study of vascular disorders in vibration- exposed forestry workers," *International Arch Occupational Environmental Health*, pp. 81, 401- 408. DOI: 10.10107/s00420-007-0225-9. , 2008.

[18] M. Bovenzi, "Health effects of mechanical vibration," *G Ital Med Lav Erg*, pp. 27(1), 58-64, 2005.

[19] M. Bovenzi, "Low back pain disorders and exposure to whole-body vibration in the workplace," *Seminars in perinatology*, 1996.

[20] Wilder DG, Pope MH, Magnusson M, Aleksiev AR, Wasserman JF Wasserman DE, "Whole body vibration exposure and occupational work hardening," *J Occup Environ Med*, 1997.

[21] Griffin MJ, Bendall H, Pannett B, Coggon D. Palmer KT, "Prevalence and pattern of occupational exposure to whole body vibration in Great Britain: findings from a national survey," *Occup Environ Med.*, 2000.

[22] X., Eger, T.R., and Dickey, J.P. Ji, "Optimizing seat selection for LHDs in the underground mining environment," *The Journal of the Southern African Institute of Mining and Metallurgy, (116), 785-792. DOI:10.17159/2411-9717*, 2016.

[23] P. Donati, "Survey of technical preventative measures to reduce whole-body vibration effects when designing mobile machinery," *Journal of Sound and Vibration, 253(1), 169-183. DOI: 10.1006/jsvi.2001.4254*, 2002.

[24] J., and van Niekerk, J.L. Gunaselvam, "Seat selection guidelines to reduce whole-body vibration exposure levels in the SA mining industry," *The Journal of the Southern African Institute of Mining and Metallurgy, (105), 675-686*, 2005.

[25] M., Rui, M., Nergo, C., D'Agostin, F., Angotzi, G., Bianchi, S., et al. Bovenzi, "An epidemiological study of low back pain in professional drivers," *Journal of Sound and Vibration, 298, 514-539. DOI: 10.1016/j.jsv.2006.06.001.*, 2006.

[26] M.J. Griffin, "Measurement, evaluation, and assessment of peripheral neurological disorders caused by hand-transmitted vibration," *International Archives of Occupational and Environmental Health*, pp. 81, 559-573. DOI: 10.1007/s00420-007-0253-5., 2008.

[27] M., Burstrom, L., Lundstrom, R., and Nilsson, T. Hagberg, "Incidence of Raynaud's phenomenon in relation to hand-arm vibration exposure among male workers at an engineering plant a cohort study," *Journal of Occupational Medicine and Toxicology, 3(13), 1-6. DOI: 10.1186/1745-6673-3-13*, 2008.

[28] R., Jiang, D., Thompson, A., Eger, T., Krajnak, K., Sauve, J., and Schweigert, M. House, "Vasospasm in the feet in workers assessed for HAVS," *Occupational Medicine. 61:115. [PubMed: 21196472]*, 2011.

[29] British Standards Institution. British Standard Guide to Measurement and evaluation of human exposure to whole-body mechanical vibration and repeated shock. BS 6841:1987,.

[30] Della Vedova A, Nataletti P, Alessandrini B, Poian T. Bovenzi M, "Work-related disorders of the upper limb in female workers using orbital sanders.," *int Arch Occup Environ Health.*, 2005.

[31] International Organization for Standardization. ISO 2631-1: Mechanical vibration and shock – Evaluation of human exposure to whole-body vibration – whole-body vibration – Part 1: General Requirements. Geneva, , 1997.

[32] International Organization for Standardization. ISO 5349-1: Mechanical vibration and shock – Guidelines for the measurement and the assessment of human exposure to hand-transmitted vibration. Geneva, , 2001.

[33] T., Thompson, A., Leduc, M., House, R., Krajnak, K., Goggins, K., and Godwin, A. Eger, "Vibration induced white-feet: Overview and field study of vibration exposure and reported symptoms in workers," *WORK, 47(1), 101-110. DOI: 10.3233/WOR-131692*, 2014.

[34] A., House, R., Eger, T., and Krajnak, K. Thompson, "Vibration-white foot: a case report," *Occupational Medicine, 60, 572-574*, 2010.

[35] G.S. Paddan, "Transmission of vertical vibration from the floor to the head in standing subjects," *Proccedings of the UK Group on Human Response to Vibration, Shrivenham, 21-22*, 1987.

[36] E. and Griffin, MJ. Concettoni, "The apparent mass and mechanical impedance of the hand and the transmission of vibration to the fingers, hand, and arm," *Journal of Sound and Vibration, 325, (3), pp. 664-678*, 2009.

[37] K., Godwin, A., Larieviere, C., and Eger, T. Goggins, "Study of the biodynamic response of the foot to vibration exposure," *Occupational Ergonomics, 13, 53-66*, 2016.

[38] Hashiguchi T, Furuta M, Kondo T, Miyao M, Yamada S Sakakibara H, "Circulatory disturbances of the foot in vibration syndrome," *Int Arch Occup Environ Health.63(2):145-8*, 1991.

[39] G.S. et al. Paddan, "Effect of seating on exposures to whole body vibration in vehicles," *Journal of sound and vibration; 253(1): 215-241*, 2001.

[40] Bovenzi M., "Health effects of mechanical vibration," *G Ital Med Lav Erg, 27(1), 58-64*, 2005.

[41] Yanagi H, Kinugawa Y, Sakakibara H, Yamada Hashiguchi T, "Pathological changes of finger and toe in patients with vibration syndrome," *Nagoya J Med Sci*, no. May;57 Suppl:129-36., 1994.

[42] U. Hedlund, "Raynaud's Phenonmenon of fingers and toes of miners exposed to local and whole-body vibration and cold," *International Archives of Occupational and Environmental Health, 61, 457-461*, 1989.

[43] N., & Sim, C. S. Choy, "A case of Raynaud's phenomenon of both feet in a rock drill operator with hand-arm vibration syndrome," *Korean J Occup Environ Med, 20(2), 119-126*, 2008.

[44] T., Futatsuka, M., Imanishi, H., & Yamada, S. Takeuchi, "Pathological changes observed in the finger biopsy of patients with vibration-induced white finger," *Scandinavian Journal of Work, Environment & Health, 12(4), 280-283. doi:10.5271/sjweh.2140*, 1986.

[45] M., Sakakibara, H., Yamada, S., Hashiguchi, T., Toibana, N., & Koshiyama, H. Hirata, "Nerve conduction velocities in the lower extremities among patients with vibration syndrome," *Central European Journal of Public Health, 3 Suppl, 78-80*, 1995.

[46] B. and Grzesik, J. Harazin, "The transmission of vertical whole-body vibration to the body segments of standing subjects," *Journal of Sound and Vibration, 215(4), 775- 787*, 1998.

[47] R.G., Schopper, A.W., McDowell, T.W., Welcome, D.E., Wu, J.Z., Smutz, W.P., Warren, C., and Rakheja, S. Dong, "Vibration energy absorption (VEA) in human fingers-hand-arm system," *Medical Engineering & Physics, 26(6), 483-492*, 2004.

[48] M. and Griffin, M.J. Morioka, "Frequency weightings for fore-and-aft vibration at the back: Effect of contact location, contact area, and body posture," *Industrial Health, 48, 538-549. DOI: 10.1080/08990220500420400*, 2005.

[49] Y., Wosk, J., Voloshin, A., and Liberty, S. Folman, "Cyclic impacts on heel strike: a possible biomechanical factor in the etiology of degenerative disease of the human locomotor system," *Archives of Orthopaedic and Trauma Surgery, 104(6), pp. 363-365*, 1986.

[50] K. G., Wagenaar, R. C., Kubo, M., Lafiandra, M. E., and Obusek, J. P. Holt, "Modulation of Force Transmission to the Head While Carrying a Backpack Load at Different Walking Speeds," *Journal of Biomechanics, 38(8), pp. 1621-1628*, 2005.

[51] E. L., Burr, D. B., Caterson, B., Fyhrie, D., Brown, T. D., and Boyd, R. D. Radin, "Mechanical Determinants of Osteoarthrosis," *Semin. Arthritis Rheum, 21(3Suppl 2), pp. 12-21*, 1991.

[52] Martin, R. B., Burr, D. B., Caterson, B., Boyd, R. D., and Goodwin C. Radin E. L., "Effects of Mechanical Loading on the Tissues of the Rabbit Knee," *J Orthop Res, 2(3), pp. 221-34*, 1984.

[53] Chadefaux D., Cazzaniga C Tarabini M., "Modelling of the vibrations transmissibility in the feet of standing subjects".

[54] M.J. Griffin Y. Matsumoto, "Dynamic response of the standing human body exposed to vertical vibration: influence of posture and vibration magnitude," *Journal of sound and Vibration 212 85-107*, 1998.

[55] W. Ammann H. Bachmann, "Vibration in Structures Induced by Man and Machines," *Structural Engineering Documents, 3rd edition, international association for Bridge and Structural Engineering*, 1987.

[56] M., Solbiati, S., Moschioni, G., Saggin, B., and Scaccabarozzi, D. Tarabini, "Analysis of non-linear response of the human body to vertical whole-body vibration," *Ergonomics, 57(11), 1711-1723. DOI: 10.1080/00140139.2014.945494*, 2014.

[57] D/Tech Systems, Chandler, John Wiley & Sons, LTD David I. G. Jones, "Handbook of Viscoelastic Vibration Damping," 2001.

[58] G. J., McLure, H., Newell, E. N. Campbell, "Compressive behaviour after simulated service conditions of some foamed materials intended as orthotic shoe insoles," *Rehabil. Res. Dev., 21, 57-65*, 1984.

[59] S. Albert, "A subjective comparison of Spenco and R.P.T. soft tissue supplements used in footgear," *Orthot. Prosthet., 35 (3), 17-21*, 1981.

[60] B. Wood, "The painful foot," *In: Kclley, W. Harris, E. Ruddy. 5. Sledge, C. (eds). A textbook of rheumatology Philadelphia. P. A.: W. B. Saunders. 472-484*, 1981.

[61] R. B., Thompson, D. E. Beach, "Selected soft-tissue research: an overview from Carville," *Phys. Ther., 59, 30-33*, 1979.

[62] Lord Corporation, "Lord User's Guide, ," 2000.

[63] M. & Pope, M.H. Cardinale, "The effects of whole body vibration on humans: Dangerous or advantageous?," *Acta Physiologica Hungarica, 90(3), 195- 206*, 2003.

[64] International Organization for Standardization. ISO 2631: Mechanical vibration and shock – Evaluation of human exposure to whole-body vibration – whole-body vibration – Part 1: General Requirements. Geneva, , 1997.

[65] A. Gefen, "The in vivo elastic properties of the plantar fascia during the contact phase of walking," *Foot and Ankle International, 24(3), pp. 238-244*, 2003.

[66] A., and Leichter, I. Simkin, "Role of the calcaneal inclination in the energy storage capacity of the human foot—a biomechanical model," *Medical and Biological Engineering and Computing, 28(2), pp. 149-152*, 1990.

[67] W., and Voloshin, A. S. Kim, "Role of plantar fascia in the load bearing capacity of the human foot," *Journal of biomechanics, 28(9), pp. 1025-1033*, 1995.

[68] H., and Voloshin, A. Wee, "Transmission of vertical vibration to the human foot and ankle," *Annals of Biomedical Engineering, 41(6), 1172-1180. DOI: 10.1007/s10439-013-0760-3.*

[69] R.R. Coermann, "The mechanical impedance of the human body in sitting and standing positions at low frequencies," *Human Factors, 4, 227-253*, 1962.

[70] Tarabini M., Lievers W., Eger T. Goggins K., "Biomechanical response of the human foot when standing in a natural position while exposed to vertical vibration from 10-200 Hz.," *Ergonomics*, 2018.

[71] M., Solbiati, S., Moschioni, G., Saggin, B., and Scaccabarozzi, D. Tarabini, "Analysis of non-linear response of the human body to vertical whole-body vibration," *Ergonomics, 57(11), 1711-1723. DOI: 10.1080/00140139.2014.945494* , 2014.

[72] Delphine Chadefaux et al., "Development of a two-dimensional biodynamic model of the foot-ankle system exposed to vibration ," *Journal of sound and vibration*, 2018.

[73] Palmer KT, Syddall H, Pannett B, Cooper C, Coggon D. Griffin MJ, "Risk of hand-arm vibration syndrome according to occupation and sources of exposure to hand-transmitted vibration: A national survey," *Am J Ind Med*, pp. 39(4):389-96, 2001.

[74] G.S. et al. Paddan, "Effect of seating on exposures to whole body vibration in vehicles," *Journal of sound and vibration*, pp. 253(1): 215-241, 2001.

[75] G.S. Paddan, "Transmission of vertical vibration from the floor to the head in standing subjects," *Proccedings of the UK Group on Human Response to Vibration, Shrivenham*, pp. 21-22, 1987.

[76] M.J. Griffin Y. Matsumoto, "Mathematical models for the apparent masses of standing subjects exposed to vertical whole-body vibration," *Journal of sound and vibration , 260 431-451*, 2003.

[77] M.J. Griffin L. Wei, "Mathematical models for the apparent mass ot the seated human body exposed to vertical vibration".

[78] Tammy Eger, Katie Goggins, Francesco Corti, Filippo Goi M. Tarabini, "Effect of the shoe sole on the vibration transmitted from the supporting surface to the feet".

[79] Y & Griffin, Michael Matsumoto, "Comparison of biodynamic responses in standing and seated human bodies," *Journal of Sound and Vibration - J SOUND VIB. 238. 691-704. 10.1006/jsvi.2000.3133*, 2000.

1 Appendix A

1.1 Comparison of the transmissibility functions changing the optimization frequency boundary.

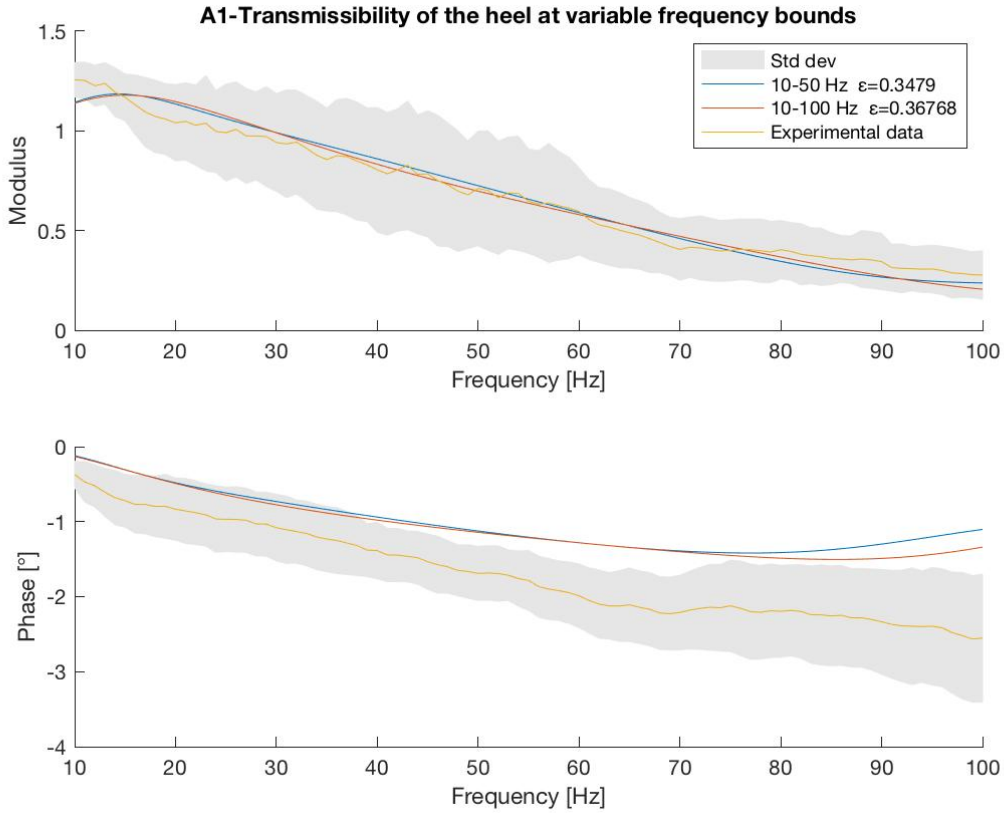

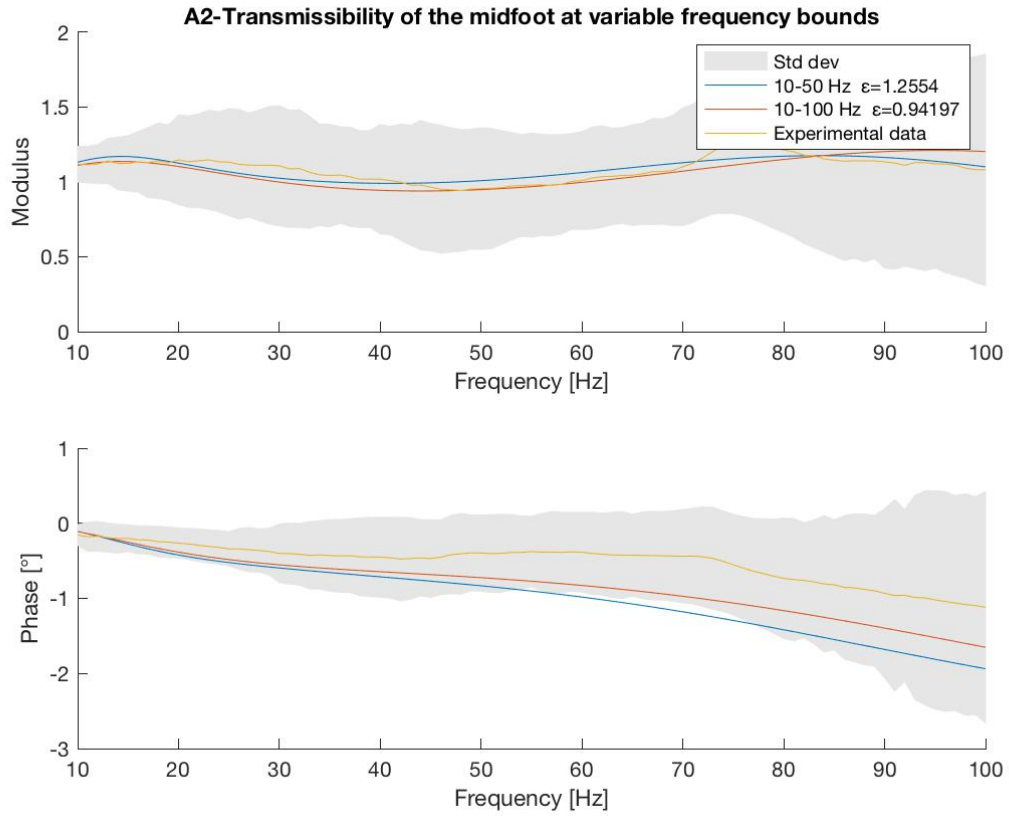
A2-Transmissibility of the midfoot at variable frequency bounds
Std dev
10-50 Hz ε=1.2554
10-100 Hz ε=0.94197
Experimental data
Modulus
Frequency [Hz]
Phase [°]
Frequency [Hz]

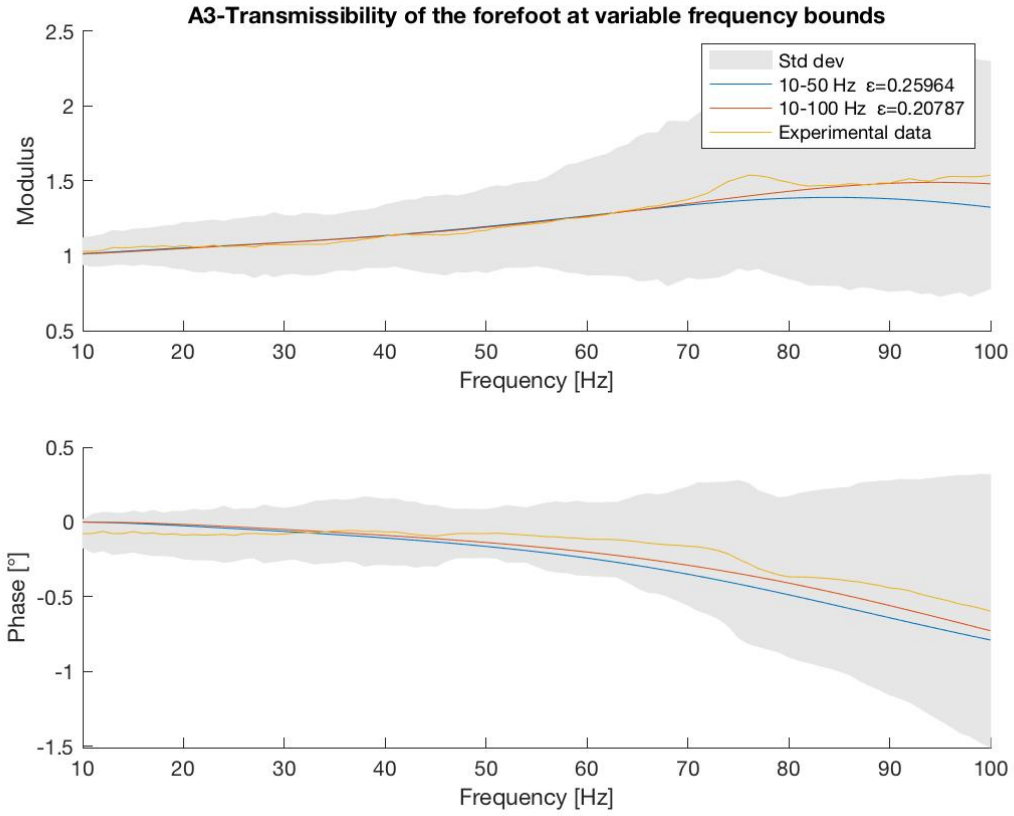
A3-Transmissibility of the forefoot at variable frequency bounds
Std dev
10-50 Hz ε=0.25964
10-100 Hz ε=0.20787
Experimental data
Modulus
Frequency [Hz]
Phase [°]
Frequency [Hz]

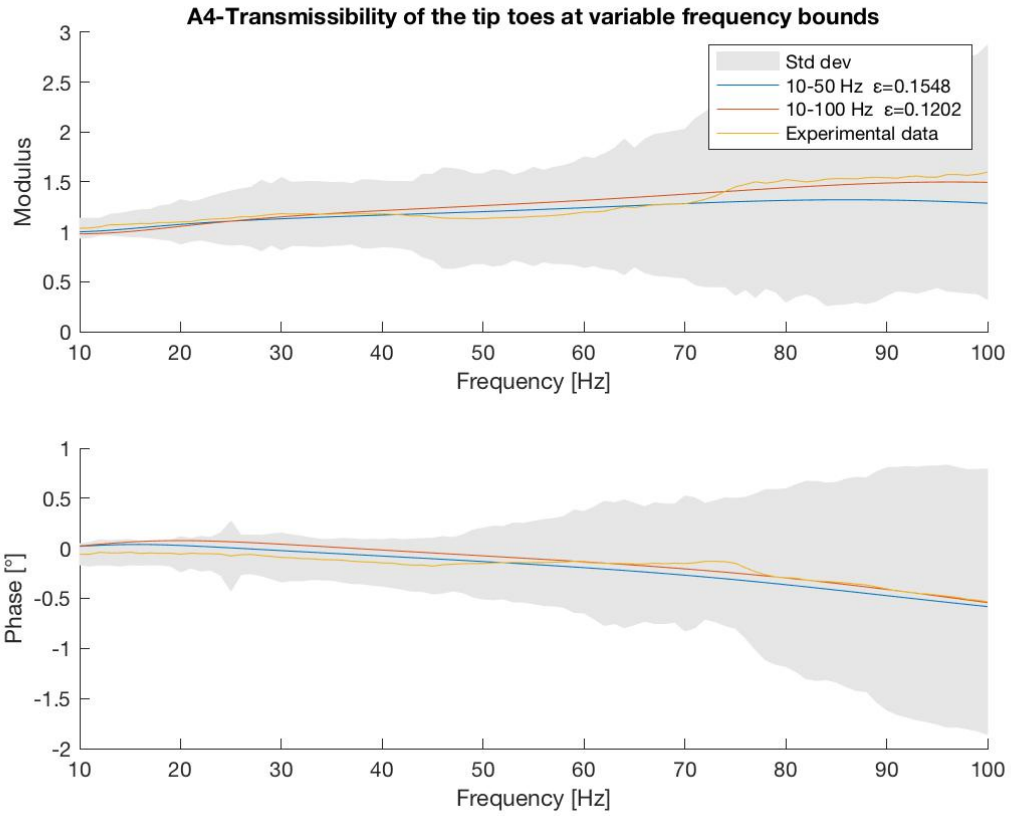
A4-Transmissibility of the tip toes at variable frequency bounds
Std dev
10-50 Hz ε=0.1548
10-100 Hz ε=0.1202
Experimental data
Modulus
Frequency [Hz]
Phase [°]
Frequency [Hz]

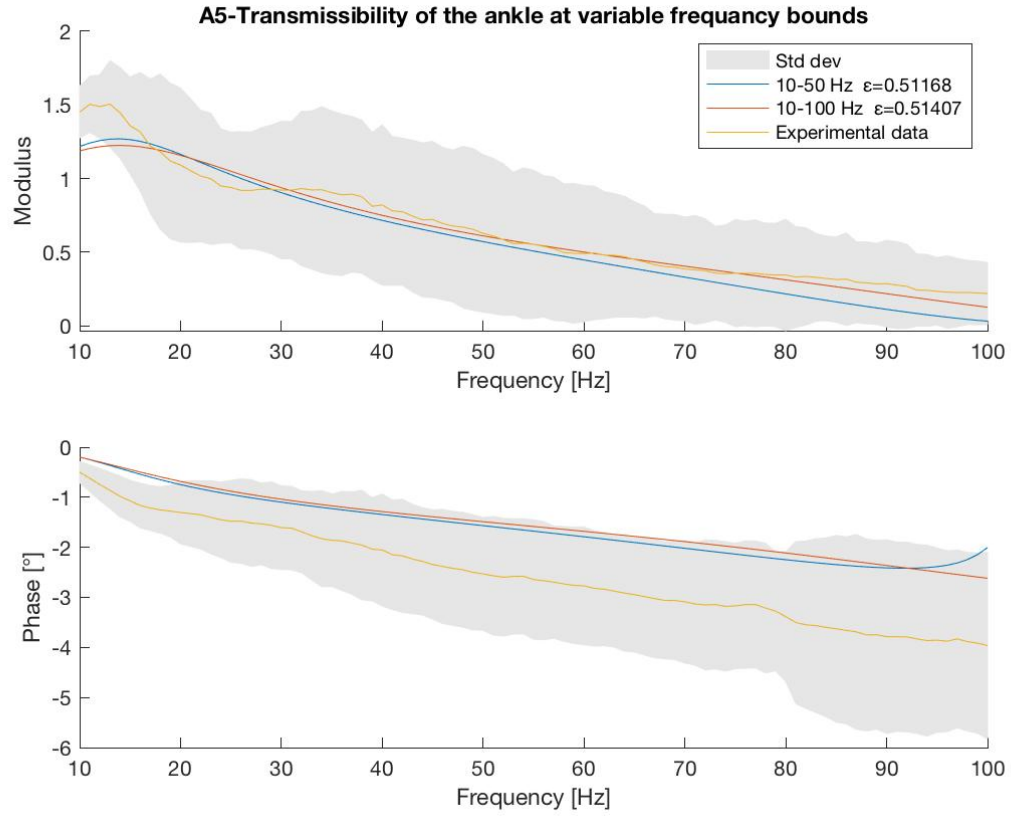
A5-Transmissibility of the ankle at variable frequancy bounds
Std dev
10-50 Hz ε=0.51168
10-100 Hz ε=0.51407
Experimental data
Modulus
Frequency [Hz]
Phase [°]
Frequency [Hz]

Least square error ε evaluated on the interval of 10-100Hz						
	T1	T2	T3	T4	T5	Average least square error
10-50Hz	0,34	1,25	0,26	0,15	0,51	0,506
10-100Hz	0,37	0,94	0,21	0,12	0,51	0,430

Table 21 - Comparison between least square errors computed on the range of 10-100Hz on the transmissibility function with parameters optimized on the boundary of 10-50Hz and 10-100Hz

Least square error ε evaluated on the interval of 10-50Hz						
	T1	T2	T3	T4	T5	Average least square error
10-50Hz	0,43	0,54	0,04	0,02	0,68	0,343
10-100Hz	0,45	0,40	0,03	0,02	0,65	0,308

Table 22 - Comparison between least square errors computed on the range of 10-50Hz on the transmissibility function with parameters optimized on the boundary of 10-50Hz and 10-100Hz